UNIVERSITÀ DEGLI STUDI DI NAPOLI FEDERICO II

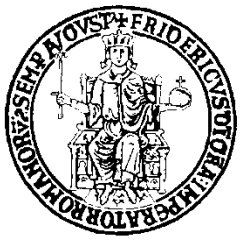

FACOLTÀ DI INGEGNERIA

Dipartimento di Ingegneria Industriale

DOTTORATO DI RICERCA IN INGEGNERIA AEROSPAZIALE NAVALE E DELLA QUALITÀ XXVII CICLO

ADS-B BASED SENSE AND AVOID APPLICATIONS FOR GENERAL AVIATION/UNMANNED AIRCRAFT

Coordinatore
Prof. Luigi De Luca

Tutor
Prof. Domenico Accardo
Prof. Giancarmine Fasano
Ing. Federico Corraro

Candidato
Ing. Martina Orefice

Marzo 2015

Index

Acronyms

ACAS	Airborne Collision Avoidance System
ADS-B	Automatic Dependent Surveillance - Broadcast
ADS-R	Automatic Dependent Surveillance – Re-broadcast
ARV	Air Referenced Velocity
ATS	Air Traffic Services
A/V	Aircraft/Vehicle
ASACAS	Autonomous Separation And Collision Avoidance System
CAB	Civil Aeronautics Board (CAB)
CDTI	Cockpit Display of Traffic Information
CFR	Code of Federal Regulations
ENU	East-North-Up
FAA	Federal Aviation Administration
FLARE	Flare Laboratory for Aeronautical Research
FOV	Field Of View
GNC	Guidance, Navigation and Control
IMC	Instrument Meteorological Condition
LIDAR	Laser Imaging Detection and Ranging
MASPS	Minimum Aviation Systems Performance Standards
MMW	Millimetre Wave
MOPS	Minimum Operational Performance Standards
MS	Mode Status
NACp	Navigation Accuracy Category for Position
NACv	Navigation Accuracy Category for Velocity
NAS	National Airspace System
NED	North-East-Down
SAA	Sense And Avoid
SIL	Surveillance Integrity Level
SV	State Vector
TAS	True Air Speed
TCAS	Traffic Alert and Collision Avoidance System

TIS-B	Traffic Information Service - Broadcast
TSAA	Traffic Situation Awareness with Alerting
UAV	Unmanned Aerial Vehicle
VFR	Visual Flight Rules
VLA	Very Light Aircraft
VMC	Visual Meteorological Condition
WP	Way Point

Abstract

This work focuses on the application of ADS-B surveillance data as inputs for conflict detection algorithms, in order to support future self-separation as well as collision avoidance systems. In particular, an approach is here proposed for conflict detection between ownship and surrounding ADS-B OUT equipped aircraft, which uses traffic position and velocity data provided by the on-board ADS-B IN device. The intended system applicability is for both manned commercial aircraft, as an aid to pilots, and Unmanned Aircraft Systems (UAS), where high automation levels are required, as part of an autonomous Sense-And-Avoid system.

In the first part of the work, a detailed analysis on state of the art of the SAA systems is shown investigating the architectures based on cooperative and non-cooperative sensors.

In the expected evolution of surveillance systems for aircraft applications in the next years, the Automatic Dependent Surveillance Broadcast (ADS-B) implementation on-board vehicles plays a fundamental role hence, in the second part, a detailed analysis about ADS-B system is reported. The advantages and the drawbacks related to the adoption of this sensor for a SAA architecture are also investigated.

In the third part the architecture of the proposed system is presented including a description of the software modules, focusing on the specific applications devoted to surveillance data processing and conflicts identification and prioritization.

Finally test scenarios, and the related results, are presented and discussed. In particular off-line and real-time tests, with an hardware in the loop architecture, have been carried out.

The activities hereafter reported have been carried out in the framework of a collaboration between the Italian Aerospace Research Centre (CIRA), where the author is employed in the field of air transport sustainability, and the University of Naples “Federico II”.

Chapter 1

Survey on Sense And Avoid Systems

1.1 Introduction

Unmanned Aerial Vehicles (UAVs) have grown exponentially in the last decade and a lot of applications proved UAV reason for existence. Most of those applications are military but more and more civil and commercial opportunities are opening for UAVs. In fact, the size of UAVs is extremely variable and it makes possible to perform some tasks impracticable or dangerous for manned aircraft, such as detecting, monitoring and measuring the evolution of natural disasters, like forest fires or landslips [1].

Especially in U.S., numerous efforts have been made, by governments and industries, in order to integrate UAVs in the NAS. Among the years, an extensive research has been carried out especially in the framework of navigation and control techniques regarding UAVs [2] but some lacks still remain in terms of safety. In fact the major obstacle to integrate UAVs in the NAS is the lack of a sense-and-avoid capability similar to the one provided by on-board pilots, and the consequent possibility of mid-air collisions. Therefore, although the efficiency of those systems have been proved under different and various conditions, their safety, reliability and compliance with aviation regulations still has to be proved.

Certainly, the fundamental difference between a UAV and a manned aircraft is the physical absence of the pilot on-boards who also interacts with the ground-based air traffic control (ATC) system. Essentially an UAV is remotely piloted although it is capable of numerous automate operations. It implicates that the pilot has not direct situational awareness and the one of the most significant challenges, is the replacement of the “see-and-avoid” capability, with the “sense-and-avoid”

one [3]. In the following a regulatory and technology survey of sense-and-avoid systems will be reported.

1.2 Regulatory state of the art of SAA systems

Since the pilot remotely controls the UAV it is necessary to replace the "see-and-avoid" capacity with the "sense-and-avoid" capacity.

The U.S. regulatory survey of sense-and-avoid, carried out by Douglas M. Marshall et al. [4], gives an indication about the challenges related to the integration of UAVs into the NAS.

The cornerstone of the current VFR, i.e. the concept of "see and be seen" had its first appearance in a Federal regulation, in the Air Commerce Act of 1926. Only in 1955 the CAB (the predecessor of FAA) inserted the sentence "see and be seen" in a document [5] which stated "the philosophy behind the Visual Flight Rules is that aircraft being flown in accordance with these rules are operated in "see and be seen" weather conditions permitting the pilots to observe and avoid other traffic". Starting from this, in 1968, the FAA published an amendment confirming the pilot's responsibility and now the amendment 91 CFR states "When weather conditions permit, regardless of whether an operation is conducted under instrument flight rules or visual flight rules, vigilance shall be maintained by each person operating an aircraft so as to see and avoid other aircraft." [6] and in addition pilots are responsible to not "operate an aircraft so close to another aircraft as to create a collision hazard" [7].

Although the term "operate", as reported in FAA Section 1.1 (" [operate] means use, cause to be used, or authorize to use aircraft, for the purpose…of air navigation including the piloting of aircraft, with or without the right of legal control" [8]) may include UAV operations, there isn't a specific part set aside for unmanned aircraft (but it exists the counterpart for the operation of moored balloons, kites, unmanned rockets, and unmanned free balloons [9]). Only in 1981 the Advisory Circular 91.57 referred directly to unmanned aircraft: it introduced the standards for model aircraft.

Over the years many efforts have been done in order to develop SAA requirements and in 2004 the RTCA Special Committee 203 (SC-203) was

formed. It had the task of produce the MASPS for several systems including the MASPS for Sense And Avoid. The quantitative performance standards for a SAA system (MASPS), would have been published on December 2013 [10] (but the document will not be issued).

In 2005 and 2007 the FAA emitted two policy statements that pronounced pilot's duty to see-and-avoid other aircraft and, concerning the UAV, the responsibility of the pilot to conducts visual line-of-sight operations [11].

Between December 2008 and March 2009, the FAA organized several workshops in order to define the capabilities that a SAA system should have to be compliant with the current rules governing the "see-and-avoid". The workshop published a document in October 2009 [12], where the sense-and-avoid concept was defined as "the capability of [an unmanned aircraft] to remain well clear from and avoid collisions with other airborne traffic". Moreover the workshop defines that a SAA system would be characterized by two components:

- A Self-Separation component that assures a safe separation based on a variable time-based threshold. In this way the aircraft remain "well-clear" of each other;
- A Collision Avoidance component that operates when the safe separation is lost and an extreme manoeuver is needed to prevent a collision, i.e. penetrating the collision volume. In fact, for the collision avoidance maneuver, a distance based threshold is considered.

The SC-203 sunset on June 2013 and, contextually, the SC-228 was created. The committee has the task of produce the MOPS for Unmanned Aircraft Systems planned for July 2016 [13]. The committee delivered two White Papers in December 2013: Detect and Avoid (DAA) White Paper and Command and Control (C2) White Paper [14].

Currently the FAA Regulation states that an UAV "must provide equivalent levels of safety, comparable to see-and-avoid requirements for manned aircraft" [15] and the UAV that wants to operate in U.S. NAS must obtain Certificates of Authorization. Note that an equivalent level of safety to the see capabilities of manned aircraft implies that the SAA system must be able to detect "other aircraft

within a range of ±15° elevation and ±110° azimuth and respond in sufficient time so that a collision is avoided by a minimum of *500 ft*. The *500 ft* margin of safety derives from what is commonly defined as a near midair collision." [16].

In the European framework, relevant effort is devoted to support the definition of suitable standards allowing the integration of UAS into the civil airspace. EDA (the European Defense Agency) funded the ongoing project MIDCAS (Mid-air Collision Avoidance System), started in 2009 and expected to be completed by 2015, whose budget has been set to approximately 50 M€. The specific aim of MIDCAS is to identify adequate technology, contribute to standardization and demonstrate a SAA system for UAS able to fulfill the requirements for traffic separation and mid-air collision avoidance in non-segregated airspace. The MIDCAS SAA system is currently in the final test campaign, using a UAV in real world environment, and the project findings are shared with European regulatory bodies to provide the technical background for them to establish SAA standards. Therefore, the outcomes of the MIDCAS project will be used as baseline input for the process of standardization of UAV integration into non-segregated airspace

1.3 Challenges on Certification of SAA systems

In order to defines a set of SAA standards, for the certification and operational approval of UAVs, the Workshop of 2009 identified a set of requirements categorized by sub-function. They are reported in Table 1.1 that is an extract of the document emitted by the FAA "Sense, and Avoid Technology for Unmanned Aircraft Systems " [17]:

Function No.	Function	Requirements	Detect	Sense	Avoid
1.0	Detect conflicting traffic	• Continuously scan for threats	×		
		• Minimizes false alarms	×		
		• Minimizes misses		×	
		• Provides operator threat data		×	×
		• Covers a field of view of 110° horizontal and ±15° azimuth	×		
		• Tracks all threats within a minimum range		×	
		• Determines closure rates		×	
2.0	Determine Right of Way	• Autonomously makes move in accordance with (IAW) FAA/International Civil Aviation Organization (ICAO) regulations			×
		• Operator makes move IAW FAA/ICAO regulations			×
3.0	Analyze Flight Paths	• Determines if target is heading toward danger zone (maintain 500-foot separation)		×	
		• Calculate flight paths based on sensors available information		×	
		• Updates time available for maneuver		×	×
4.0	Maneuver	• Maneuver IAW FAA guidelines			×
		• Allows operator maneuver			×
		• Maneuvers continuously in loss link/loss of command control (C^2)			×
		• Maintains at least 500-foot separation		×	×
		• Returns to original flight path after maneuver		×	
5.0	Communicate	• Continuously reports to ground system; allows operator override		×	×
		• Available bandwidth exists to carry message packets		×	×
		• May use stand-alone telemetry or platform communications		×	×
		• Priority communication to maintain safety of flight		×	
		• Reports targets when threat parameters are met; updates solution until no longer a target		×	×

Table 1.1 - Requirements for SSA systems [17]

Nevertheless, a wide range of possible solutions are available and a trade-off between the sub-functions is needed in order to take into account, for example, the traffic characteristics of the interested airspace class, the aircraft performance and the size, weight, cost and performance of the sensors. Moreover, also the architecture of the SAA system has to be taken into account. An issue is the pilot control latency and the communication link, and how the UAV pilot remotely controls the UAV. The pilot, on the ground, would receive surveillance data from the UAV, evaluate the situation and communicate the avoidance manoeuver on-board after the decision on when and how avoid the threat has been taken. But

another solution would be to use an automatic collision avoidance algorithm on-board the UAV with no communication with the pilot [18].

Another trade-off is related to the interaction between the sensors and the avoidance manoeuvres. In fact the accuracies and performance of the sensing system are strictly related to the used sensors and so the collision avoidance manoeuvre could respect the minimum required distance or consider an extra-size in order to compensate the possible measurement errors [18].

For those reasons is not possible to adopt a common SAA algorithm for all UAVs, unlike the manned collision avoidance system TCAS II that uses a single threat algorithm [19].

In the following, a review on possible sensors solution and SAA architecture will be given.

1.4 SAA Available Technologies Survey

"Currently is no recognized technology solution that could make these aircraft capable of meeting regulatory requirements for see-and-avoid and command and control" is a statement of Nick Sabatini (associate FAA administrator for aviation safety) articulated before the House Committee on Transportation and Infrastructure, Subcommittee on Aviation on Unmanned Aircraft Activities in 2006 [20]. The situation is not very changed ever since, due to the complexity of sense-and-avoid technologies and an initial FAA certification of an airborne SAA will not take place until the next year [21]. For this reason, a great effort has been made, during the lasts years, by industry and agencies in order to identify a technological solution that could satisfy an equivalent level of safety of manned aircraft.

The technologies that have been used, during the years, can be divided in two macro-areas [22]:

- Cooperative Technologies that typically require a transponder on board the aircraft; they require other aircraft to be equipped with the same devices when sharing the same airspace.

- Non Cooperative Technologies that identify all the aircraft not equipped with a transponder or, for example, gliders, hot air balloons and so on; they do not require other aircraft to be equipped with the same devices when sharing the same airspace.

Note that, in a multi-sensor approach, a data fusion system is required to integrate the best features of the dissimilar sensors while ensuring high reliability and limiting the computational burden so as to enable real time software implementation.

1.4.1 Cooperative Technologies

TCAS

Traffic Alert and Collision Avoidance System (TCAS) [19] is the principal collision avoidance systems and it uses transponder in order to transmit information. Therefore it generates alerts for the pilot for potential collision threats related to transponder-equipped aircraft. In addition to traffic advisories (TA) the TCAS II can provide resolution advisories (RA) supporting the pilot in the conflict resolution [23]-[24]. Note that the suggested collision avoidance maneuver is generated in a cooperative manner with the other aircraft. TCAS is mandated on all aircraft with 10 seats or more. Nevertheless this systems was never intended to replace see-and-avoid and, moreover, a safe horizontal maneuver is not guaranteed due to the low accuracy of bearing measurements.

ADS-B

Automatic Dependent Surveillance – Broadcast (ADS-B) is a relatively new technology and it was developed in order to support aircraft operation and overcome the ground based radar surveillance [25]-[26]. Actually, it allows both ground station and pilots to detect other ADS-B equipped aircraft with more much precision than ever.

ADS–B consists of two different services: ADS-B OUT and ADS-B IN. In a typical application, aircraft equipped with ADS-B OUT technology compute their own precise position through satellite-based GPS. This information, along with other such as altitude, velocity, identification (and others which will be described

in the following chapter) are transmitted in broadcast via a discrete frequency via a data-link. Those information can be received by other aircraft equipped with ADS-B IN technology or ground station improving the awareness of pilots about the surrounding traffic conditions and reducing the risk of misleading controllers orders due to stress condition. The main expected outcome of ADS-B technology is the improvement of the Separation Assurance function and in the future the ADS-B will enable pilots to perform self-Separation Assurance manoeuvres [27]-[28]. The introduction of ADS- B will provide specific benefits to support the integration of UAV into civil airspace. Moreover, General Aviation aircraft will be provided with a system that will ensure a remarkable increase in the overall situational awareness and a reduction in the number of collision threats.

1.4.2 Cooperative technologies on UAV

Cooperative technologies are widely used on manned aircraft due to their proved reliability. Moreover those systems have been already certified and approved for use. Nevertheless there are some disadvantage that must be taken into account when the cooperative sensors are intended to use on UAVs. First of all, cooperative technologies, effectively, work only when all the aircraft in the shared airspace possess and utilize them. They provide no SAA capability against ground obstacles, i.e. terrain and mountains, and they were developed assuming that a pilot would be in the loop evaluating warnings and taking the appropriate manoeuvres. Moreover, some of those systems, such as TCAS, might be cost prohibitive for some users. For these reasons, a recertification might be needed for use in UAVs, in order to maintain the equivalent level of safety of manned aircraft [17].

1.4.3 Non-Cooperative Technologies

Active Microwave Sensors

Active microwave sensors represent a suitable option to provide the required situational awareness in the case of medium/large UAV platforms which have to attain a reliable full autonomy from ground. In fact, airborne radars

provide direct and typically accurate range estimates (also range rate if Doppler processing is used). Moreover, they can guarantee large detection range, low levels of missed or false detections (ground echoes have to be properly filtered), and can be not much affected by weather conditions, so that the all-time all-weather operation can be guaranteed.

It is worth noting that, in the choice of wavelength, maximizing detection range, minimizing sensor dimensions to enable installation on-board a lightweight aircraft, and improving as much as possible angular resolution are contradicting requirements. In fact, radars operating at low frequencies are relatively unaffected by atmosphere, but are large in size and unable to provide required spatial resolution, due to main lobe width, which is directly proportional to operating wavelength $\sigma_{3dB} = K\frac{\lambda}{l}$. The parameter K is a coefficient whose value depends on the considered aperture and feeding, and l is the antenna length in the considered direction. In conventional architectures the main lobe width coincides with the achievable angular resolution. A higher frequency radar, instead, is smaller in size and provides better resolution for given aperture size, but is more susceptible to atmospheric and weather effects, and in particular to rain, as it results if we consider atmospheric attenuation produced by fog and rain.

Frequencies ranging from C-band (about 6 GHz) to Ka and W band (35 and 94 GHz, respectively) have been used and/or proposed in sense and avoid applications.

Besides angular resolution, other important performance parameters are the detection range, the range and Doppler resolution, the achievable field of regard and scan rate.

The detection range for a given target can be calculated in probabilistic terms on the basis of achievable signal-to-noise ratio (SNR) and the number of impulses integrated to perform target detection [29].

Given a field of regard, the achievable scan rate depends on the radar pulse repetition frequency (PRF, which in its turn influences average power consumption and maximum unambiguous range), number of integrated pulses for each resolution cell, and main lobe width.

Compared with mechanically scanned systems, electronically scanned arrays have the significant advantage of beam agility, i.e., the beam can pointed adaptively without the constraints of mechanical inertia. Thus, track update rate for a given target can be increased without significant effects on the revisit rate in the rest of the sensor field of regard.

However, electronic scanning allows beam pointing within angular limits which are smaller than typical sense and avoid requirements. In general, standalone radar architectures are typically characterized by coarse angular resolutions (order 1°) and low update rates (order 1 Hz), since finer resolution essentially implies larger antenna dimensions. In general radars are demanding in terms of cost, size, weight and required electric power, so that they do not represent an affordable sensing solution for small unmanned platforms, considering current technological levels. However, increasing efforts are being made towards miniaturization and adaptation to small UAV.

Laser (LIDAR)

Laser systems work similarly to conventional radar: laser scans are taken at regular interval and processed by an echo-analysis software. The obstacles and intruders can be used as input to automated collision avoidance systems [30]. Due to their high configurability, laser systems can be used in several atmospheric conditions reducing the false alarms. Moreover, they are capable to detect small obstacles up to *5 mm* of diameter and large obstacles such as buildings and bridge.

Electro Optical Systems

Electro-optical sensors are largely used in the framework of collision avoidance systems for small UAV thanks to the low cost, power consumption and weight. In particular they are often used as standalone systems or in integrated architectures comprising radar or other systems, to produce an estimate of vehicle states through a multi sensor fusion.

In terms of wavelength, visible band sensors are usually exploited to detect the sunlight scattering from other aircraft, while during nighttime when no Sun

scattering is available, the best solution is to use a Thermal Infra Red sensor that can detect the energy emitted by the same object.

Important parameters relevant to EO detection and tracking performance are related to the available field of view and angular resolution.

In general, standalone EO systems require heavy computational resources in order to fulfill real-time full image detection of obstacles, and their output can suffer from a high false alarm rate since background removal processing is less accurate as the image size increases. Moreover, EO detection range is very much affected by weather and illumination conditions and it can be poor.

Acoustic Sensors

Acoustic sensors can be used to detect and track aircraft basing on the signal emitted from a propeller-driven aircraft which comprises a strong narrowband tone imposed onto a broadband random component.

1.4.4 Cooperative and Non-cooperative technologies summary

The advantages and drawbacks for existing technologies are indicated in Table 1.2, which is an extract of the accurate analysis conducted by Yu X. et al. in [31]. Moreover, the effective detection ranges of the introduced sensors are illustrated in Figure 1.1 (which is extracted from Ref. [31])

	Information provided	VMC	IMC	SWAP	Cost	Others
TCAS	Range Altitude	√	√	×	×	Well proven Widely used
ADS-B	Position Altitude Velocity	√	√	×	×	Well proven
SAR	Range Bearing	√	√	×	×	Typically poor accuracy
LIDAR	Range	√	√	×	×	Easy configuration Narrow FOV
EO system	Azimuth	√	×	√	√	Data link required
	Elevation					Lack of direct range
Acoustic system	Azimuth	√	×	√	√	Data link required
	Elevation					Lack of direct range Delay
IR system	Azimuth	√	×	√	√	Data link required
	Elevation					Lack of direct range

Note: SWAP: size, weight, and power; √: favorable/applicable; and ×: not favorable/applicable.

Table 1.2 - The characteristics of sensor technologies [31]

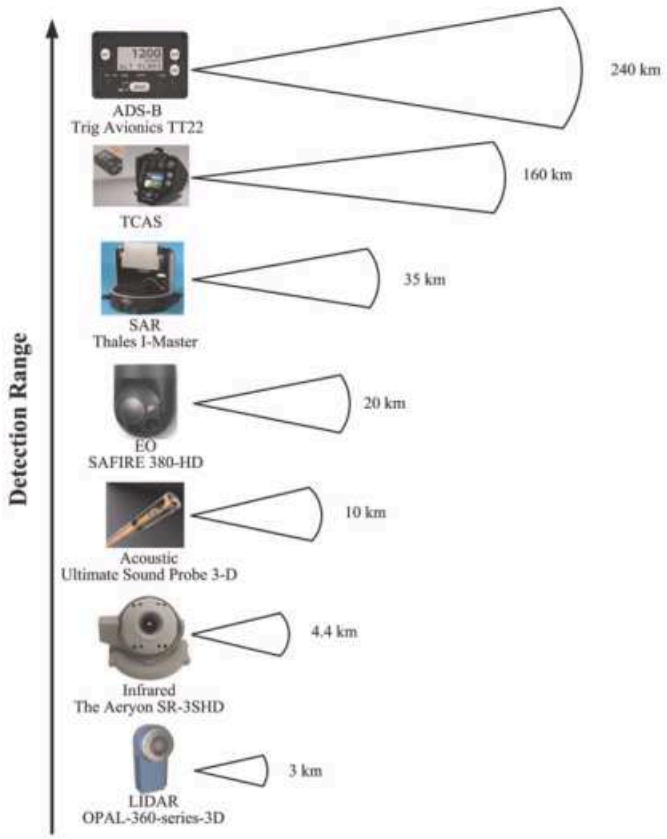

Figure 1.1 - Detection range of typical sensors [31]

Moreover in [32] are reported the mainly characteristics of most used sensors in SAA. They can be summarized as follows:

- Optical Sensors (Pixel/Visual):
  - Low cost, size and weight;
  - Suffer atmospheric disturbances;
  - A visual radar is highly comparable to a human's ability of observe (equal level of safety);
  - To achieve the required FOV, sensors have to be arrayed in various position on the aircraft, taking up valuable external area.
- Infrared Sensors:
  - Higher cost than EO;
  - Low size and weight;
  - Able to conduct nighttime operations;
  - Operate under harsh weather conditions;
  - To achieve the required FOV, sensors have to be arrayed in various position on the aircraft, taking up valuable external area;
  - Unable to pick up objects lacking some type of heat signature (cables or gliders);
  - Development and integration would be very costly.
- Microwave Radar (MMW Radar):
  - Very mature technology;
  - Detect intruder aircraft at great distances;
  - High size and weight.
- Laser Radar (LIDAR):
  - the size of the cone is very small and it makes possible to target a specific obstacle;
  - the revisit rate is poor and it takes multitude of laser sensors to achieve the same rate as a microwave radar;
  - extremely underdeveloped;
  - High cost;

- Inadequate in adverse weather (light can be absorbed and reflected).

1.4.5 SAA architectures and methods

During the latest years a great effort has been made, by industry and agencies in order to identify a technological solution that could satisfy an equivalent level of safety of manned aircraft. In the following, a review on the available SAA system architectures and algorithms is presented.

Regarding the "sense" function, for a sense-and-avoid system on UAVs, MIT Lincoln Laboratory developed the Airborne Sense and Avoid (ABSAA) Radar panel which is an unique light-weight sensor performing quick and repeatable scanning of the search region. The radar solution meets the all-weather and day/night requirements [33] - [34].This prototyping effort was focused on the General Atomics Predator B which nominally could carry 2 or 3 separate radar arrays to cover a total of 220° in azimuth and 30° in elevation [35]. Others radar approaches for the sense function can be found in [36] and [37]. In the first a prototype radar, for mini-UAV, is presented. This radar is able to differentiate other miniature rotorcraft by their Doppler signature. Moreover a performance analysis related to the signature matching algorithms is presented. The second introduces a radar technology and shows the test that have been performed in order to evaluate the performance of a digital beam forming concept associated with flood light illumination: it allows combining wide angle coverage, high velocity resolution, and high refresh rate.

Several different approaches have been considered in literature for vision-based flying object detection, ranging from optical flow to morphological filtering [38]. An emerging technologies based on the Active Electronically Scanned Array (AESA) couple the radar-based technology and EO systems: the EO system scans and records images while the radar is shifting through its various modes [39].

A visual approach is proposed by Zarandy A. et al. in [40]: their prototype uses 5 pieces of 1.2 Megapixel miniature cameras, an FPGA board with a Spartan 6 (XC6SLX45T), and a 128Gbyte Solid-State Disk drive for recording raw video data. The paper focus on image processing algorithms and it proves that the

designed system is able to identify 10 meter sized aircraft from at least 2000 meters under regular daylight image conditions.

Another vision-based approach is proposed by Fasano et al. in [41]: the obstacle detection and track confirmation are based on morphological filtering and on a local image analysis. The tracking is performed through a Kalman Filter in order to establish aircraft position and velocity. The proposed technique has been tested using flight data gathered in a sense and avoid research project carried out by the Italian Aerospace Research Center (CIRA) and the Department of Industrial Engineering of the university of Naples "Federico II"

Two devices based on electro-optical systems, in order to perform the "sense" function for a sense-and-avoid module, are reported in [42] and [43].

A trade analysis of EO sensors, used to provide a sense and avoid capability for Global Hawk, is reported in [44]. It is assumed that Global Hawk has three cameras, whose coverage do not overlap, that provide a FOV of ±100° by ±15°. The analysis suggested that the EO system is suitable for detecting larger aircraft but may not be ideal for detecting smaller aircraft with enough lead time for Global Hawk to avoid them.

Detection and tracking strategies based on acoustic array can be found in [45]÷[47]. These systems use array of microphones located on board an aircraft and a combination of narrow and broad band processing techniques to characterize the temporal variation of the received tone of an approaching aircraft and estimate its propeller blade rate, together with its speed and the time and distance to the closest point of approach.

Scientific Applications and Research Associates, Inc. (SARA) proposed an acoustic sensor for use on small UAVs. The Passive Acoustic Non-cooperative Collision Alert System (PANCAS) is characterized by a series of microphones mounted in order to compute bearing information for sound at each frequency. A proprietary algorithm is considered in order to minimize false alarms, due to fixed and random errors (atmospheric effects, wind effects, signal processing errors), and to determine the threshold to apply a collision avoidance manoeuver [48].

The sense-and-avoid system proposed by Ramasamy S. et al. (2014) [49] considers cooperative and non-cooperative sensors and it includes:

- Visual camera;
- Thermal camera;
- Lidar;
- MMW Radar;
- Acoustic Sensors;
- Transponder;
- ADS-B;
- TCAS/ACAS.

The avionic sensors and sensor decision tree is reported in Figure 1.2.

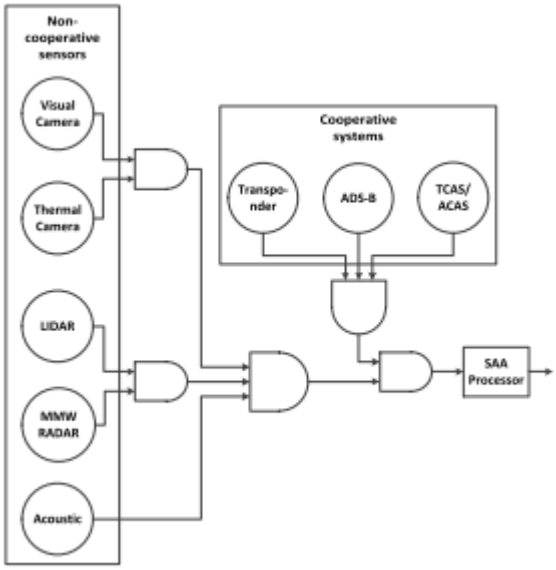

Figure 1.2- Avionic Sensors and Sensor Decision Tree proposed by Ramasamy S. et al [49]

Referring to non-cooperative sensors an high level tracking detection is performed by using a Kalman filter starting from the continuous cameras detection and range information provided by LIDAR. The Track-To-Track (T^3) algorithm is used for sensor fusion. This method combines the estimates instead of the observation from different sensors. The ADS-B system is used to obtain the state of the intruders and an Interacting Multiple Model (IMM) algorithm is considered for data fusion [50]. The risk of collision is, then, evaluated considering the probability of a near mid-air event for the predicted trajectory over the time horizon by employing Monte Carlo approximations. Finally the

volume that must be avoided by the host UAV can be obtained computing and combining the navigation and tracking error ellipsoids.

Another multi-sensor data integration for an autonomous sense-and-avoid system is reported in [51] and [52]. The suite of SAA sensors used is shown in Figure 1.3. The proposed system is called Multi-Sensor Integrated Conflict Avoidance (MuSICA) and the data integration is performed by an Extended Kalman Filter (EKF) and a measurements-to-track association. The collision avoidance algorithm is called Jointly Optimal Conflict Avoidance (JOCA) and it computes an optimal avoidance manoeuvre considering hierarchical constraints in order to make the maneuver as human-like as possible. JOCA hierarchical constraints are reported in Figure 1.4.

Figure 1.3 - SAA sensors proposed by Chen R. H. et al. in [51]

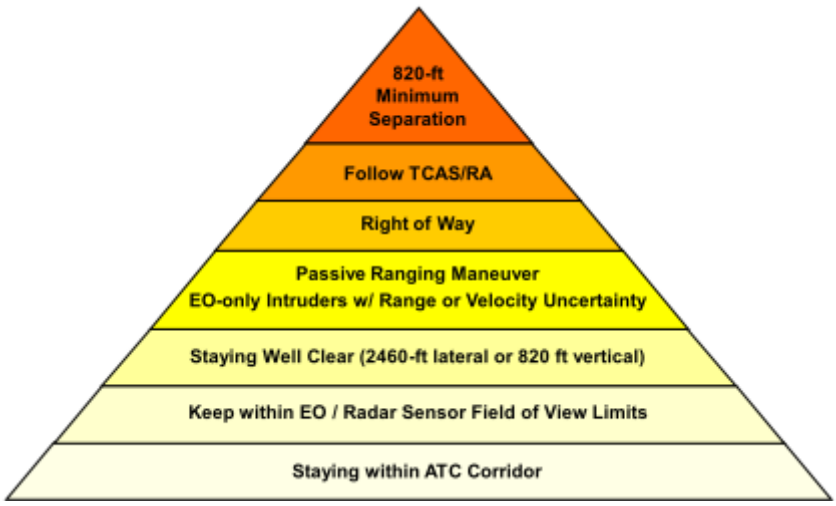

Figure 1.4 - JOCA hierarchical constraint as proposed by Graham S. et al. in [52]

In [53] a SAA algorithm based on the Laser Obstacle Avoidance Marconi (LOAM) system is proposed. LOAM system, developed and tested by SELEX-ES and the Italian Air Force Research and Flight Test Centre [30], is a low-weight/volume navigation aid system for rotary-wing/UA platform specially designed to detect potentially dangerous obstacles placed in or nearby the flight trajectory and to provide the crew with warnings and information of the detected obstacles. A laser beam scans periodically the area around the flight trajectory in the FOV and using a dedicated signal processing algorithms, optimized for low-level obstacle detection, the system provides obstacle shapes. Measurements uncertainties are taken into account, adding a Gaussian error to every data and computing a statistic of the position error for obstacles near and far from the aircraft. If a collision risk is established by the impact warning processing, a collision avoidance maneuver is computed having the smaller possible correction and which is compatible with a safe flight plan. Here too, an ellipsoidal avoidance volume is associated to the obstacle considering the two-sigma standard deviation of the total obstacle detection and tracking errors.

A SAA algorithm based on the surveillance data provided by electro-optical sensors and an airborne radar can be found in [54]. The conflict detection criterion is based on the definition of the closest point of approach and the resolution maneuver is computed considering the minimum variation from the original path. In particular, the collision volume is assumed to be spherical and the resolution maneuver is computed considering the tangent to that sphere. The sphere radius is related to the Near Mid-Air Collision (NMAC) parameter as defined in [55]: "A Near Mid-Air Collision is defined as an incident associated with the operation of an aircraft in which a possibility of collision occurs as a result of proximity of less than 500 feet to another aircraft, or a report is received from a pilot or a flight crew member stating that a collision hazard existed between two or more aircraft".

A sense-and-avoid system, which uses an ADS-B Transceiver, is reported in [56]-[57]. The collision detection algorithm considers the GPS position obtained by the ADS-B device and a threat is declared if an aircraft or a fixed obstacle is predicted to enter a collision or near collision course with the ownship aircraft within a certain time frame. The collision avoidance algorithm considers a

behavior-based approach derived from a guidance method developed for unmanned maritime vehicles. In particular, it represent a multi-objective optimization problems using a set of behavior that may include “Reach Target”, “Avoid Small Threats”, “Avoid Large Threats” and “Follow Right-of-Way Rules”. These behaviors may or may not produce objective functions for which a priority weighting is assigned. Objective function are defined considering a set of explicit constraints constructs representing the dynamic characteristics of the UAV: horizontal velocity, vertical velocity, and direction. Note that the behaviors are based on the closest point of approach. Hence, the sense-and-avoid algorithm uses interval programming (IvP) methods to balance objective functions for each behavior [58]. Concerning the avoidance volume computation, one possible assumption considers the turning and climb-descendent performance, creating a cylindrical volume. Another solution is to use time-based thresholds based on the definition of tau parameter [19].

A range-based method used to create dynamic alerting thresholds is reported in [59]. The relative dynamics of the incoming aircraft and the “sense” feature, are assumed to be evaluated through the ADS-B system. The alerting thresholds are defined based on the geometric relationship of the encounter and the UAV’s maneuvering ability and the four kinds of alarms include: “Dangerously Close”, “Perform Maneuver”, ”Vertical Maneuver” and “Super Maneuver Only”.

A collision avoidance approach, based on the conflict probing is presented in [60]. Conflict probing consists of predicting the future separation between ownship and hazards for a set of ownship velocity vectors, up to a predefined prediction horizon. The probing data indicates which velocity vectors will lead to a future conflict and the related time to conflict. Conflict probing can provide a common framework for the computation of coordinated conflict avoidance maneuvers that include integration of multiple types of hazards and constraints such as vehicle performance and right-of-way rules.

Another approach relying on the use of ADS-B data for trajectory prediction and conflict detection is proposed in [61]. The methodology addresses the problem from a probabilistic point of view aimed to assess the conflict probability based on the approximation of the conflict zone by a set of blocks.

The Mid-Air Collision Avoidance (MIDCAS) Project proposes a SAA system based on the data coming from a set of sensors comprising EO, IR, Radar, ADS-B and Transponder. The collision volume can be defined in two ways, starting from the NMAC parameter: the first one defines the collision volume as a spheroid with vertical half axis of *350 ft*, and horizontal half-axis of *500 ft*; the second defines the collision volume as a cylindrical volume centered on the UAV with a horizontal radius of *500 ft* and a vertical height of *200 ft*. the system shows threats information display and it computes an automated collision avoidance maneuver [62].

Finally, in Europe, the general aviation and UAVs are currently experiencing the introduction of other and cheaper cooperative means for conflict detection (as alternative to TCAS), such as FLARM [63]. Each FLARM device evaluates its position and altitude with a high precision GPS receiver. Based on other information, such as speed, acceleration, heading, track, a flight plan can be calculated and sent over a radio channel to all nearby aircraft equipped with FLARM too. Therefore, a motion prediction algorithm calculates a collision risk for each received aircraft based on an integrated risk model. The FLARM device gives the alerts to the pilot which can take resolutive actions. The newer FLARM incorporates a very accurate ADS-B and transponder (SSR) Mode-C/S receiver in order to include all the transponder equipped aircraft in the collision prediction algorithm.

Chapter 2

Automatic Dependent Surveillance – Broadcast

2.1 Introduction

The Automatic Dependent Surveillance – Broadcast (ADS-B) is a, relatively, new technology that has been under development several years before its recent adoption [64]. This technology was, actually, developed for support air traffic controllers improving the manned aircraft situational awareness: it was intended to replace the primary and secondary surveillance radars. However, it also appeared as a potential solution for the sense and avoid issue in UAVs.

2.2 ADS-B Description

The Automatic Dependent Surveillance - Broadcast is a cooperative surveillance technology. There are two main services related to this technology:

- ADS-B OUT service supports the air traffic data transmission between the aircraft and the ATC;
- ADS-B IN service supports the aircraft data transmission between the aircraft themselves.

The aircraft equipped with ADS-B OUT technology compute their own precise position through satellite-based GPS and automatically transmit these parameters. The information are broadcasted via a radio-link and can be received by ground operators or other aircraft equipped with ADS-B IN technology. The FAA identified two links for the transmission of data:

- Universal Access Transceiver (UAT) for general aviation users that operates at *978 MHz* UHF frequency;
- *1090 MHz* Mode S Extended Squitter (ES) for private or commercial operators.

The UAT data link is approved by FAA for use in all airspace except class A (above *18000 ft*) and it is intended to support also other services such as Flight Information Service – Broadcast (FIS-B) and Traffic Information Service – Broadcast (TIS-B). In this way UAT users can receive ground-based aeronautical data (FIS-B) and reports from proximate traffic (TIS-B) through a multilink gateway service that provides ADS-B reports for 1090ES-equipped aircraft and non-ADS-B equipped radar traffic. This physical layer is now available only in U.S. [65]. Moreover, through the ADS-R ground station it is possible to obtain on the UAT link the data of aircraft transmitting on *1090 MHz* link and vice versa: messages are crosslink translated from UAT to 1090ES and from 1090ES to UAT [66].

The existing mode S transponder supports a message type known as the Extended Squitter (ES) message that may includes ADS-B data. ATC ground station and aircraft equipped with TCAS already have the Mode S receiver and it would be enhanced in order to support the ES information exchange according to the TSO C–166B [67]. The technical link standards 1090ES does not support FIS-B service due to the bandwidth limitations of ES. In Europe there is not a physical layer for ADS-B and only the 1090ES link is used.

In both forms the position is updated, at least, once per second. There are many benefits related to the introduction of ADS-B including the followings [68]:

- ADS-B implementation improves situational awareness of pilots and air traffic controllers improving the shared information about the surrounding traffic;
- Aircraft that uses UAT link can receive weather reports and weather radar through FIS-B data;
- Aircraft that uses either UAT or 1090ES link can obtain NOTAMs and others flight information;
- ADS-B ground stations are cheaper compared to primary and secondary radar systems;
- ADS-B IN device is able to indicate traffic information with respect to targets that may be located up to even 200 nautical miles far awayfrom the device [69].

2.3 ADS-B Messages and Reports

This section describes the information broadcasted through ADS-B OUT devices according to REF DO-338 [67]. In the following it will be referred to ADS-B Message to indicate a block of data, that is formatted and transmitted, containing the information elements used to create ADS-B reports. On the other hand, an ADS-B Report contains the information elements, assembled by an ADS-B receiver, using messages received from a transmitting participant. Among all types of reports that may be assembled by the ADS-B IN device the followings will be considered:

- The Mode Status (MS) report contains operational information about the transmitting participant;
- The State Vector (SV) report contains information about an aircraft current kinematic state.

Reports may contain the following information:

1) *Time of Applicability* (TOA): it indicates the time at which the reported values were valid. Time of Applicability is provided in all reports. Note that the Time of Applicability of position measurements (TOAp) may differ from the Time of Applicability of velocity measurements (TOAv). The TOA field contains always the TOAp. Also TOAp and TOAv are transmitted in SV report.
2) Identification:
   - Call Sign/Flight ID: it is a message of 8 alphanumeric characters. For aircraft not receiving ATS services and military aircraft it is not required. It is reported in the MS report.
   - Participant Address and Address Qualifier: this message is necessary to differentiate a message transmitted by an A/V from another A/V. Aircraft with Mode-S transponders using ICAO 24 bit address shall use the same one for ADS-B; another kind of address is used otherwise. All A/Vs addresses must be unique in the operational domain. The Address Qualifier message indicates if the Address field contains the 24-bit ICAO address or another

kind of address. Both Participant Address and Address Qualifier are included in all ADS-B Reports.

- ADS-B Emitter Category: it is included in MS Report and it describes the type of A/V (i.e. Light, Small Aircraft, Large Aircraft).
- Mode 3/A Code: the ADS-B Transmitting Subsystem may have the capability to disable the transmission of this information. The broadcast of this information is only a transitional feature to support ATC automation systems but may be removed in future.

3) A/V Length and Width Codes: these messages describe the amount of space that an aircraft occupies. They are required to be transmitted by aircraft above a certain size and they are included in the MS report.
4) Position (it is included in the SV Report)
   - Geometric position referenced to the WGS-84 ellipsoid characterized by:
     - Horizontal position (latitude and longitude);
     - Geometric Height.
   - Barometric Pressure Altitude;
5) Horizontal Velocity:
   - Ground-referenced or geometric velocity: it is communicated in the SV Report;
   - Air-Referenced Velocity (ARV): it is communicate in the Air-Referenced Velocity report (out of the scope of this work);
6) Vertical Rate: it is reported in the SV Report. One of the two types of vertical rate (barometric and geometric) it is reported and it is obtained from the best source.
7) Heading: it indicates the orientation of A/V and it is described as an angle measured clockwise from magnetic north or true north (the reference direction is reported in the MS Report). The heading is communicated in the SV Report and in the ARV report.

8) Capability Class (CC) Code – used to indicate the capabilities of a transmitting ADS-B participant:
   - TCAS/ACAS Operational: the CC code shall be set to one if the TCAS/ACAS system is operational, otherwise it shall be set to zero;
   - 1090 MHz ES Receiver Capability: the CC code for "1090ES IN" shall be set to one if the transmitting aircraft has the capability to receive ADS-B 1090ES Messages, otherwise zero;
   - ARV Report Capability Flag;
   - Target State (TS) Report Capability Flag;
   - Trajectory Change (TC) Report Capability Level;
   - UAT Receive Capability: the CC code for "UAT IN" shall be set to zero if the aircraft is not fitted with the capability to receive ADS-B UAT Messages; otherwise one;
   - Other Capability Codes are expected to be defined in later versions of the MASPS.
9) Operational Mode (OM) Codes – used to indicate the current operating mode of a transmitting ADS-B participant.
   - TCAS/ACAS Resolution Advisory Active Flag: the CC code for "TCAS/ACAS Resolution Advisory Active" shall be set to zero i it is certain that the TCAS II or ACAS computer is not issuing a Resolution Advisory (RA); otherwise one.
   - IDENT Switch: it is a one-bit field that is activated by an IDENT switch. This flag shall be set to one for a period of 20±3 seconds, after it shall be reset to zero.
   - Reserved For Receiving ATC Services Flag: it a one-bit OM code and if it set to one indicates that the aircraft is receiving ATC services; otherwise it is set to zero;
   - Other Operational Mode Codes are expected to be defined in later versions of the MASPS.
10) Navigation Integrity Category (NIC): it specifies an integrity containment region. It is related to the Source Integrity Level (SIL)

that specifies the probability of the reports horizontal position exceeding the containment radius defined by the NIC without alerting, assuming no avionics faults. It is reports in the SV Report.

11) Navigation Accuracy Category for Position (NACp): it is used to describe the accuracy of position information in ADS-B Messages and it reported in the MS Report.
12) Navigation Accuracy Category for Velocity (NACv): it is used to describe the accuracy of velocity information in ADS-B Messages and it reported in the MS Report.
13) Source Integrity Level (SIL): it specifies the probability of the reports horizontal position exceeding the containment radius defined by the NIC without alerting, assuming no avionics faults. This probability is covered by the System Design Assurance (SDA) parameter.
14) Barometric Altitude Integrity Code (NIC_{BARO}): it is a one-bit flag that indicates if the barometric pressure altitude, in the SV Report, has been cross-checked against another source of pressure altitude. The NIC_{BARO} value is reported in the MS Report.
15) Emergency/Priority status: it is reported in MS Report.
16) Geometric Vertical Accuracy (GVA):it is a 2-bit field and it shall be set by using the Vertical Figure of Merit (VFOM)(95%) from the GNSS source used to report the geometric altitude.
17) TACAS/ACAS Resolution Advisory (RA) Data Block: the message subfields are specified in RTCA DO-185B [19].
18) ADS-B Version Number: it is a 3-bit field that specify the ADS-B Transmitting Subsystem Version.
19) Selected Altitude Type: it is a 1-bit field used to indicate the source of Selected Altitude data.
20) MCP/FCU (Mode Control Panel/Flight Control Unit) or FMS (Flight Management System) Selected Altitude Field: it is an 11-bit field that shall contain either MCP/FCU Selected Altitude or FMS Selected Altitude.

21) Barometric Pressure Setting (Minus 800 millibars) Field;
22) Selected Heading Status Field;
23) Selected Heading Sign Field;
24) Selected Heading Field;
25) State of MCP/FCU Mode Bits;
26) Mode Indicator: Autopilot Engaged Field: it is a 1-bit field that is set to zero if the Autopilot in not Engaged or Unknown; otherwise it is set to one.
27) Mode Indicator: VNAV (Vertical Navigation) Mode Engaged Field: it is a 1-bit field that is set to zero if the VNAV Mode is not Active or Unknown; otherwise it is set to one.
28) Mode Indicator: Altitude Hold Mode Field: it is a 1-bit field that is set to zero if the Altitude Hold Mode is not Active or Unknown; otherwise it is set to one.
29) Mode Indicator: Approach Mode Field: it is a 1-bit field that is set to zero if the Approach Mode is not Active or Unknown; otherwise it is set to one.
30) Mode Indicator: LNAV (Lateral Navigation) Mode Field: it is a 1-bit field that is set to zero if the LNAV Mode is not Active or Unknown; otherwise it is set to one.
31) Single Antenna Flag (SAF): it is a 1-bit field that indicates if the ADS-B transmitting Subsystem is operating with a single antenna (the field is then set to one, otherwise to zero). The conventions shall be applied both to Transponder-Based and Stand Alone ADS-B Transmitting Subsystem.
32) System Design Assurance: it is a 2-bit field that shall define the failure condition that the position transmission chain is designed to support.
33) GPS Antenna Offset: it is an 8-bit field that define the position of the GPS antenna in accordance with:
    - Lateral Axis GPS Antenna Offset shall be used to encode the lateral distance of the GPS Antenna from the longitudinal axis;

- Longitudinal Axis GPS Antenna Offset shall be used to encode the longitudinal distance of the GPS Antenna from the NOSE of the Aircraft.

2.4 ADS-B Regulations

The use of ADS-B in the U.S. NAS for surveillance application has been regulated by FAA in 2010 with some amendments to Part 91 [70]. In particular the FAA published the Final Rule for ADS-B Out equipage and it mandates performance requirements for ADS-B avionics that will be required to fly in certain airspace by 1th January 2020. Note that this rule does not mandate ADS-B IN device: a new Aviation Rulemaking Committee (ARC) was expected in June 2010 to decide ADS-B IN strategy. The designed frequencies are:

- 1090 MHz Extended Squitter (1090ES) for commercial aircraft and for all aircraft flying in Class A airspace (Flight Level 180 and above);
- Universal Access Transceiver 978 MHz (UAT) for general aviation and airport vehicles.

The final rule defines also the airspace where the ADS-B OUT will be mandated.

Since 2009, several standards and guidance have been published.

Regarding ICAO documents there are:

- ICAO DOC 9871 Technical Provisions for Mode S Services and External Squitter [71];
- ICAO DOC 9861 Manual on the Universal Access Transceiver (UAT) [72].

The FAA provided the following Advisory Circulars:

- AC 20-165 Airworthiness Approval of Automatic Dependent Surveillance - Broadcast (ADS-B) Out Systems [73];
- AC 90-114 Automatic Dependent Surveillance-Broadcast (ADS-B) Operations [74];
- AC 150/5220-26 Airport Ground Vehicle Automatic Dependent Surveillance – Broadcast (ADS-B) Out Squitter Equipment [75];

- AC 20-172A Airworthiness Approval for ADS-B In Systems and Applications [76].

The Technical Standard Order relate to the ADS-B service are:

- TSO-C166b Extended Squitter Automatic Dependent Surveillance - Broadcast (ADS-B) and Traffic Information Service - Broadcast (TIS-B) Equipment Operating on the Radio Frequency of 1090 Megahertz (MHz) [67];
- TSO-C154c, Universal Access Transceiver (UAT) Automatic Dependent Surveillance Broadcast (ADS-B) Equipment Operating on Frequency of 978 MHz [77];
- TSO-C195a, Avionics Supporting Automatic Dependent Surveillance – Broadcast (ADS-B) Aircraft Surveillance Applications (ASA) [78];

Concerning the RTCA documents there are:

- RTCA DO-260B Minimum Operational Performance Standards for 1090 MHz Extended Squitter Automatic Dependent Surveillance - Broadcast (ADS-B) and Traffic Information Services - Broadcast (TIS-B) [79];
- RTCA DO-282B Minimum Operational Performance Standards for Universal Access Transceiver (UAT) Automatic Dependent Surveillance - Broadcast (ADS-B) [80];
- RTCA DO-317B Minimum Operational Performance Standards (MOPS) for Aircraft Surveillance Applications (ASA) System [81];
- RTCA DO-249 Development and Implementation Planning Guide for Automatic Dependent Surveillance Broadcast (ADS-B) Applications [82];
- RTCA DO-242A Minimum Aviation System Performance Standards for Automatic Dependent Surveillance Broadcast (ADS-B) [83];
- RTCA DO-338 Minimum Aviation System Performance Standards (MASPS) for ADS-B Traffic Surveillance Systems and Applications (ATSSA) [66];

These and others documents can be found in [84].

ADSB-Out application in the Europe has been regulated with UE 1207/2011 [85].

2.5 Realities and Challenges in ADS-B system

Starting from 2020 FAA, as well as EUROCONTROL, have mandated ADS-B OUT in all aircraft as part of next generation air transportation systems NextGen and SESAR. The employment of such a system may lead several advantages such as [86]:

- Optimization of runway control/taxing improving the handling of aircraft on the ground (their position is known with high precision);
- Improvement of accuracy and ATC safety during take-off and landing;
- Reduction of mid-air collision risk;
- Introduction of UAV in NAS permitting the SAA function with high precision.

Nevertheless, a lot of challenges still remains related to the integration of ADS-B system.

An analysis carried out by Strohmeier et al. in [87], identified two relevant problems:

- In dense airspace the ADS-B system is affected by message collisions, especially when only the *1090 MHz* link is used (i.e. in Europe). The message collisions causes the most high loss rate: with few aircraft the loss rate is of about 10 percent but it rises over 45 percent with 60 ADS-B transmitter participants. This is due to the fact that not only Ads-B operates on *1090 MHz* link and a solution would be improving the channel capacity.
- There are security issues related to ADS-B. In fact, ADS-B is an open-source and it is susceptible to radio frequency attack as reported in [88]÷[90]. For example it is possible to modify the aircraft virtual trajectory, delete all ADS-B messages sent by a particular aircraft or modify the identifier of a particular aircraft.

A solution to these problems can be found in [91]: a means to increase the bandwidth capacity, through a modification of access and access protocol, is proposed together with a means for protection of flight path in terms of authentication and encryption on the data link.

Further analysis on the limitations of the ADS-B technology for the application on unmanned aerial systems has been carried out in [92], where the use of ADS-B based only surveillance on-board of small remotely piloted vehicles is considered not suitable and the fusion with electro-optical sensors is suggested as mostly mandatory.

More in particular a detailed analysis on the challenges related to a SAA system based on the displayed ADS-B data is reported in [93]. First of all requirements on the position quality have to been established. In fact, although some performance requirements are stated in DO-317B for some application, such as the enhanced visual acquisition, the performance for a SAA system must have superior. Moreover, the position information will not be available for aircraft not equipped with ADS-B or from aircraft that do not meet accuracy and integrity requirements. Also the data coming from the ground stations suffers problems such as availability, that may be limited in several ways, and low quality related mostly on the rebroadcast of data. Also the ADS-B receiver and message processing requirements have to be defined with an high level of design in order to assure the required level of safety. Finally also the availability and quality of ownship data and the Surveillance Processing are critical in the use of ADS-B data because all the surveillance and the relevant ownship data comes together to be processed for display and application-specific functions. Requirements have to be defined too. Nevertheless, it is reported that “The FAA has plans to expand the capability of ADS-B to include more advanced applications using delegated separation and/or collision avoidance. […] This work plan recognizes the need for development of increasingly complex ADS-B traffic applications from “Traffic Situation Awareness with Alerts” to “ADS-B Integrated Collision Avoidance” and even “Self Separation””.

Chapter 3
System Description

3.1 Introduction

The ADS-B surveillance data can be used as input for conflict detection algorithms in order to support future self-separation as well as collision avoidance systems. In particular the proposed conflict detection algorithm is based on the received data, of all ADS-B Out equipped aircraft, by the on-board ADS-B In device.

The overall proposed system architecture aims to manage the ADS-B raw data in order to provide the on-board application, with an usable structured database with all the available information about the surrounding traffic. The such obtained information is sent to a conflict detection algorithm and, subsequently, the tracks are prioritized in terms of the most relevant threat. The obtained data can be send to a CDTI display to support the pilot, incrementing the situational awareness, or can be used for conflict resolution algorithms.

It is worth to note that, the proposed system, for tests scope, has been involved in a conflict resolution architecture for an unmanned aircraft but, as mentioned before, it can be used also in manned applications. The conflict resolution module is out of the scope of this work.

In order to test the developed system a model of the software has been implemented in Matlab and Simulink R2009A.

3.2 Software Architecture description

The functional architecture of the proposed system is reported in Figure 3.1.

The four main module are:

- Surveillance Processing Module;

- Coarse Filter Module;
- Conflict Detection Module;
- Prioritization Module.

The ADS-B IN incoming data are sent to a Surveillance Module that generate a traffic database, containing information such as position, velocity ad participant address, with a number *M* of multiple targets. The obtained data are subject to a pre-filter in order to delete from the database the aircraft which are too far away from ownship (more details are shown in the following), reducing the number of tracks in the database to *N*. Among all the obtained tracks, the conflict detection module evaluates which ones represent a conflict to the ownship leading to *P,* the number of relevant tracks. Also in this case the number of aircraft *P* can be equal to *N*. Finally, a prioritization module gives information about the most relevant threat.

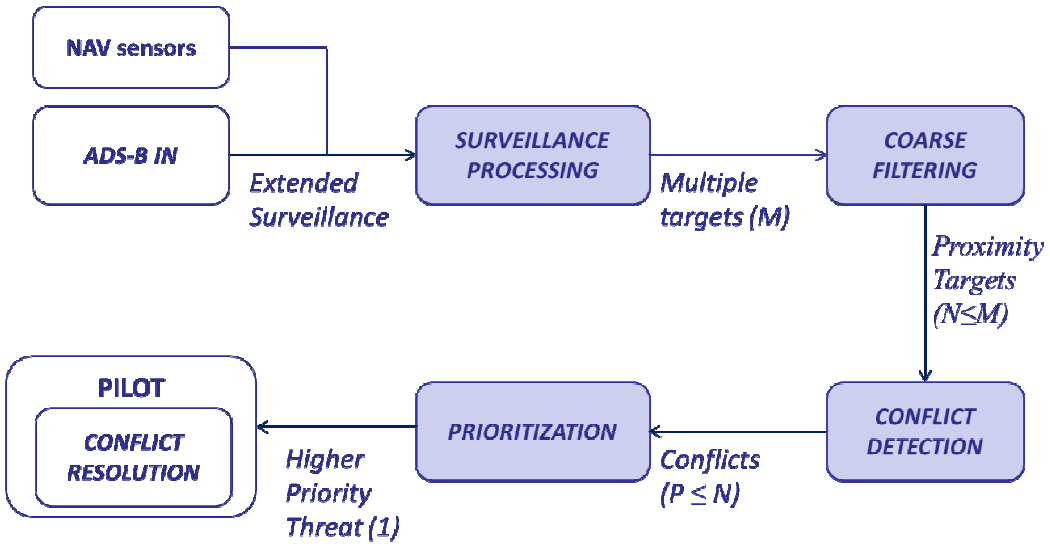

Figure 3.1 – Architecture of the Proposed System

3.3 Surveillance Processing algorithm

The Surveillance Processing module is in charge of re-elaborating the raw data coming from the ADS-B In device in order to create an air traffic database usable by on-board applications. In other words, starting from the ownship navigation data and traffic ADS-B broadcasted information, it is possible to

generate a traffic state file database easily usable by the pilot or other applications. The implemented Surveillance Processing functionalities are based on RTCA-317A Appendix C specifications [94] but they are adapted to be useful in the framework of the particular application under study. Figure 3.2 shows a functional architecture of Surveillance Processing.

Considering that:

- only the 1090MHz communication link is enabled (the only link available in Europe);
- the ADS-R and TIS-B reports are not available;

the following functionalities are implemented:

- Track Generation and Maintenance;
- Track Termination;
- Common Time Track Extrapolation;
- Traffic State File Generation.

Figure 3.2 shows an high level Simulink Architecture of Surveillance Processing.

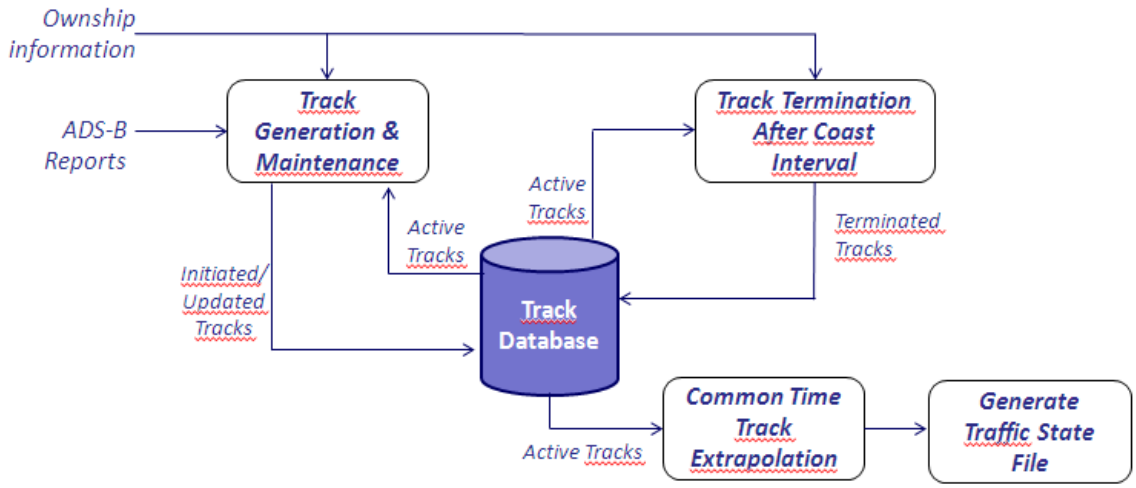

Figure 3.2 – Surveillance Processing Architecture

3.3.1 Track Generation and Maintenance

Track Generation and Maintenance module is responsible for track initiation and subsequent updates.

The module operates differently based on the received report type.

Upon a reception of a *Mode Status* report, the module searches, into a database, for a stored track with the same 24-bit address:

- If no match is found the report shall be discarded;
- If a match is found NACp, NACv, and SIL values, and the other variables related to Mode Status report, in the track shall be updated with the values in the report.

The logic adopted when a *State Vector* report is received, is shown in high level flow chart in

Figure 3.3 - SV report reception - high level flow chart of generation and maintenance module

.

Upon a reception of a *State Vector* report, the module search for a stored track with the same 24-bit address as the report; there are two possible ways to operate:

1. If no match is found a new track could be generated. To generate a new track, the sentences *a.* and *b.* shall be both verified:
    a. The measurements in the reports shall be valid:
        i. if the target is airborne, the validity flags of Geometric Altitude, Horizontal Position, Vertical Rate and Horizontal Velocity are considered;
        ii. if the target is on the ground the validity flags of Geometric Altitude, Horizontal Position, and Ground Speed are considered;
    b. Two consecutive reports of the same track shall correlate: upon the reception of a new report, the latter is recorded but not stored into the database. If a consecutively incoming report correlates with the first, according to the same validation and correlation criterion used for the updating of a track into the database and discussed in the following, the new track is generated and stored into the database. Otherwise, the first report is discarded and the incoming one is recorded without generating a new track.

    When a new track is generated track it is automatically validated and can be considered as reference track for the incoming new reports.

2. If a match is found, and the track has been previously validated, the validity of the incoming report is checked, as shown in paragraph 3.3.1.1.

   If the report validity checks are passed, the module could update an existing track state component through the state assembly function, otherwise the report is rejected.

   The assembly function could generate a filtered state vector through position or velocity measurements:

   - if the target position measurements and velocity measurements are valid the generation and maintenance module could update the state vector through position or velocity measurements based on the most recent measurement;
   - if the target position measurements are valid but the Velocity Measurements are invalid, the module could generate an assembled state vector through position measurements;
   - if the target Velocity Measurements are valid but the Position measurements are invalid, the module could generate an assembled state vector through velocity measurements.

   In any of the previous cases, to effectively generate an assembled state vector, the measurement time of applicability, of the position or velocity depending on the case, shall be greater than the time of applicability of the stored track but lower than the time of applicability of ownship measurement data. Simultaneously the assembled state vector calculation, also the assembled uncertainties are computed on the basis of the uncertainties related to the measurements and the ones related to the stored track. The state filtering equation are presented in the paragraphs 3.3.1.2.2 and 0. It is worth nothing that, when a match is found the stored track position and velocity are extrapolated to the time of applicability of the incoming report according to the paragraph 3.3.1.2.

   If none of the previous condition is verifies the report is discarded and it is not considered for update.

Once the assembled state vector has been computed, the track update is performed if spatial correlation occurs, detailed equations can be found in paragraph 3.3.1.3.

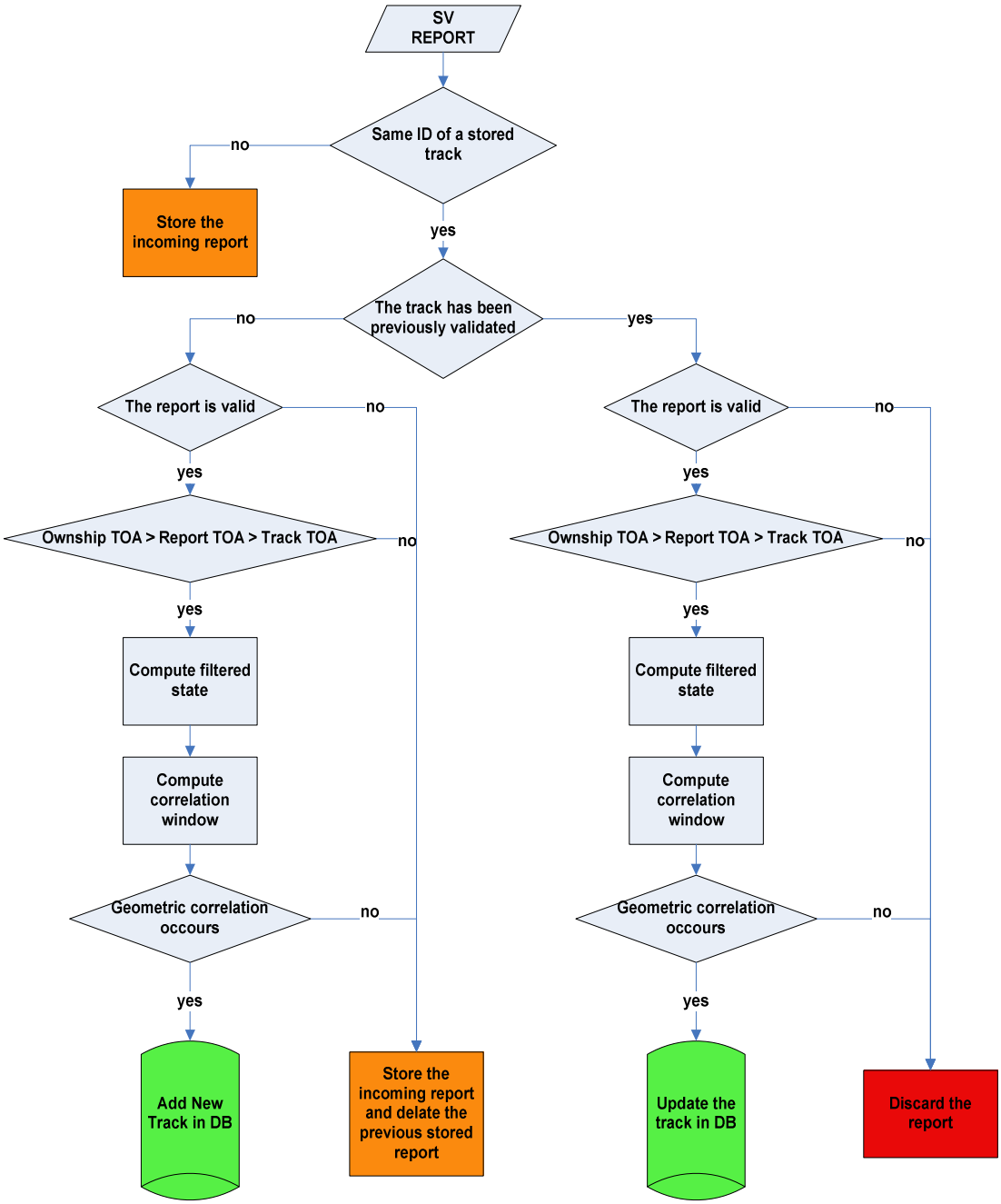

Figure 3.3 - SV report reception - high level flow chart of generation and maintenance module

Therefore, if spatial correlation occurs the module updates the track and in particular the state vector and uncertainties with the assembled state and assembled uncertainties, the time of applicability of the stored track with the time of applicability used to generate the assembled state, and all the other variables related to the State Vector report with the values in the report.

If spatial correlation fails the state vector report is discarded.

3.3.1.1 Reports validity checks

The performed report validity checks are different based on the indication of validity flag of the incoming measurements:

1. If position measurements and velocity measurements are valid the module performs an horizontal velocity validation, an horizontal position validation and a vertical position validation.
2. If the report contains only valid position measurements the horizontal position validation and vertical position validation are performed.
3. Finally if only velocity measurements are valid the horizontal velocity validation is performed.

The report validation criteria, according to RTCA 317 [94] Appendix D, are the following.

Horizontal velocity validation

$$|V_1 - V_0| < 2 \cdot V_u + A \cdot T \quad (1)$$

Where, considering an ENU reference frame:

- V_0 is the last validated velocity on the horizontal plane;
- V_1 is the velocity on the horizontal plane, contained in the report to be validated;
- V_u is the velocity uncertainty;
- A is assumed to be 14.7 m/s^2 as reported in [94] Appendix D;
- T is the time difference between the incoming report and the last validated velocity report.

Horizontal position validation

$$D < 4 \cdot K + (V + 2 \cdot V_u) \cdot T + 0.5 \cdot A \cdot T^2 \quad (2)$$

Where, considering an ENU reference frame:

- D is the horizontal distance between the last validated position and the one contained in the report to be validated;
- K is the horizontal position uncertainty at 95%;
- V is the magnitude of reported velocity;
- V_u, A are the same of above;
- T is the time difference between the incoming report and the last validated position report.

Vertical position validation

$$|A_1 - A_0| < 250\,ft + 10000\,fpm \cdot \frac{T}{60} \quad (3)$$

Where:

- A_0 is the last validated altitude;
- A_1 is the altitude contained in the report to be validated;
- T is the time difference between the incoming report and the last validated altitude report.

3.3.1.2 State Estimation: the Kalman Filter

In order to produce an accurate estimation of the track state recorded into the database, a Kalman filter is implemented. The filter is based on a constant velocity model of the intruders.

3.3.1.2.1 Prediction

The stored track position and velocity are predicted to the time of applicability of the incoming report according to the Eq.(4). A constant velocity dynamic model, for the target, has been adopted but more information about target dynamic models can be found in [95].

$$
\begin{aligned}
\hat{x}_{t_k} &= x_{t_{k-1}} + \dot{x}_{t_{k-1}} \cdot \Delta t \\
\hat{y}_{t_k} &= y_{t_{k-1}} + \dot{y}_{t_{k-1}} \cdot \Delta t \\
\hat{z}_{t_k} &= z_{t_{k-1}} + \dot{z}_{t_{k-1}} \cdot \Delta t \\
\hat{\dot{x}}_{t_k} &= \dot{x}_{t_{k-1}} \\
\hat{\dot{y}}_{t_k} &= \dot{y}_{t_{k-1}} \\
\hat{\dot{z}}_{t_k} &= \dot{z}_{t_{k-1}}
\end{aligned}
\tag{4}
$$

Where:

- $\left(x_{t_{k-1}}, y_{t_{k-1}}, z_{t_{k-1}}\right)$ is the position, in local ENU coordinates, of the track stored into the database and related to the last update;
- $\left(\dot{x}_{t_{k-1}}, \dot{y}_{t_{k-1}}, \dot{z}_{t_{k-1}}\right)$ is the velocity, in local ENU coordinates, of the track stored into the database and related to the last update;
- Δt is the time difference between the report time and the time of the last track update.

Also the covariance matrix is predicted according to the Eq. (5).

$$
\begin{aligned}
\sigma^2_{\hat{x}_{t_k}} &= \sigma^2_{x_{t_{k-1}}} + (\Delta t)^2 \sigma^2_{\dot{x}_{t_{k-1}}} + 2dt\sigma_{x\dot{x}_{t_{k-1}}} + \frac{Q(\Delta t)^4}{4} \\
\sigma^2_{\hat{\dot{x}}_{t_k}} &= \sigma^2_{\dot{x}_{t_{k-1}}} + (\Delta t)^2 Q \\
\sigma_{\hat{x}\hat{\dot{x}}_{t_k}} &= \sigma_{x\dot{x}_{t_{k-1}}} + (\Delta t)\sigma^2_{\dot{x}_{k-1}} + \frac{Q(\Delta t)^3}{3} \\
\sigma^2_{\hat{y}_{t_k}} &= \sigma^2_{y_{t_{k-1}}} + (\Delta t)^2 \sigma^2_{\dot{y}_{t_{k-1}}} + 2\Delta t\sigma_{y\dot{y}_{k-1}} + \frac{Q(\Delta t)^4}{4} \\
\sigma^2_{\hat{\dot{y}}_{t_k}} &= \sigma^2_{\dot{y}_{t_{k-1}}} + (\Delta t)^2 Q \\
\sigma_{\hat{y}\hat{\dot{y}}_{t_k}} &= \sigma_{y\dot{y}_{t_{k-1}}} + (\Delta t)\sigma^2_{\dot{y}_{t_{k-1}}} + \frac{Q(\Delta t)^3}{3} \\
\sigma^2_{\hat{z}_{t_k}} &= \sigma^2_{z_{t_{k-1}}} + (\Delta t)^2 \sigma^2_{\dot{z}_{t_{k-1}}} + 2\Delta t\sigma_{z\dot{z}_{t_{k-1}}} + \frac{Q(\Delta t)^4}{4} \\
\sigma^2_{\hat{\dot{z}}_{t_k}} &= \sigma^2_{\dot{z}_{t_{k-1}}} + (\Delta t)^2 Q \\
\sigma_{\hat{z}\hat{\dot{z}}_{t_k}} &= \sigma_{z\dot{z}_{t_{k-1}}} + (\Delta t)\sigma^2_{\dot{z}_{t_{k-1}}} + \frac{Q(\Delta t)^3}{3}
\end{aligned}
\tag{5}
$$

Where Q is the process noise variance and it is assumed to be $0.065g^2$ as reported in [94] Appendix C.

The initial covariance matrix can be computed as:

$$\begin{pmatrix} \sigma^2_{x_{t0}} & \sigma_{x\dot{x}_{t0}} \\ \sigma_{x\dot{x}_{t0}} & \sigma^2_{\dot{x}_{t0}} \end{pmatrix} = \begin{pmatrix} \sigma^2_{epu} & \sigma_{epu}\sigma_{hva} \\ \sigma_{epu}\sigma_{hva} & \sigma^2_{hva} \end{pmatrix}$$
$$\begin{pmatrix} \sigma^2_{y_{t0}} & \sigma_{y\dot{y}_{t0}} \\ \sigma_{y\dot{y}_{t0}} & \sigma^2_{\dot{y}_{t0}} \end{pmatrix} = \begin{pmatrix} \sigma^2_{epu} & \sigma_{epu}\sigma_{hva} \\ \sigma_{epu}\sigma_{hva} & \sigma^2_{hva} \end{pmatrix} \quad (6)$$
$$\begin{pmatrix} \sigma^2_{z_{t0}} & \sigma_{z\dot{z}_{t0}} \\ \sigma_{z\dot{z}_{t0}} & \sigma^2_{\dot{z}_{t0}} \end{pmatrix} = \begin{pmatrix} \sigma^2_{vepu} & \sigma_{vepu}\sigma_{vva} \\ \sigma_{vepu}\sigma_{vva} & \sigma^2_{vva} \end{pmatrix}$$

Where [96]:

- σ_{epu} is the standard deviation of estimated position uncertainty and it is derived from NACp according to Table 3.1;
- σ_{vepu} is the standard deviation of vertical estimated position uncertainty and it is derived from NACp according to Table 3.1;
- σ_{hva} is the standard deviation of horizontale velocity accuracy and it is derived from NACv according to Table 3.2;
- σ_{vva} is the standard deviation of vertical velocity accuracy and it is derived from NACv according to Table 3.2.

NAC_P	**95% Horizontal and Vertical Accuracy Bounds (EPU and VEPU)**	**Comment**
0	EPU ≥ 18.52 km (10 NM)	Unknown accuracy
1	EPU < 18.52 km (10 NM)	RNP-10 accuracy
2	EPU < 7.408 km (4 NM)	RNP-4 accuracy
3	EPU < 3.704 km (2 NM)	RNP-2 accuracy
4	EPU < 1852 m (1NM)	RNP-1 accuracy
5	EPU < 926 m (0.5 NM)	RNP-0.5 accuracy
6	EPU < 555.6 m (0.3 NM)	RNP-0.3 accuracy
7	EPU < 185.2 m (0.1 NM)	RNP-0.1 accuracy
8	EPU < 92.6 m (0.05 NM)	e.g., GPS (with SA)
9	EPU < 30 m and VEPU < 45 m	e.g., GPS (SA off)
10	EPU < 10 m and VEPU < 15 m	e.g., WAAS
11	EPU < 3 m and VEPU < 4 m	e.g., LAAS

Table 3.1 – Navigation Accuracy Category for Position

NAC_V	Horizontal Velocity Accuracy (95%)	Vertical Geometric Velocity Accuracy (95%)
0	Unknown or ≥ 10 m/s	Unknown or ≥ 50 feet (15.24 m) per second
1	< 10 m/s	< 50 feet (15.24 m) per second
2	< 3 m/s	< 15 feet (4.57 m) per second
3	< 1 m/s	< 5 feet (1.52 m) per second
4	< 0.3 m/s	< 1.5 feet (0.46 m) per second

Table 3.2 – Navigation Accuracy Category for velocity

3.3.1.2.2 State Filtering with position updates

Let us consider the innovation variances computed as follows:

$$\begin{aligned}\sigma_{v_x}^2 &= \sigma_{\hat{x}}^2 + \sigma_{epu}^2 \\ \sigma_{v_y}^2 &= \sigma_{\hat{y}}^2 + \sigma_{epu}^2 \\ \sigma_{v_z}^2 &= \sigma_{\hat{z}}^2 + \sigma_{vepu}^2\end{aligned} \tag{7}$$

where:

- $\left(\sigma_{\hat{x}}^2, \sigma_{\hat{y}}^2, \sigma_{\hat{z}}^2\right)$ are predicted track position variances;
- σ_{epu} and σ_{vepu} are defined as above and related to the measurements of the incoming report.

The filtered state can be computed as follows:

$$\begin{aligned}x_a &= \hat{x} + k_{0x}\left(x_m - \hat{x}\right) \\ y_a &= \hat{y} + k_{0y}\left(y_m - \hat{y}\right) \\ z_a &= \hat{z} + k_{0z}\left(z_m - \hat{z}\right) \\ \dot{x}_a &= \hat{\dot{x}} + k_{1x}\left(x_m - \hat{x}\right) \\ \dot{y}_a &= \hat{\dot{y}} + k_{1y}\left(y_m - \hat{y}\right) \\ \dot{z}_a &= \hat{\dot{z}} + k_{1z}\left(z_m - \hat{z}\right)\end{aligned} \tag{8}$$

where $\left(x_m, y_m, z_m\right)$ are the measured positions, and the gain vectors are computed as:

$$k_{0x} = \frac{\sigma_{\hat{x}}^2}{\sigma_{v_x}^2}; \quad k_{1x} = \frac{\sigma_{\hat{x}\hat{\dot{x}}}}{\sigma_{v_x}^2}$$
$$k_{0y} = \frac{\sigma_{\hat{y}}^2}{\sigma_{v_y}^2}; \quad k_{1y} = \frac{\sigma_{\hat{y}\hat{\dot{y}}}}{\sigma_{v_y}^2} \tag{9}$$
$$k_{0z} = \frac{\sigma_{\hat{z}}^2}{\sigma_{v_z}^2}; \quad k_{1y} = \frac{\sigma_{\hat{z}\hat{\dot{z}}}}{\sigma_{v_z}^2}$$

Also the assembled state covariance matrices are computed according to Eq.10-12.

$$\begin{aligned}\sigma_{xa}^2 &= (1-k_{0x})\sigma_{\hat{x}}^2 \\ \sigma_{x\dot{x}a} &= (1-k_{0x})\sigma_{\hat{x}\hat{\dot{x}}} \\ \sigma_{\dot{x}a}^2 &= \sigma_{\hat{\dot{x}}}^2 - k_{1x}\sigma_{\hat{x}\hat{\dot{x}}}\end{aligned} \tag{10}$$

$$\begin{aligned}\sigma_{ya}^2 &= (1-k_{0y})\sigma_{\hat{y}}^2 \\ \sigma_{y\dot{y}a} &= (1-k_{0y})\sigma_{\hat{y}\hat{\dot{y}}} \\ \sigma_{\dot{y}a}^2 &= \sigma_{\hat{\dot{y}}}^2 - k_{1y}\sigma_{\hat{y}\hat{\dot{y}}}\end{aligned} \tag{11}$$

$$\begin{aligned}\sigma_{za}^2 &= (1-k_{0z})\sigma_{\hat{z}}^2 \\ \sigma_{z\dot{z}a} &= (1-k_{0z})\sigma_{\hat{z}\hat{\dot{z}}} \\ \sigma_{\dot{z}a}^2 &= \sigma_{\hat{\dot{z}}}^2 - k_{1z}\sigma_{\hat{z}\hat{\dot{z}}}\end{aligned} \tag{12}$$

3.3.1.2.3 State Filtering with velocity updates

In the case of velocity updates, the innovation variances can be computed as follows:

$$\begin{aligned}\sigma_{v_x}^2 &= \sigma_{\hat{\dot{x}}}^2 + \sigma_{hva}^2 \\ \sigma_{v_y}^2 &= \sigma_{\hat{\dot{y}}}^2 + \sigma_{hva}^2 \\ \sigma_{v_z}^2 &= \sigma_{\hat{\dot{z}}}^2 + \sigma_{vva}^2\end{aligned} \tag{13}$$

where:

- $\left(\sigma_{\hat{\dot{x}}}^2, \sigma_{\hat{\dot{y}}}^2, \sigma_{\hat{\dot{z}}}^2\right)$ are extrapolated track velocity variances;
- σ_{hva} and σ_{vva} are defined as above.

As in the previous case, it is possible to define the gain vectors as:

$$k_{0x} = \frac{\sigma_{\hat{x}\hat{\dot{x}}}}{\sigma^2_{\nu_x}}; \quad k_{1x} = \frac{\sigma^2_{\hat{\dot{x}}}}{\sigma^2_{\nu_x}}$$
$$k_{0y} = \frac{\sigma_{\hat{y}\hat{\dot{y}}}}{\sigma^2_{\nu_y}}; \quad k_{1y} = \frac{\sigma^2_{\hat{\dot{y}}}}{\sigma^2_{\nu_y}} \tag{14}$$
$$k_{0z} = \frac{\sigma_{\hat{z}\hat{\dot{z}}}}{\sigma^2_{\nu_z}}; \quad k_{1x} = \frac{\sigma^2_{\hat{\dot{z}}}}{\sigma^2_{\nu_z}}$$

The filtered status and covariances are computed as shown in Eq. 15-18.

$$\begin{aligned} x_a &= \hat{x} + k_{0x}\left(\dot{x}_m - \hat{\dot{x}}\right) \\ y_a &= \hat{y} + k_{0y}\left(\dot{y}_m - \hat{\dot{y}}\right) \\ z_a &= \hat{z} + k_{0z}\left(\dot{z}_m - \hat{\dot{z}}\right) \\ \dot{x}_a &= \hat{\dot{x}} + k_{1x}\left(\dot{x}_m - \hat{\dot{x}}\right) \\ \dot{y}_a &= \hat{\dot{y}} + k_{1y}\left(\dot{y}_m - \hat{\dot{y}}\right) \\ \dot{z}_a &= \hat{\dot{z}} + k_{1z}\left(\dot{z}_m - \hat{\dot{z}}\right) \end{aligned} \tag{15}$$

$$\begin{aligned} \sigma^2_{xa} &= \sigma^2_{\hat{x}} - k_{0x}\sigma_{\hat{x}\hat{\dot{x}}} \\ \sigma_{x\dot{x}a} &= (1 - k_{1x})\sigma_{\hat{x}\hat{\dot{x}}} \\ \sigma^2_{\dot{x}a} &= (1 - k_{1x})\sigma^2_{\hat{\dot{x}}} \end{aligned} \tag{16}$$

$$\begin{aligned} \sigma^2_{ya} &= \sigma^2_{\hat{y}} - k_{0y}\sigma_{\hat{y}\hat{\dot{y}}} \\ \sigma_{y\dot{y}a} &= (1 - k_{1y})\sigma_{\hat{y}\hat{\dot{y}}} \\ \sigma^2_{\dot{y}a} &= (1 - k_{1y})\sigma^2_{\hat{\dot{y}}} \end{aligned} \tag{17}$$

$$\begin{aligned} \sigma^2_{za} &= \sigma^2_{\hat{z}} - k_{0z}\sigma_{\hat{z}\hat{\dot{z}}} \\ \sigma_{z\dot{z}a} &= (1 - k_{1z})\sigma_{\hat{z}\hat{\dot{z}}} \\ \sigma^2_{\dot{z}a} &= (1 - k_{1z})\sigma^2_{\hat{\dot{z}}} \end{aligned} \tag{18}$$

where $(\dot{x}_m, \dot{y}_m, \dot{z}_m)$ are the measured velocities.

3.3.1.3 Spatial Correlation

In order to ensure that the incoming report represents an updated measurement of the stored track, a spatial correlation test is performed. The spatial correlation window is computed based on an estimated maximum distance

between two positions. In particular is possible to estimate the maximum horizontal (r_h) and vertical (r_v) distances between the filtered and the track position; note that in Eq.16 σ'_{epu} and σ'_{vepu} are computed through Table 3.1 using NACp-1.

Therefore, the spatial correlation is proved if $d_h < r_h$ and $d_v < r_v$ where:

- $d_h = \sqrt{(x_a - x)^2 + (y_a - y)^2}$ is the horizontal distance between filtered and track horizontal position;
- $d_v = |z_a - z|$ is the vertical distance between filtered and track horizontal position.

3.3.2 Track Termination algorithm

The *Track Termination* function deletes from the database, the tracks whose time of applicability of the last correlated report is higher than a predefined threshold. The threshold used in this application is 15s according to TSAA target discontinuation threshold [97]-[98].

Moreover, this time interval is the needed time to exit the safety bubble in the hypothesis that the intruder aircraft need to cover the max dimension of the safety bubble. This statement will be better explained in paragraph 3.5.1.

3.3.3 Common Time Track Extrapolation algorithm

The *Common Time Track Extrapolation* function extrapolates all the track, recorded into the database, at a common time of applicability. In particular, all the tracks are extrapolated at ownship data time of applicability. In this way the position and velocities of the surrounding aircraft are updated to the current time and can provide the pilot, CDTI or any other application, with the most recent data. The extrapolation process is performed assuming that the tracks are moving with constant velocity:

$$\begin{aligned} \bar{x} &= x_t + \dot{x}_t dt \\ \bar{y} &= y_t + \dot{y}_t dt \\ \bar{z} &= z_t + \dot{z}_t dt \end{aligned} \tag{19}$$

$$\begin{aligned} \bar{\dot{x}} &= \dot{x}_t \\ \bar{\dot{y}} &= \dot{y}_t \\ \bar{\dot{z}} &= \dot{z}_t \end{aligned} \tag{20}$$

where:

- $(\bar{x}, \bar{y}, \bar{z})$ are the tracks extrapolated positions;
- $(\bar{\dot{x}}, \bar{\dot{y}}, \bar{\dot{z}})$ are the tracks extrapolated velocities;
- dt is the time difference between the ownship data time of applicability and the last updated time of applicability of the tracks.

3.3.4 Traffic state file generation algorithm

The *Traffic state file generation* function adapts the database in order to remove from database all the information not needed for the specific application under study. In other words, among all the information communicated by the ADS-B device only a subset is maintained. For this application the saved information is:

- target latitude, longitude and geometric altitude;
- target Participant address;
- target north velocity, east velocity and vertical rate;
- target data time of applicability;
- number of stored reports.

3.4 Coarse Filtering algorithm

As mentioned in the previous Chapter, the ADS-B In device can receive information about aircraft that may be located vary far from the ownship up to 40 nautical miles. Of course if the distance is too large the targets should not represent a real possible threat for the ownship but in the case of separation and of a possible conflict.

For this reason the *Coarse filtering* function is in charge to delete from database all the aircraft which are far from the ownship more than a predefined threshold. However the threshold cannot be excessively reduced due to the need

of assuring in any case enough time for the eventual implementation of a resolution manoeuver [54].

Therefore, the threshold value is computed considering two aircraft with an head-on approach geometry and a cruise velocity of 55m/s for each aircraft (this is a common value for general aviation).

Moreover, considering a collision avoidance look ahead time of 35s [99]-[100], the range threshold is assumed equal to 4000m.

$$R = \dot{r} \cdot dt = 110 \cdot 35 = 3850m \rightarrow R_T = 4000m$$

3.5 Conflict detection algorithm

The tracks resulting from the coarse filter module are sent to the *Conflict detection* module which performs the pair-wise check on the conflict condition between them and the ownship. The conflict condition applied is based on the distance at the closest point of approach ($\vec{d}_{AB}$), between the ownship and the specific aircraft, and on the closure rate ($\dot{r}$). This criterion is usually used in literature [54].

The ownship and the intruder are modelled as a point-of-mass object A and B respectively, with three degree of freedom and velocity $\vec{V}_A$ and $\vec{V}_B$. The predicted trajectory of both ownship and intruder, is a straight line propagation according to the velocity $\vec{V}_A$ and $\vec{V}_B$, respectively. The relative velocity is computed as:

$$\vec{V}_{AB} = \vec{V}_A - \vec{V}_B \tag{21}$$

The conflict criterion is based on the implementation of a safety bubble centred in the intruder aircraft, with a nominal radius set according to FAA minimum required safety distance $R_0 = 500ft \approx 152.4m$. So the intruder aircraft became a spherical object centred in the point-of-mass modelling the intruder.

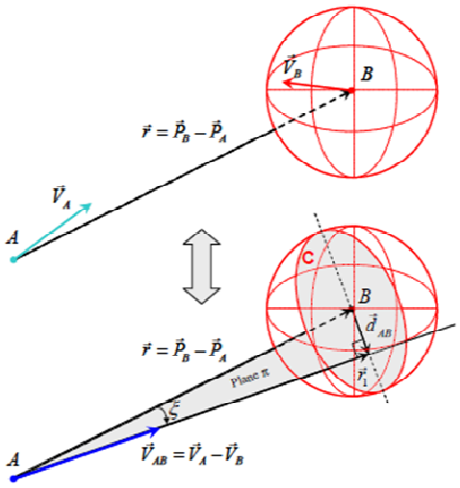

Figure 3.4 – Ownship-Intruder geometry (Figure extracted from [54])

Therefore, the implemented conflict condition is:

$$\left\|\vec{d}_{AB}\right\| < R \quad \text{and} \quad \dot{r} < 0 \tag{22}$$

where:

- $\vec{d}_{AB} = \dfrac{\vec{r} \cdot \vec{V}_{AB}}{\left\|\vec{V}_{AB}\right\|^2} \vec{V}_{AB} - \vec{r}$;
- $R = R_0 + R_{extra}$ is the safety bubble radius equal to the minimum value with in addition a suitable extra size to be determined;
- $\dot{r} = \dfrac{\vec{r} \cdot \vec{V}_{AB}}{\left\|\vec{r}\right\|}$.

Note that $\vec{r}$ is the position of the intruder in the relative reference system centred in the ownship.

The extra-size radius is introduced in order to take into account the relative motion between the ownship and the intruder aircraft, or the uncertainties about traffic position and velocity measurements. Two possible way are introduced, in the following, in order to compute the extra-size radius R_{extra}. The choice of the method to integrate in the software architecture, will follow the performance test reported in the next chapter.

3.5.1 Extra-size Radius computation: time-to-go approach

The first method proposed for the computation of the safety bubble extra-size radius, is based on the closure rate $\dot{r}$. In particular the safety bubble radius can be computed as:

$$R = R_0 + k \cdot \dot{r} \tag{23}$$

Where k is a parameter (with time dimension) whose value has to be set. In the application under study this value is set to 5s that is a mean value between the value used along the horizontal direction (8s) and the vertical direction (2s) in the TSAA application [97]. This assumption can be considered valid because the safety bubble has been assumed with spherical shape so there are not differences along the two directions.

Note that, considering an head-on conflict geometry between the ownship and an intruder aircraft, with both aircraft moving at 55m/s the closure rate is $\dot{r} = 110 m/s$. The safety radius is:

$$R = R_0 + k \cdot \dot{r} \approx 152.4 + 5 \cdot 110 \approx 702 m \tag{24}$$

Considering that the velocity of the intruder aircraft is 55m/s, it will take about 13s to cover 702m. Therefore, in order to be conservative the maximum data age for this application, introduced in paragraph 3.3.2, is of 15s.

3.5.2 Extra-size Radius computation: uncertainties approach

The second method proposed for the computation of the extra-size safety bubble is related to the broadcast of two information such as the NACp and NACv parameters related to each report. Those parameters give information regarding the accuracy of the incoming position and velocity measurements. In particular, the horizontal and vertical accuracy (σ), at 95%, can be computed referring to Table 3.1 for what concerns the position measurements, and to Table 3.2 for the velocity measurements.

In this case the safety radius is defined as:

$$R = R_0 + \sigma_{\Delta d_{cpa}} \tag{25}$$

where $\sigma_{\Delta d_{cpa}}$ is the variance of d_{cpa} estimate. It possible to verify that the closest point of approach can be computed as in Eq. 26.

$$\left\| d_{cpa} \right\| = \sqrt{\left(r_x^2 + r_y^2 + r_z^2 \right) - \frac{\left(r_x V_x + r_y V_y + r_z V_z \right)^2}{\left(V_x^2 + V_y^2 + V_z^2 \right)}} \tag{26}$$

The differential of d_{cpa} is:

$$\begin{aligned} \Delta d_{cpa} = & \left(\frac{\partial d_{cpa}}{\partial r_x} \cdot \right)^2 \Delta r_x + \left(\frac{\partial d_{cpa}}{\partial r_y} \right)^2 \cdot \Delta r_y + \left(\frac{\partial d_{cpa}}{\partial r_z} \right)^2 \cdot \Delta r_z + \\ & + \left(\frac{\partial d_{cpa}}{\partial V_x} \right)^2 \cdot \Delta V_x + \left(\frac{\partial d_{cpa}}{\partial V_y} \right)^2 \cdot \Delta V_y + \left(\frac{\partial d_{cpa}}{\partial V_z} \right)^2 \cdot \Delta V_z \end{aligned} \tag{27}$$

Where:

$$\begin{aligned} \frac{\partial d_{cpa}}{\partial r_x} &= \frac{1}{a} \left(r_x - \frac{b}{c} \cdot V_x \right) \\ \frac{\partial d_{cpa}}{\partial r_y} &= \frac{1}{a} \left(r_y - \frac{b}{c} \cdot V_y \right) \\ \frac{\partial d_{cpa}}{\partial r_z} &= \frac{1}{a} \left(r_z - \frac{b}{c} \cdot V_z \right) \end{aligned} \tag{28}$$

$$\frac{\partial d_{cpa}}{\partial V_x} = \frac{1}{a}\left[\frac{b}{c^2}\left(-r_x c + V_x b\right)\right]$$
$$\frac{\partial d_{cpa}}{\partial V_y} = \frac{1}{a}\left[\frac{b}{c^2}\left(-r_y c + V_y b\right)\right] \tag{29}$$
$$\frac{\partial d_{cpa}}{\partial V_z} = \frac{1}{a}\left[\frac{b}{c^2}\left(-r_z c + V_z b\right)\right]$$

$$a = \sqrt{\left(r_x^2 + r_y^2 + r_z^2\right) - \frac{\left(r_x V_x + r_y V_y + r_z V_z\right)^2}{\left(V_x^2 + V_y^2 + V_z^2\right)}}$$
$$b = r_x V_x + r_y V_y + r_z V_z \tag{30}$$
$$c = V_x^2 + V_y^2 + V_z^2$$

The variance can be computed as:

$$\begin{aligned}\mathrm{var}\left[\Delta d_{cpa}\right] = &\frac{\partial d_{cpa}}{\partial r_x}\mathrm{var}\left[\Delta r_x\right] + \frac{\partial d_{cpa}}{\partial r_y}\mathrm{var}\left[\Delta r_y\right] + \frac{\partial d_{cpa}}{\partial r_z}\mathrm{var}\left[\Delta r_z\right] + \\ &+ \frac{\partial d_{cpa}}{\partial V_x}\mathrm{var}\left[\Delta V_x\right] + \frac{\partial d_{cpa}}{\partial V_y}\mathrm{var}\left[\Delta V_y\right] + \frac{\partial d_{cpa}}{\partial V_z}\mathrm{var}\left[\Delta V_z\right] = \sigma^2_{\Delta d_{cpa}}\end{aligned} \tag{31}$$

The values $\mathrm{var}\left[\Delta r_x\right], \mathrm{var}\left[\Delta r_y\right], \mathrm{var}\left[\Delta r_z\right], \mathrm{var}\left[\Delta V_x\right], \mathrm{var}\left[\Delta V_y\right], \mathrm{var}\left[\Delta V_z\right]$ can be computed with NACp and NACv values through Table 3.1 and Table 3.2.

3.6 Prioritization algorithm

As result of conflict detection module, multiple conflicts can be detected. In fact, more than one aircraft may pose a conflict to the ownship. For this reason a proper prioritization criterion has to be implemented. The aim of this module is to define the most dangerous vehicle.

The prioritization criterion is strictly connected to the conflict detection algorithm and in particular to the dimensioning of the safety bubble radius.

Therefore, two possible approaches are presented related to the two safety bubble dimensioning introduced above.

3.6.1 Prioritization criterion: time-to-go approach

The first method presents a prioritization criterion based on the closure rate. This criterion is a simplification of the ACAS *tau* parameter evaluation [99]-[100].

In particular, the time-to-go (*TTG*) parameter is defined as [100]:

$$TTG = \frac{r}{\dot{r}} \tag{32}$$

Therefore, the aircraft with lower *TTG* has higher priority respect to the ones with higher *TTG*. The priority target (*PT*) is therefore:

$$PT = \min\left(\frac{r}{\dot{r}}\right) = \min(TTG) \tag{33}$$

3.6.2 Prioritization criterion: uncertainties approach

As mentioned in paragraph 3.5.2, the safety bubble radius can be computed adding to the nominal radius a value equal to the standard deviation of the distance at the closest point of approach σ. It is possible to perform the conflict detection check with respect to three spheres which surround the intruder aircraft:

$$\begin{aligned} R_1 &= R_0 + \sigma \\ R_2 &= R_0 + 2\sigma \\ R_3 &= R_0 + 3\sigma \end{aligned} \tag{34}$$

In the hypothesis of normal distribution, it is possible to compute the three probabilities of conflict related to three volumes. The first probability is related to the sphere with radius:

$$R = R_0 + \sigma \tag{35}$$

The second volume is the space included between the sphere at 1σ and the one at 2σ. The third volume is included between the sphere at 2σ and the one at 3σ. Therefore the conflict probabilities (*CP*) can be computed as:

$$\begin{aligned} CP_1 &= P\{1\sigma\} = 0.6827 \\ CP_2 &= P\{2\sigma\} - P\{1\sigma\} = 0.9545 - 0.6827 = 0.2718 \\ CP_3 &= P\{3\sigma\} - P\{2\sigma\} = 0.9973 - 0.9545 = 0.0428 \end{aligned} \tag{36}$$

The prioritization criterion is then:

$$PT = \max\left(CP \cdot \frac{\dot{r}}{r} \right) = \max\left(CP \cdot inv(TTG) \right) \tag{37}$$

The *TTG* is included as a scale factor in order to take into account the approaching geometry.

Note that, with this method, the extra-size value is related to the measurement uncertainties and so to the NACp and NACv values.

Chapter 4
Implementation and Test

4.1 Introduction

This section will show the algorithm modelling, the simulation environment and the main test scenarios and related results.

In particular in the first part, a description of the algorithms, introduced above, will be presented.

In the second part, tests will be shown in order to verify the effectiveness working of the surveillance processing and in order to assess one of the two methods, explained in the previous chapter, of conflict detection and prioritization.

In the third part, the assessed software architecture will be inserted in an more complex system to support a conflict resolution algorithm. Note that the conflict resolution algorithm is out of the scope of this work and more information can be found in [54]. Therefore offline test scenarios will be described and the results will be shown and discussed.

The last part will be about the real-time simulation tests. Therefore a description of the facility will be shown. Further the test scenarios will be presented and the related results will be discussed.

4.2 Sense and Detect Algorithm modelling

The overall system architecture, and related algorithms, discussed in the previous chapter have been modelled in Matlab and Simulink R2009A.

4.2.1 Surveillance Processing Simulink Scheme

Figure 4.6 shows the implemented Simulink scheme modelling the Surveillance Processing algorithms. The represented scheme is slightly different

from the one in Figure 3.2 but it is possible to identify the main modules descripted in the previous chapter. In particular:

- The "*GenAndMain1090*" block (Figure 4.1) implements, as a unique Matlab function, all the functionalities introduced in the paragraph 3.3.1 and related sub-paragraph. In particular it is in charge of generate new tracks into the database and update the existing ones.

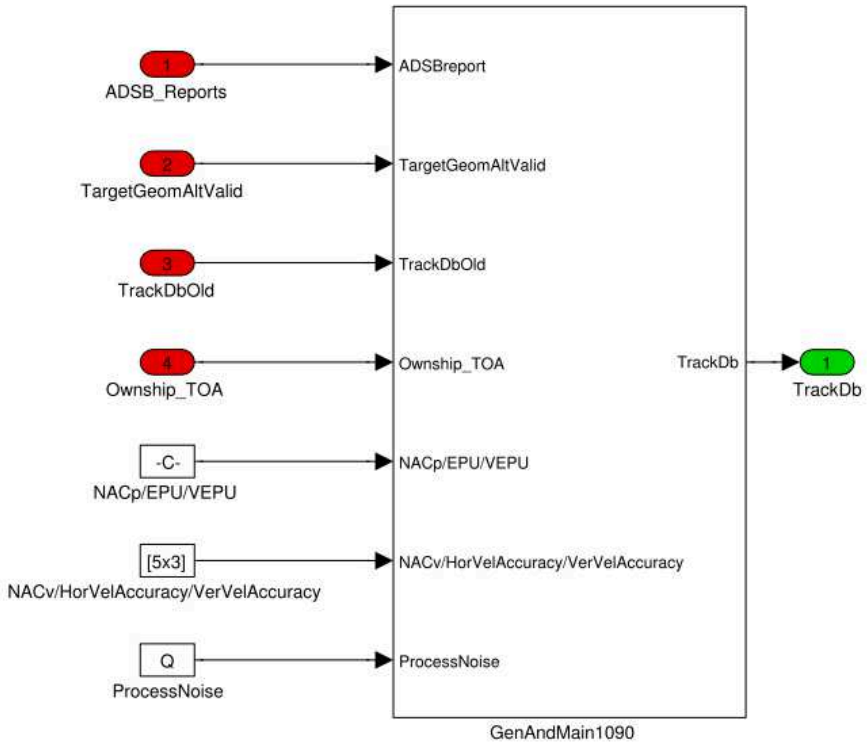

Figure 4.1- Generation And Maintenance Simulink Scheme

The input variables of this module are explained in the following:

- *ADSB_Reports* is a bus containing all the ADS-B traffic information;
- *TargetGeomAltValid* is a vector related to the validity flag of the available geometric altitude value. Note that the Generation and Maintenance module works only with geometric altitude and the validity flag is managed by another block explained in the following;
- *TrackDbOld* is a bus representing the track database used in the closed loop with a one-step delay. This feedback signal is

used to updated the stored track and to add new track into the database;

- *Ownship_TOA* is a constant value related to the time of applicability of ownship position and velocity measuraments;
- *NACp/Epu/Vepu* is a matrix implementing Table 3.1;
- *NACv/HorVelAccuracy/VerVelAccuracy* is a matrix implementing Table 3.2;
- *Q* is a constant tunable variable related to the process noise. As mentioned above, for this application it is assumed to be $0.065g^2$ according to [94] Appendix C.

The output variable *TrackDb* is a bus representing the track database.

- The *"TrackTermination"* block is a Matlab function that updates the database according to the track termination algorithm introduced in the paragraph 3.3.2 and it is represented in Figure 4.2.

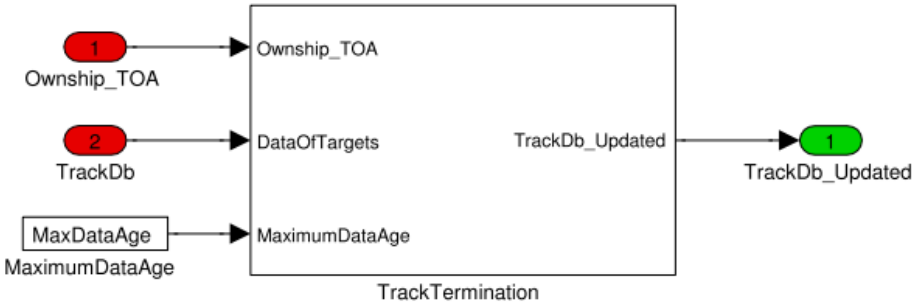

Figure 4.2 - Track Termination Simulink Scheme

The input variables are the following:

- *Ownship_TOA* that is a constant value related to the time of applicability of ownship position and velocity measuraments;
- *TrackDb* which is a bus containing the tracks information;
- *MaximumDataAge* that is a tunable parameter, which represents the maximum elapsed time, from the last update before the track has been deleted from the database.

The output bus *TrackDb_Updated* contains all the tracks that are available at the current time.

- The "*CommonTimeTrackExtrapolation*" block is a Matlab function that implements the functionality described in the paragraph 3.3.3, that is the extrapolation of traffic data to a common time of applicability. The Simulink scheme is represented in Figure 4.3.

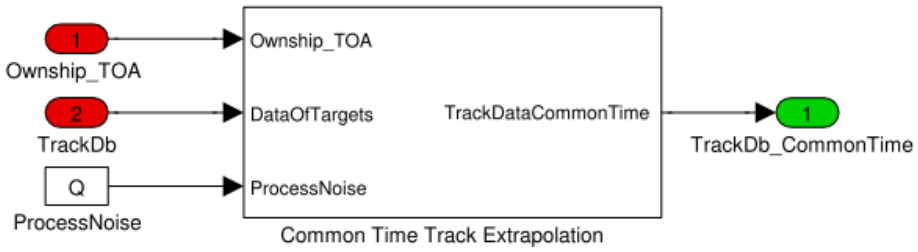

Figure 4.3 - Common Time Track Extrapolation Simulink Scheme

The input variables are:

- *Ownship_TOA* that is a constant value related to the time of applicability of ownship position and velocity measuraments;
- *TrackDb* which is a bus containing the tracks information;
- *Q* that is a constant tunable variable related to the process noise. As mentioned above, for this application it is assumed to be $0.065g^2$ according to [94] Appendix C.

The output bus *TrackDb_CommonTime* contains all the tracks extrapolated to a common time of applicability.

As mentioned above, the Generation and Maintenance module works with geometric altitude information. Nevertheless, this information is not always available and a dedicated module is introduced. The *"BaroAltitude2WGS84"* block is a Matlab function, represented in Figure 4.4, which implements the follow functionalities:

- If the ADS-B provide a track with a valid pressure altitude measurement and an invalid geometric altitude measurement, the module computes the geometric altitude based on the valid pressure altitude. Note that in this case also the geometric altitude measurement becomes "valid".
- If the ADS-B provide a track with a valid geometric altitude measurement and an invalid pressure altitude measurement, no conversion is performed.

- If the ADS-B provide a track with a valid geometric altitude measurement and a valid pressure altitude measurement, no conversion is performed.
- If the ADS-B provide a track with an invalid geometric altitude measurement and an invalid pressure altitude measurement, no conversion is performed.

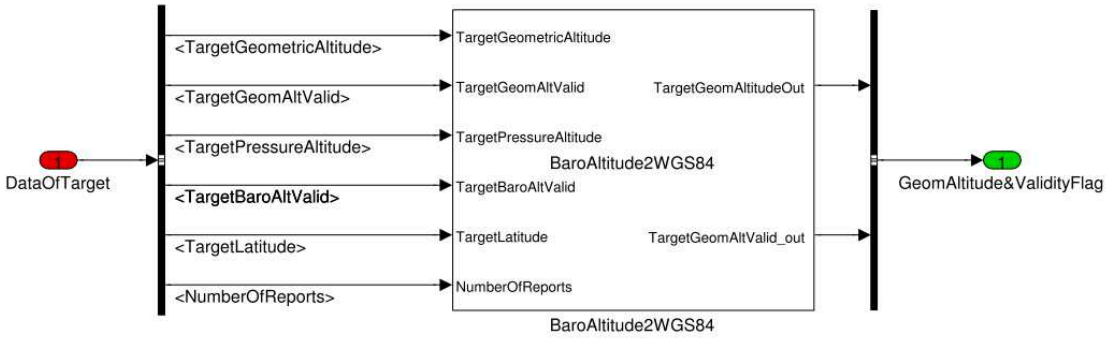

Figure 4.4 - Barometric Altitude to Geometric Altitude conversion Simulink Scheme

Only a subset of the traffic information is used for this computation and in particular:

- The targets geometric altitude field;
- The targets geometric altitude validity flag field;
- The targets barometric altitude field;
- The targets barometric altitude validity flag field;
- The targets latitude field;
- The number of reports field;

The output bus includes information about the targets geometric altitude and related validity flag.

The *"SelectValidatedTrack"* subsystem selects, among all the stored track, the ones that can be considered valid, and that can be recorded into the database, according to the track validation criterion described in the paragraph 3.3.1.

The *"Out_DatabaseCreation"* subsystem, represented in Figure 4.5, selects the traffic data useful for the application under study. In particular the information that are selected are:

- The targets latitude in WGS84 reference frame;

- The targets longitude in WGS84 reference frame;
- The targets geometric altitude in WGS84 reference frame;
- The targets east velocity in WGS84 reference frame;
- The targets north velocity in WGS84 reference frame;
- The targets vertical rate in WGS84 reference frame;
- The targets data time of applicability;
- The targets participant address;
- The number of tracks stored into the database.

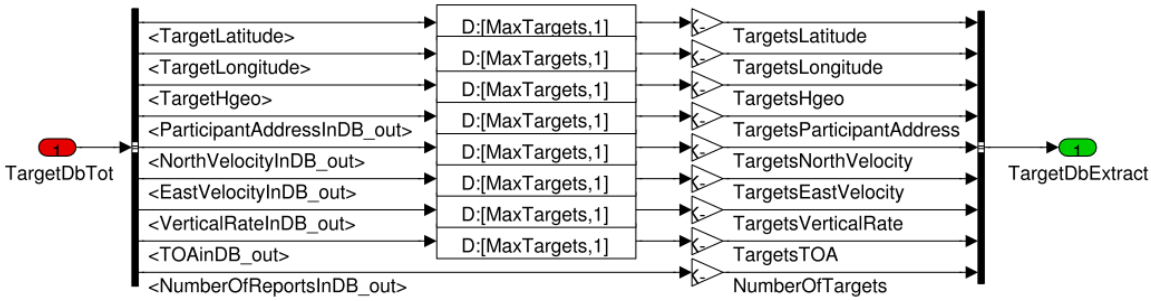

Figure 4.5 - Out Database Creation Simulink Scheme

The remaining blocks *LLH2ENU_REPORTS, LLH2ENU_DB, ENU2LLH_UnitDelay* and *ENU2LLH*, have been introduced to perform the needed reference frame conversions: this makes it possible to feed the main blocks with a more suitable data structure.

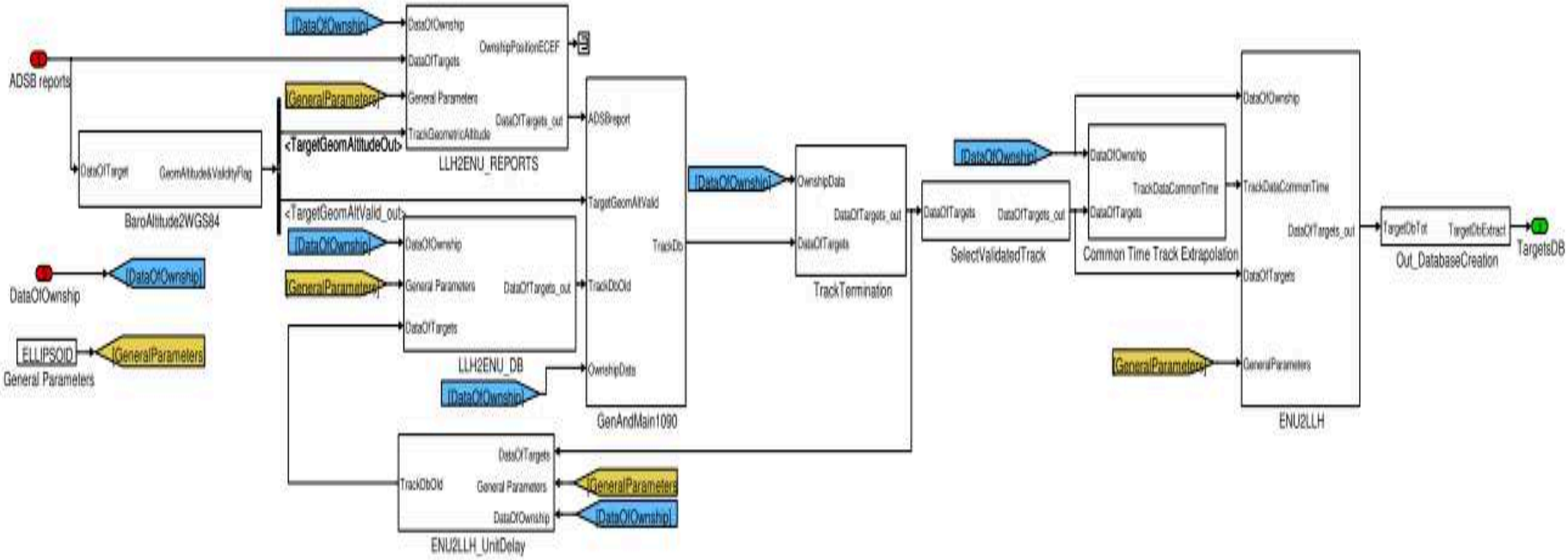

Figure 4.6 - Surveillance Processing Simulink Scheme

4.2.2 Coarse Filtering: Simulink Scheme

The coarse filtering Simulink block is represented in Figure 4.7. It implements the functionalities explained in section 3.4.

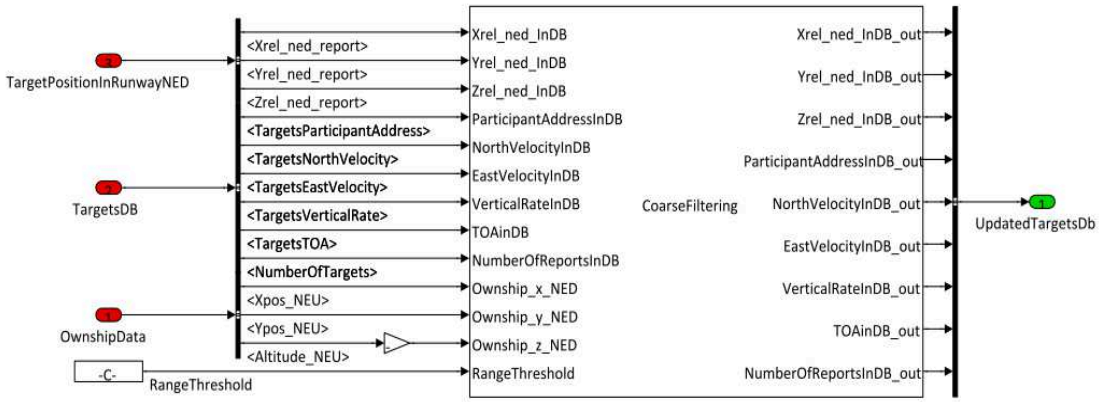

Figure 4.7 – Coarse Filtering Simulink Scheme

The input data are:

- A bus which identifies the targets position in a local NED reference frame;
- A bus which includes he targets east velocity, north velocity, vertical rate and participant address;
- A bus related to the ownship position in the local NED reference frame;
- A constant tunable value which identifies the coarse filter range threshold.

The out variable is a bus which includes all the traffic information of the aircraft whose distance from the ownship is lower than the specified threshold.

4.2.3 Conflict detection and prioritization Simulink scheme: time-to-go approach

The conflict detection and prioritization Simulink modules, based on the time-to-go approach, are represented in Figure 4.8 and Figure 4.9. the implemented algorithms are described in paragraphs 3.5, 3.5.1 and 3.6.1.

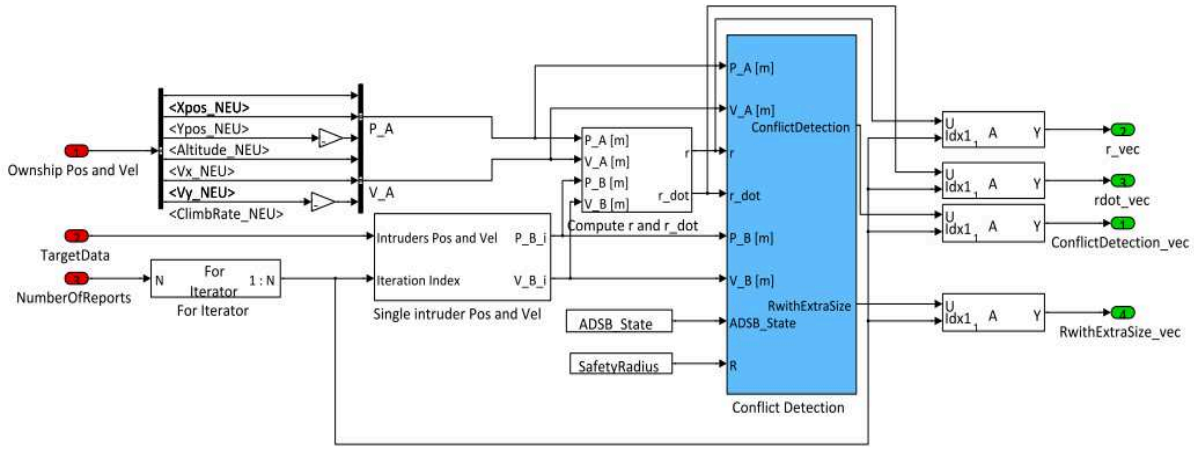

Figure 4.8 – Conflict Detection Simulink Scheme

The input variables for the conflict detection subsystem are:

- *Ownship Pos and Vel* which is a bus related to the ownship position and velocity in a NED reference frame;
- *TargetData* that is a bus including traffic information and among them the targets position and velocity;
- *NumberOfReports* that represents the number of track contained into the database.

The output variables are:

- *r_vec* which is a vector including the relative distance between the ownship and each aircraft in the database;
- *rdot_vec* which is a vector representing the closure rate between the ownship and each aircraft in the database;
- *ConflictDetection_vec* which is a vector of Boolean values: the value is 1 if the considered aircraft pose a conflict to the ownship, otherwise the value is 0;
- *RwithExtraSize_vec* which is a vector including the safety bubble radius, with extra-size, related to each intruder aircraft.

Those variables, excluding the extra-size radius, are the input variables for the prioritization subsystem. The others input variables, for prioritization module, are the bus related to the track database *TargetsDB* and the *ParticipantAddress_vec* that is a vector including the participant addresses of

aircraft stored into the database. The two main subsystems of the prioritization module are:

- *Compute_InvTTG* which evaluates the inverse of TTG for each aircraft into the database;
- *findConflictIndex* that selects among all the track available into the database the one with the high priority.

Therefore, the module outputs are:

- *ConflictDetectionIndex* which is a boolean value indicating if at least one aircraft, among the ones recorded into the database, poses a conflict to the ownship;
- *r_conflict* that is the relative distance between the ownship and the most dangerous threat;
- *rdot_conflict* that is the closure rate between the ownship and the most dangerous threat;
- *ConflictIndex* which is a row index in order to identify the most dangerous threat among all the aircraft stored into the database.

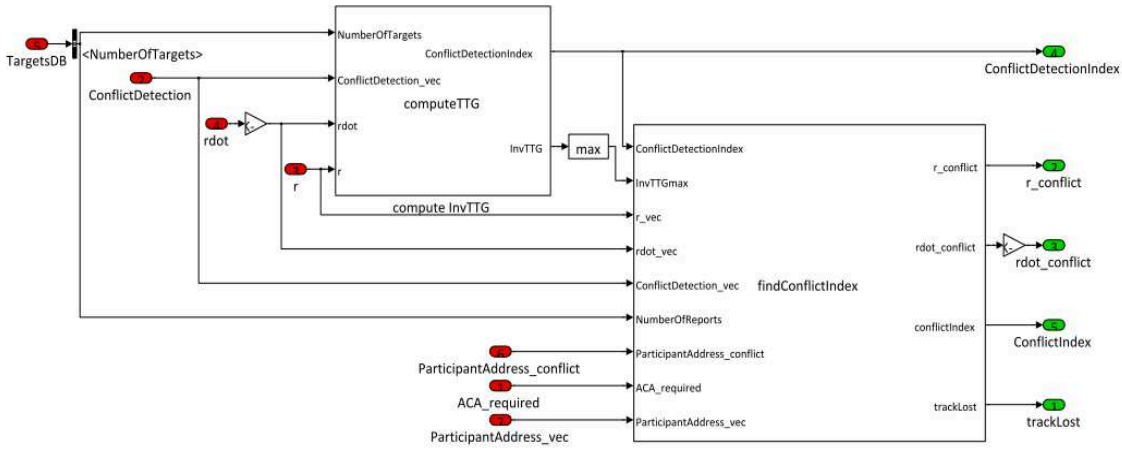

Figure 4.9 – Time-to-go approach: Prioritization Simulink scheme

4.2.4 Conflict detection and prioritization Simulink scheme: uncertainties approach

The Simulink block for conflict detection and prioritization based on the uncertainties approach, introduced in the paragraphs 3.5, 3.5.2 and 3.6.2, is represented in Figure 4.10. Both the conflict detection and the prioritization algorithms are implemented in a Matlab function whose input are:

- *DataOfOwnship* which is a bus including ownship position and velocity in a local NEU reference frame;
- *DataOfTargets* that is a bus containing information about position, velocity, measurements uncertainties (in a local NEU reference frame) and number of tracks stored into the database;
- *SafetyRadius* which presents the nominal value of safety bubble radius.

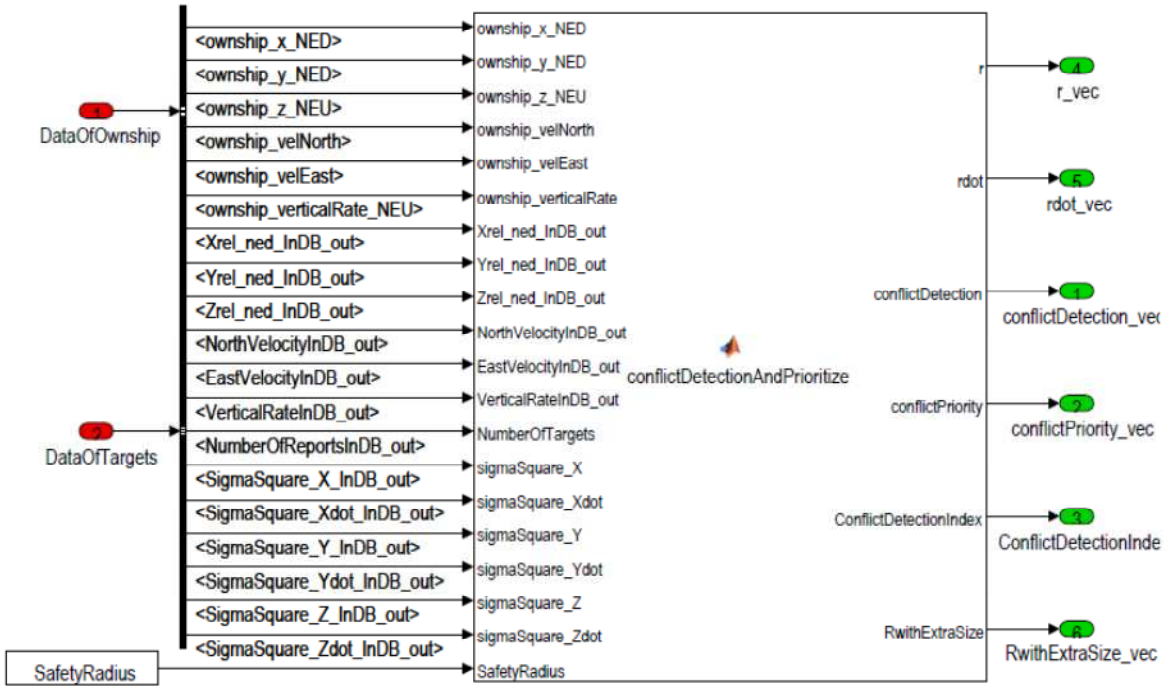

Figure 4.10 - Uncertainties Approach: Conflict Detection and Prioritize Simulink Scheme

In this case, the output variables are vectors related to the all aircraft stored into the database:

- *r_vec* is a vector containing the relative distance between the ownship and all the aircraft in the database;
- *rdot_vec* is a vector including the closure rate between the ownship and all the aircraft in the database;
- *ConflictDetection_vec* is a vector whose element are Boolean which indicate if the generic aircraft in the database poses a conflict to the ownship or not;
- *ConflictPriority_vec* is a vector indicating the order priority according to the equation (37) (paragraph 3.6.2);
- *ConflictDetectionIndex* which is a boolean value indicating if at least one aircraft, among the ones recorded into the database, poses a conflict to the ownship;
- *RwithExtraSize_vec* which is a vector including the safety bubble radius, with extra-size, related to each intruder aircraft.

4.3 Unitary Performance Tests

Prior to introduce the software architecture adopted to perform offline and real-time test, a performance test campaign has been carried out in order to establish the working of some modules. In particular unitary tests have been performed on the following modules:

- Surveillance Processing module, in order to establish the module performances*;*
- Safety bubble extra-size radius computation and Prioritization modules, in order to define which approach, between the proposed ones, has to be integrated in the assessed software architecture.

4.3.1 Surveillance Processing: Tracking Filter Test

In order to establish the performance of the introduced tracking filter, some tests have been performed [101].

The test scenarios foresee the presence of the ownship (receiver participant) and one intruder aircraft (transmitter participant) and both the aircraft move with

constant velocity. The module performance are evaluated as NACp and NACv values, of the transmitter participant, change.

A local ENU reference frame it is considered, with origin in the ownship. The latter is assumed to move, when the simulation starts, with constant velocity at *35m/s* along the *x/east* and *y/north* axis and the vertical rate is zero. The intruder starts at *5000 m* along *x* and *y* axis, with an initial velocity of *35 m/s* along the *x/east* and *y/north* axis and of *1 m/s* along the *z/up* axis. In the first scenario the NACp value of the intruder is 9 and NACv value is 3: according to Table 3.1 and Table 3.2, those values correspond to *EPU<30 m*, *VEPU<45 m*, *HVA<1 m/s* and *VVA<1.52 m/s*. The error between the estimated position along the *x* direction and the simulated one, is reported in Figure 4.11: the root mean square (rms) error is of about *6 m*. Figure 4.12 shows the error between the estimated velocity and the simulated one along the *x* direction too: the root mean square error is of about *0.5 m/s*.

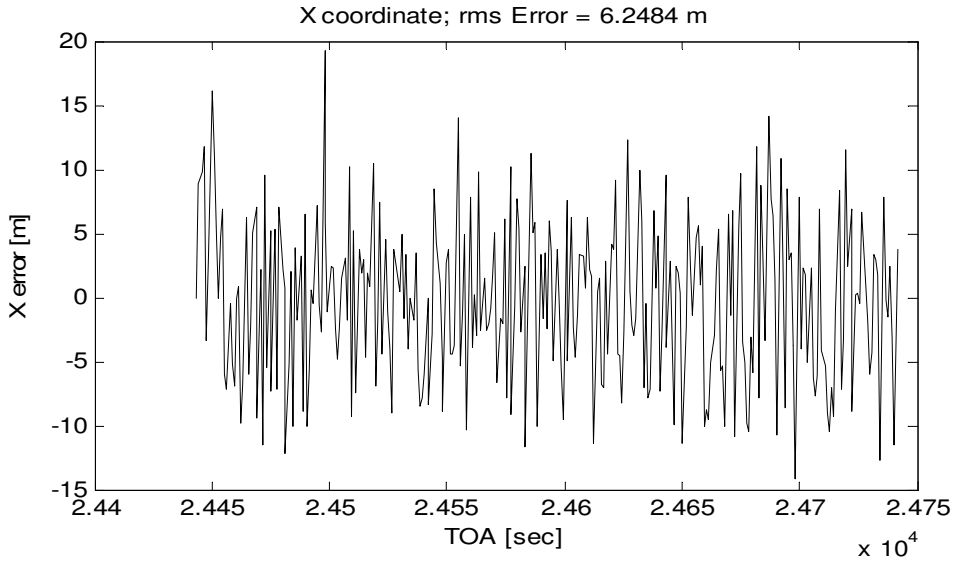

Figure 4.11 - Error [m] between the estimated x position and the simulated one – First Scenario

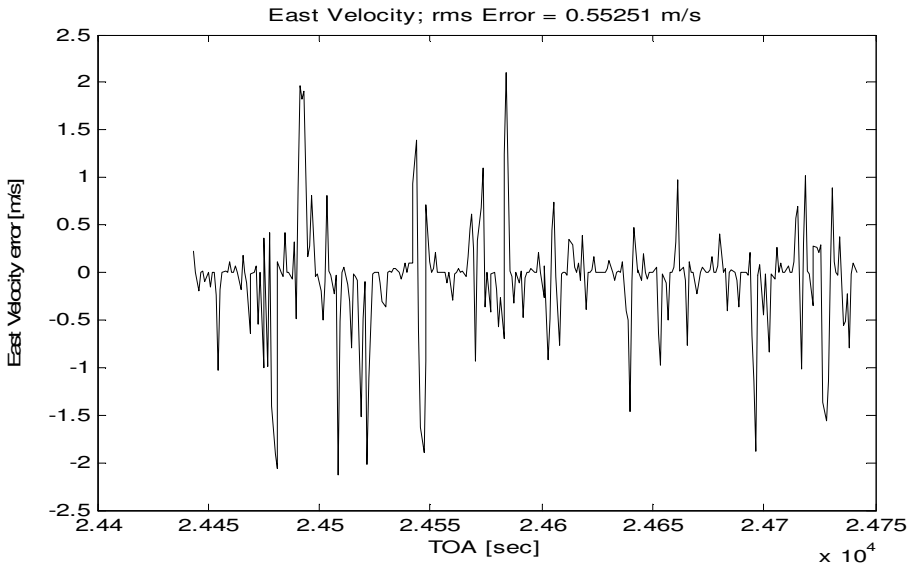

Figure 4.12 - Error [m/s] between the estimated east velocity and the simulated one – First Scenario

In the second scenario NACp and NACv values of the intruder aircraft are 7 and 2 respectively. It correspond to *EPU<185.2 m*, *VEPU<182.5 m*, *HVA<3 m/s* and *VVA<4.57 m/s*.

As reported in Figure 4.13, the rms error related to the *x* position is of about *7 m*. Therefore the rms error increases, with respect to the first scenario, due to un higher uncertainty value and to the propagation of the error in the filter prediction phase.

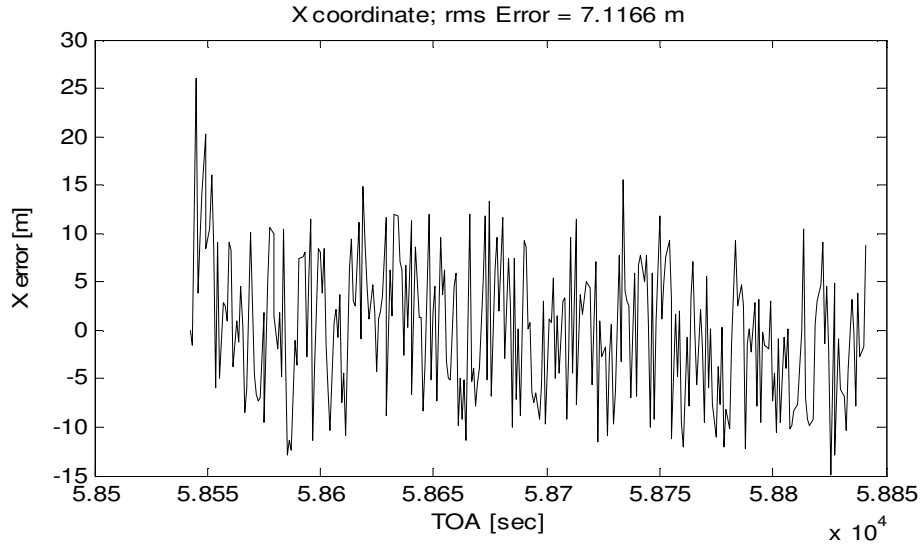

Figure 4.13 - Error [m] between the estimated x position and the simulated one – Second Scenario

Nevertheless, the rms of velocity component along the *x* axis reduces and it is of about *0.09 m/s*. This behaviour is related to the assumption of constant velocity for the intruder aircraft. In fact, the intruder dynamic model is consistent with the simulated intruder aircraft motion and the dynamic model influences the velocity estimation more than the measurements, i.e. the gain values of the Kalman filter are small.

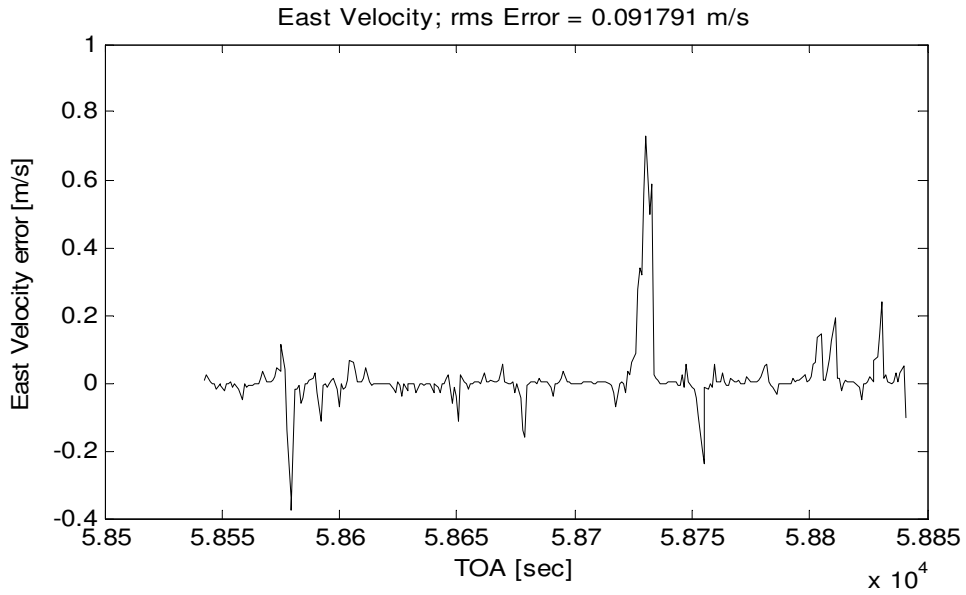

Figure 4.14 - Error [m/s] between the estimated east velocity and the simulated one – Second Scenario

In the last scenario the intruder dynamic model is not compliant with the simulated intruder aircraft motion: the intruder aircraft moves with a constant acceleration, of *0.1 m/s*^{2} along the *x/east* direction. The NACp and NACv values are the same of the previous scenario. Figure 4.16 shows that the velocity rms error is of about *0.2 m/s*: the error increases due to the difference between the assumed dynamic model and the simulated motion.

Note that in all the scenarios, the errors are compliant with the NACp and NACv values.

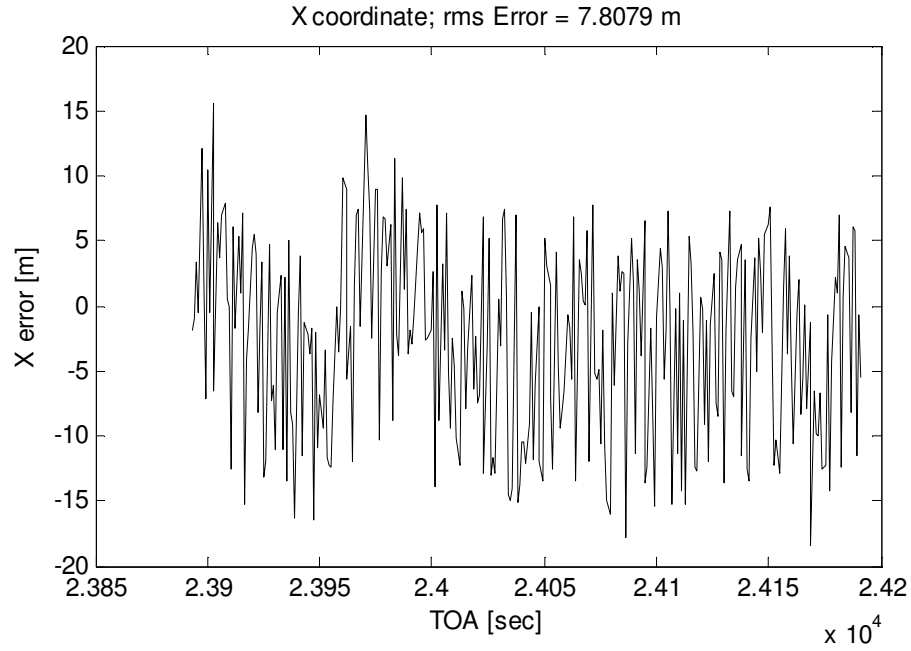

Figure 4.15 - Error [m] between the estimated x position and the simulated one – Third Scenario

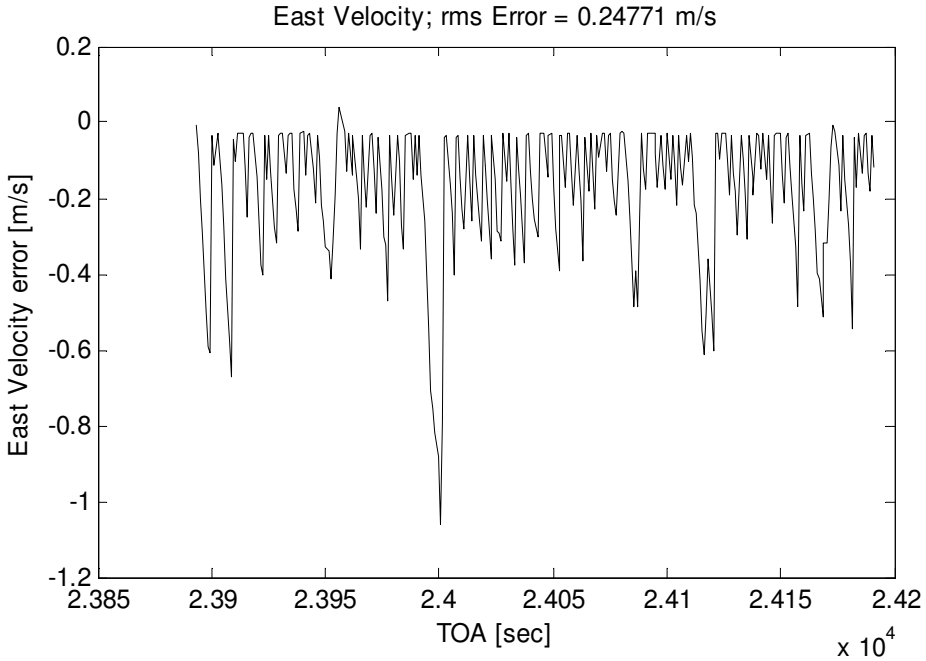

Figure 4.16 - Error [m/s] between the estimated east velocity and the simulated one – Third Scenario

4.3.2 Surveillance Processing Tests

The following simulation scenarios are introduced in order to evaluate the functionalities of Track Generation and Maintenance, Track Termination and Common Time extrapolation. It is assumed that there are not uncertainties associated to the transmitted position and velocity measurements. In other words, the exact velocity and position of intruders aircraft are received on-board.

In the first scenario an intruder and the ownship are flying in an head-on conflict geometry. A local ENU reference frame, centred in the ownship, is considered. The simulation lasts *80 s* but, at *50 s*, not valid state information are transmitted by the intruder aircraft. In Figure 4.17 three line are represented:

- The red line is related to the measurements data, received from the simulated on-board ADS-B IN device, and considered as input for the Generation and Maintenance module;
- The blue line refers to the elaborated data recorded into the database after the generation and maintenance processing;
- The green line refers to the state intruder data extrapolated at the time of applicability of Ownship measurements.

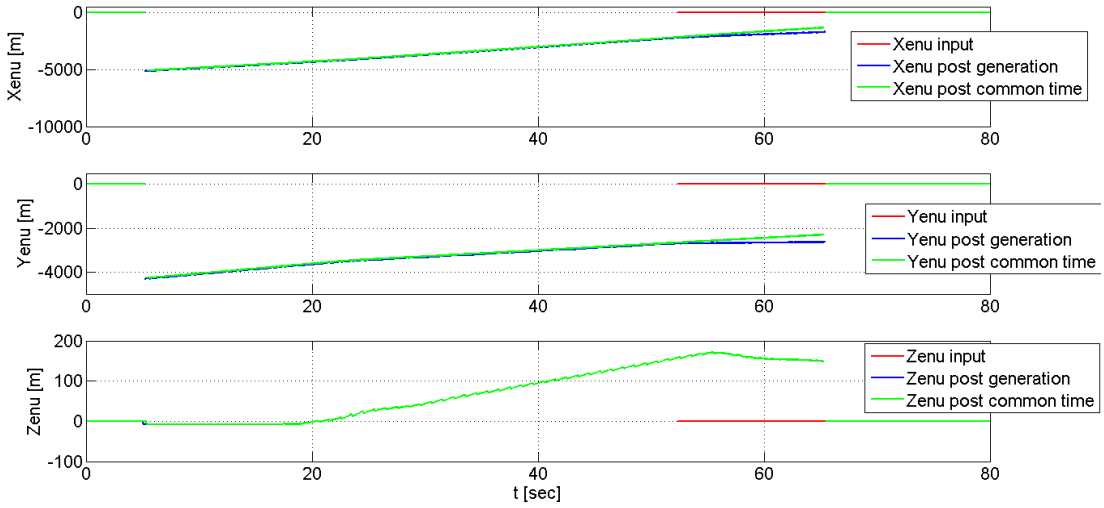

Figure 4.17 – Surveillance Processing Tests: Intruder Position - Scenario 1

As states above, at about *50 s* no valid measurements are received (Figure 4.18). The track information are propagated for the following *15 s* (lines blue and green) and then are terminated. When the track is terminated the output value for

intruder position and velocity is zero. When no valid measurements are received, the difference between the green line and the blue one became more significant. Beforehand, the update frequency was high enough to not allow to see differences between the blue and the green lines.

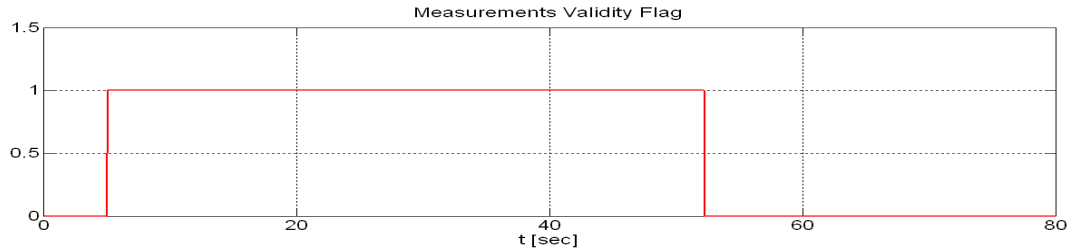

Figure 4.18 - Measurements Validity Flag - Scenario 1

In the second scenario, the conflict geometry is the same of the previous scenario but, initially the input intruder latitude oscillates so that two consecutives reports do not correlate until *50 s*. It simulates a damage in ADS-B OUT or ADS-B IN device. Since the reference frame used for Figure 4.19 is a local reference frame centred in the ownship, the latitude oscillation converts in an oscillation along *x* and *y* directions. When the signal stabilizes, and two consecutive reports correlate, the track is added into the database and the state information are output.

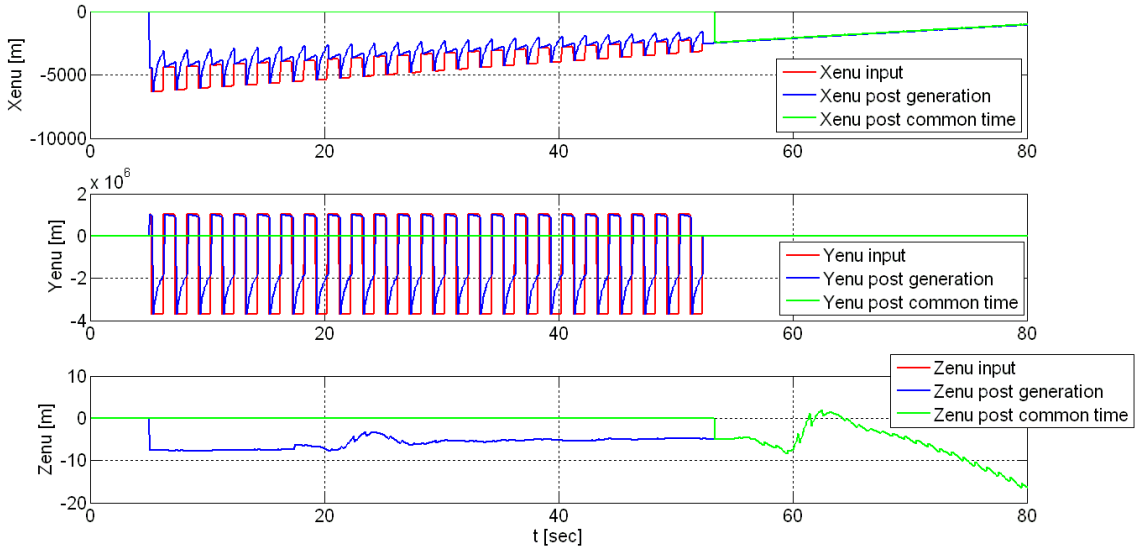

Figure 4.19 - Surveillance Processing Tests: Intruder Position - Scenario 2

The third scenario aircraft geometry is similar to the previous ones, but the latitude oscillation starts at about *50 s*. When the oscillation starts, it indicates that no valid measurements are provided to the surveillance module and, hence, the track is propagated for the following *15 s* (lines blue and green) and then it is deleted from the database (Figure 4.20). Regarding the representation of latitude oscillation the same consideration of the previous case are valid.

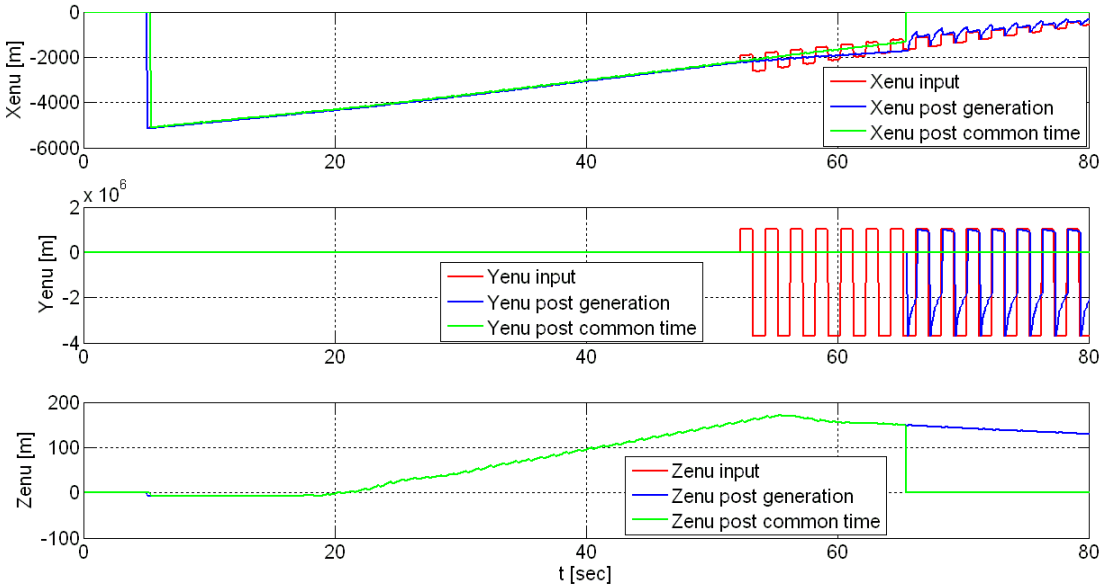

Figure 4.20 - Surveillance Processing Tests: Intruder Position - Scenario 3

In the last scenario the intruder and the ownship are, still, in an head-on geometry and the transmitter intruder latitude oscillates when the simulation time is included between *50 s* and *60 s*. It simulates that no valid traffic information are received in that time interval. Figure 4.21 shows that the intruder velocity and position are propagated in that time interval using the last validated information and when the latitude stabilizes again the track update takes into account the measurements information.

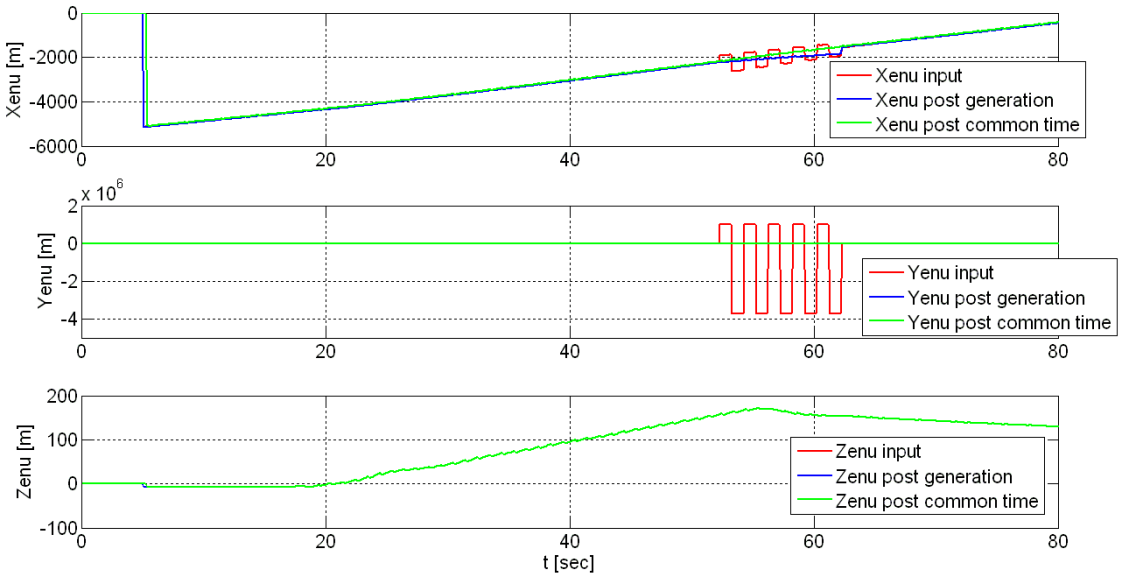

Figure 4.21 - Surveillance Processing Tests: Intruder Position - Scenario 4

4.3.3 Safety bubble extra-size radius computation

The conflict condition criterion is reported in Eq.(38):

$$\left\| d_{cpa} \right\| < R + R_{extra} \tag{38}$$

where:

- $\left\| d_{cpa} \right\|$ is the distance at the closest point of approach;
- R is the nominal value of the safety bubble radius;
- R_{extra} is the extra-size radius introduced to take into account of the relative dynamic between the ownship and the intruder aircraft or the measurements uncertainties of the intruder aircraft.

As explained in the previous chapter, two methods are introduced for the computation of the extra-size radius, related to two methods of prioritization criterion:

- A first method based on the computation of the closure rate ($\dot{r}$) between the ownship and the surrounding aircraft:

Conflict Detection	Pioritization
$\left\|d_{cpa}\right\| < R + k\dot{r}$	$\min\left(\frac{r}{\dot{r}}\right) = \min(TTG)$

Table 4.1 – Conflict Detection and Prioritization based on the closure rate

In this case the extra-size radius is the product between a scale factor *k*, assumed to be 5 for this simulation, and the closure rate. Once the conflict detection condition has been verified for more than one aircraft stored in the database, the most dangerous threat prioritization is computed based on the minimum TTG value.

- A second method based on the uncertainties related to the computation of the closest point of approach (and relate to the NACp and NACv values broadcasted by the traffic):

Conflict Detection	Pioritization
$\left\|d_{cpa}\right\| < R + \sigma_{\Delta d_{cpa}}$ $\left\|d_{cpa}\right\| < R + 2\sigma_{\Delta d_{cpa}}$ $\left\|d_{cpa}\right\| < R + 3\sigma_{\Delta d_{cpa}}$	$\max\left(P\{C\}\frac{\dot{r}}{r}\right) = \max\left(P\{C\} \cdot inv(TTG)\right)$

Table 4.2 - Conflict Detection and Prioritization based on the measurements uncertainties

In this case three bubble can be computed around the intruders aircraft. The three bubble radius are given by the nominal value and the closest point of approach standard deviation at $1\sigma_{\Delta d_{cpa}}$, $2\sigma_{\Delta d_{cpa}}$ and $3\sigma_{\Delta d_{cpa}}$. The priority threat is given by the maximum value of the product between the probability of the conflict, based on the radius that generates the conflict, and the inverse of *TTG*.

Two simulation test scenarios are described in order to define the proper method to use.

In the first scenario an intruder aircraft and the ownship move, with constant velocity, in an head-on geometry. Considering a NED reference frame centred in the runway, the initial state of the aircraft are shown in Table 4.3.

Ownship	**Intruder Aircraft**
x=1000m; y=100m; z=-300m	*x=100m; y=100m; z=-300m*
V_x*=-35m/s;* V_y*=0m/s;* V_z*=0m/s*	V_x*=35m/s;* V_y*=0m/s;* V_z*=0m/s*

Table 4.3 - Initial state of ownship and intruder aircraft

The NACp value transmitted by the intruder is assumed to be 11 (*EPU<3m, VEPU<4m*) and the NACv is equal to 4 (*HVA<0.3m/s; VVA<0.46m/s*). The safety radius computed with the two methods is represented in Figure 4.22 and Figure 4.23.

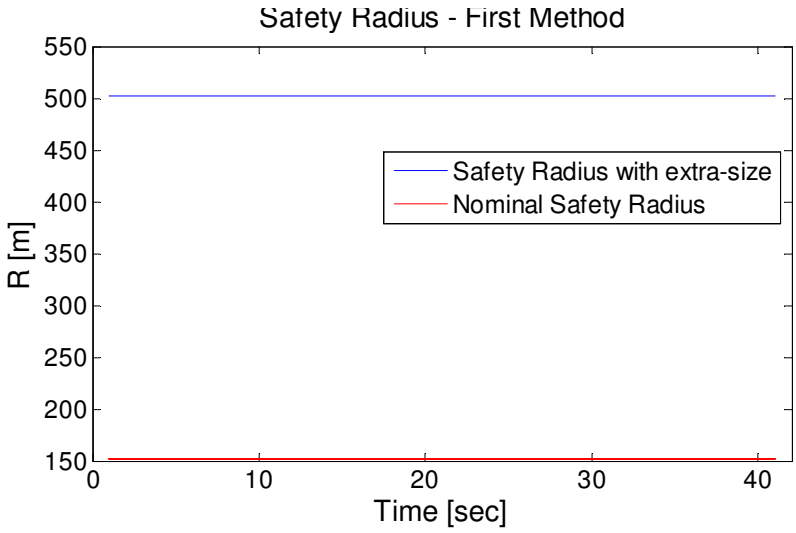

Figure 4.22 – Safety radius bubble: closure rate method – First Scenario

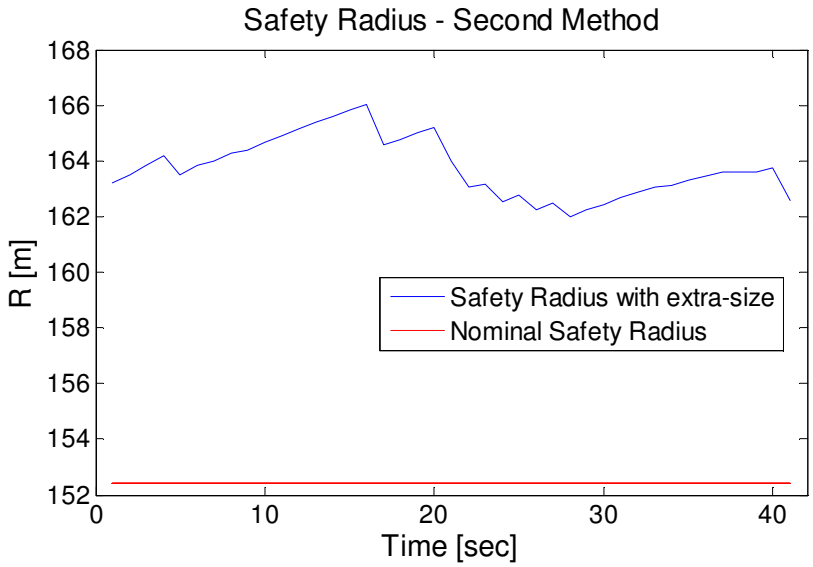

Figure 4.23 - Safety radius bubble: uncertainties method – First Scenario

The first method gives a constant value for the safety bubble radius due to the assumption of constant velocity motion for both the intruder and the ownship. The second method provides a value definitively lower than the first one, and almost constant, because the uncertainties are rather low for this simulation.

The initial state conditions, for the ownship and the intruder aircraft, are the same of the previous scenario but the NACp and the NACv values of the intruder aircraft are reduced and equal to 8 (*EPU<92.6m, VEPU<92.6*) and 3 (*HVA<1m/s, VVA<1.52m/s*), respectively. As reported in Figure 4.24 and Figure 4.25, the safety radius computed with the first method is unchanged, but the second one amplifies due to an increase of received measurements uncertainties. nevertheless, it is lower than the first one again.

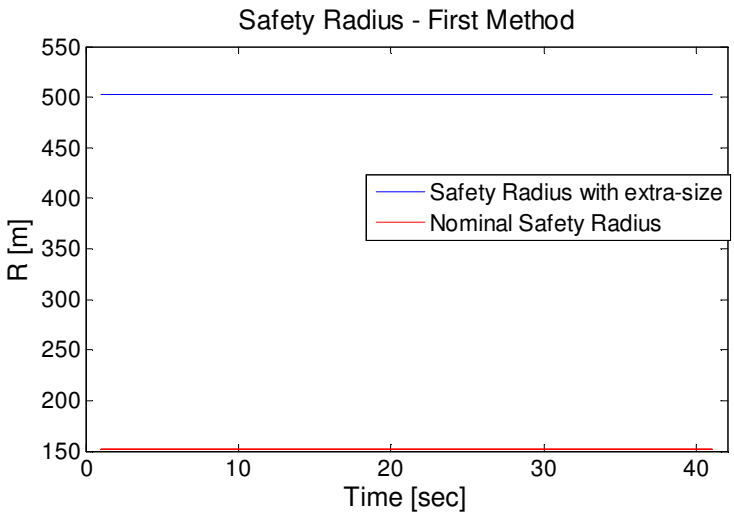

Figure 4.24 - Safety radius bubble: closure rate method – Second Scenario

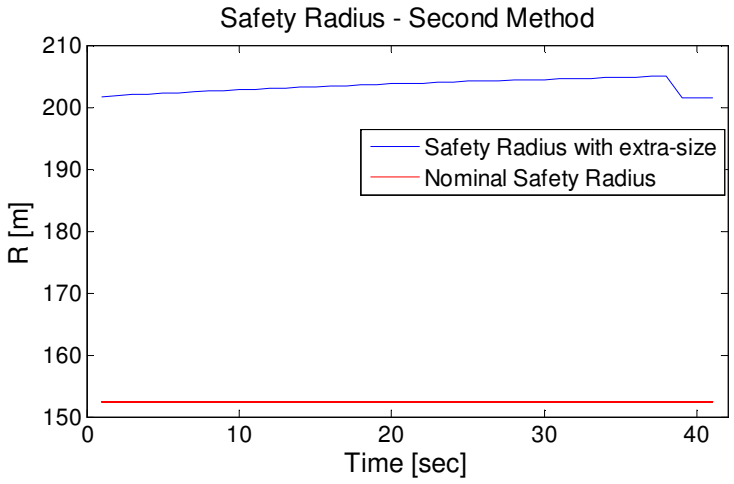

Figure 4.25 - radius bubble: uncertainties method – Second Scenario

Therefore, the method based on the closure rate provides a safety radius higher, but depending on the choice of the *k* parameter, than the safety radius related to the uncertainties method. Nevertheless the safety radius provided by the second method is strictly connected to the variation of the NACp and NACv values that can significantly change during the flight and it could led to an unstable algorithm.

The instability of the safety bubble computation and, consequently, the instability of prioritization and conflict detection algorithms could compromise the correct working of the whole architecture. Therefore, the closure rate based algorithm is chosen to be integrated in the tested software architecture.

4.4 Numerical Testing

4.4.1 Simulation Environment for Numerical Testing Description

The proposed approach has been tested by means of numerical simulations representing some relevant conflict scenarios, carried out with the aim of assessing the applicability of ADS-B data for conflict detection purposes. The intruders' motion has been simulated by using simple kinematic 3D motion model, whereas the ownship dynamics has been fully modelled by using 6 degrees-of-freedom aircraft model and suitable autopilot and auto-throttle systems [54].

The developed ADS-B based subsystems, for the surveillance and conflict detection functionalities, have been included in a more complex software architecture for an autonomous GNC application. In other words, the system has to guarantee the autonomous flight, during the entire flight mission, including the autonomous mid-air flight, the take-off and the landing, and the collision avoidance [54].

The software architecture of the whole system is represented in Figure 4.26. A brief description of the represented subsystems is provided in the following:

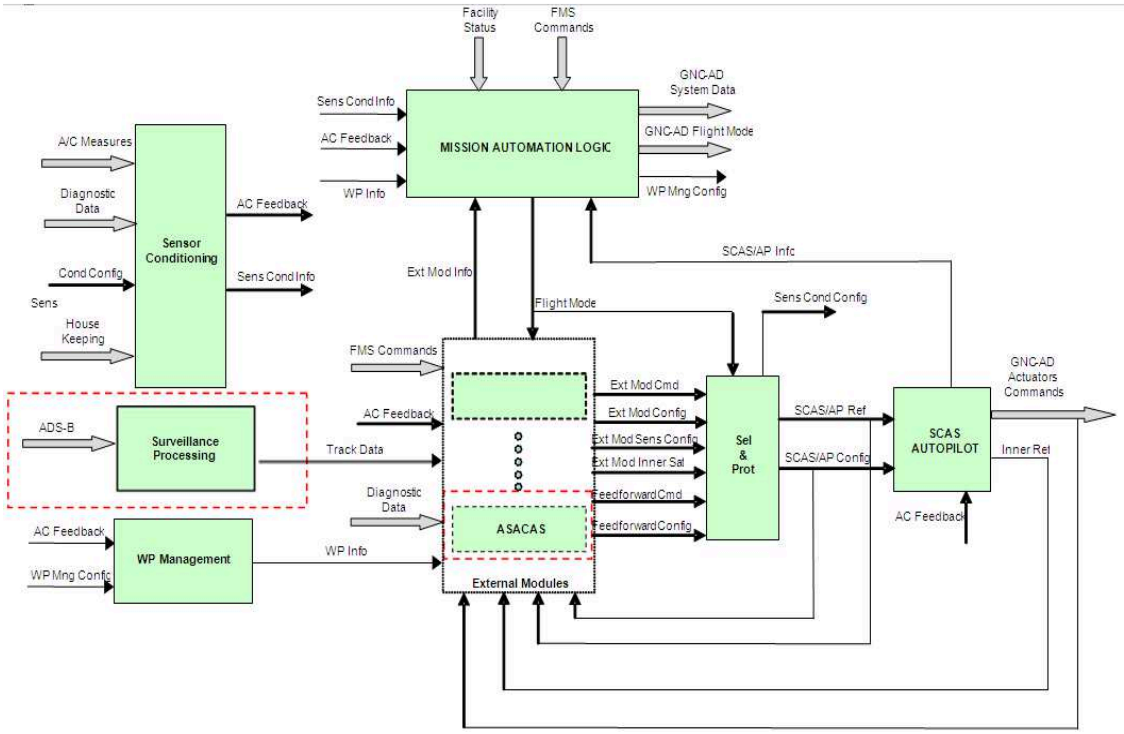

Figure 4.26 - Autonomous GNC Software Architecture

- The *Mission Automation Logic* consist of a state machine implementing the automation logic of the GNC module. It manages the activation of the other module based on the external input.
- The *External Module* subsystem includes all the modules that generates the input variables for the SCAS/Autopilot. The ASACAS module is one of those modules, and it includes conflict detection module and the other described before (with the exception of the Surveillance Processing Module).
- The *Sensor Conditioning* module performs a conversion from raw data to engineering data in order to support the autonomous GNC algorithms.
- The *Surveillance Processing* module elaborates the raw data received from the ADS-B IN device in order to feed the *External Modules* with a more suitable data structure.
- The *WP Management* module generates the WP, and the related information, to be followed.

- The *SCAS/Autopilot* module implements the velocity control (*Autothrottle*), the altitude and vertical speed control, the heading or inertial velocity control and the attitude control.
- The *Selection and Protection* module selects the state references and configuration codes to supply the *SCAS/Autopilot*. Moreover it selects the configuration command for the *Sensor Conditioning* module, and it activates the flaps based on the TAS value.

4.4.2 Numerical Testing Results

In this section, two exemplary numerical simulation trials are reported and described in order to show how the proposed system works [102]. The considered scenarios are:

- Case A – The scenario refers to typical head-on approach conflict geometry, involving ownship and one intruder flying at the same altitude;
- Case B – The scenario refers to the presence of three intruders with two of them that represent a conflict condition with ownship.

For what concerns the case A, the overall evolution of the flight is reported in Figure 4.27. The simulation of the flight starts at *5 s* of the simulation time (the previous time is needed for simulation environment initialization purposes), with vehicles, whose initial trajectories are straight lines, approaching according to head-on conflict geometry and flying at the same altitude.

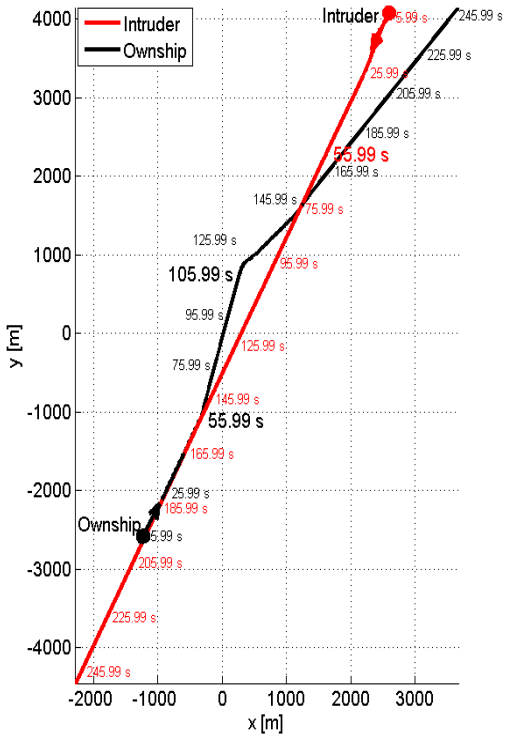

Figure 4.27 - Aircraft Trajectories - Case A

The system behaviour can be derived from the analysis of its logic evolution. In Figure 4.28 the mission automation logic signal is reported: the logic signal values 15 and 16 indicate the activation of the flight modes devoted to automatic waypoints navigation and, as evident from the figure, while the ownship is performing automatic navigation towards the selected waypoint, the logic signal value changes from 16 to 26, indicating the activation of the collision avoidance manoeuver.

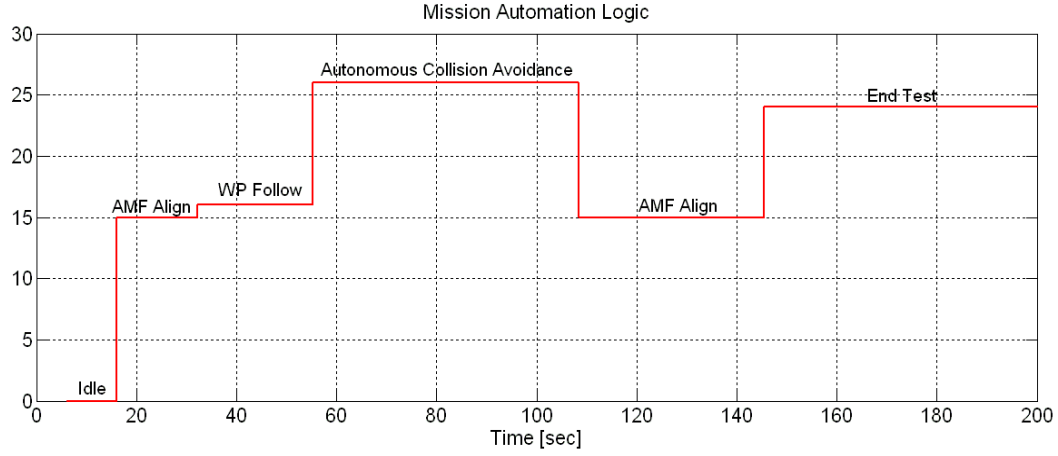

Figure 4.28 - Mission Automation Logic - Case A

The change is motivated by the satisfaction of the conflict detection condition: indeed, the vehicles are at a distance lower than the coarse filtering threshold and are approaching (see Figure 4.29) with predicted violation of the safety bubble.

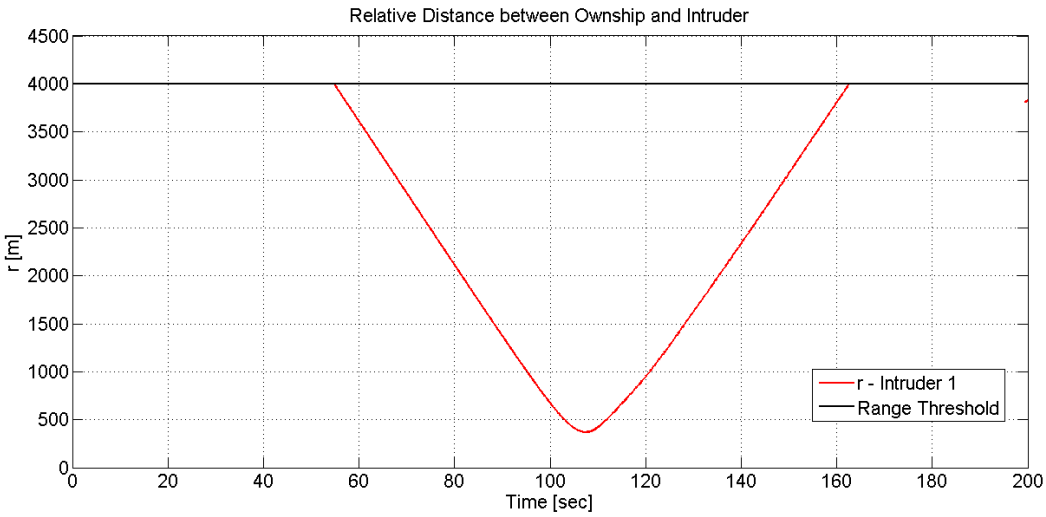

Figure 4.29 - Aircraft Relative Distance - Case A

The collision avoidance manoeuver continues until the vehicles start diverging. The vehicles start diverging at *107.4 s*, so leading to the exit from the conflict condition and to the subsequent change of the mission automation logic signal value from 26 (collision avoidance) to 15 (automatic capture of the selected waypoint) at *108.4 s*, according to the execution frequency of the software system.

Based on these considerations, the overall flight evolution for the case A, can be summarized as:

- the conflict is detected only when the distance between intruder and ownship is lower than the coarse filtering threshold and the conflict detection condition is satisfied, i.e. at *54.8 s* of simulation time;
- therefore, the conflict resolution manoeuver is calculated and implemented;
- the resolution manoeuver ends at *108.4 s*, when the ownship starts again its flight in order to capture the destination waypoint, after having deviated from its original route due to collision avoidance manoeuver implementation.

For what concerns the case B, the overall evolution of the flight is reported in Figure 4.30. The simulation of the flight starts at *5 s* of the simulation time (the previous time is needed for simulation environment initialization purposes), with vehicles, whose initial trajectories are straight lines, approaching according to lateral conflict geometry and flying at the same altitude.

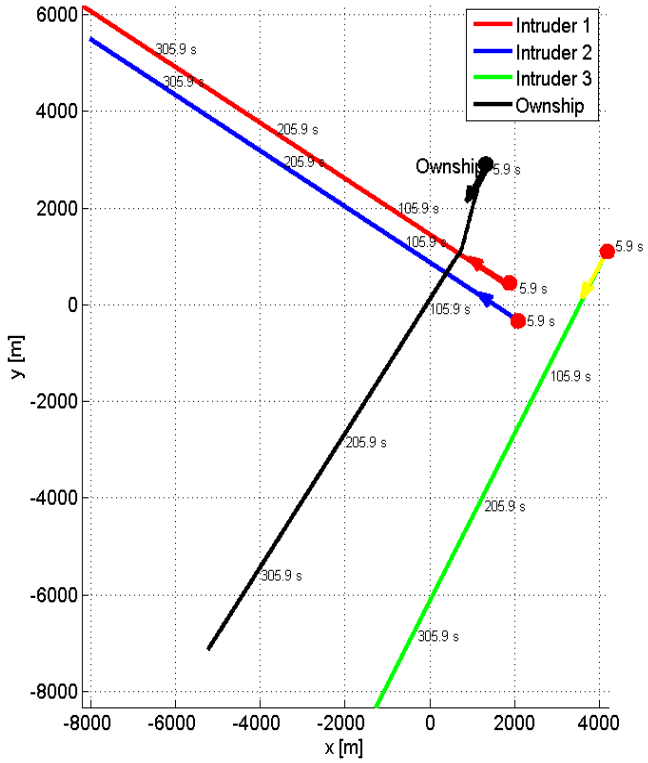

Figure 4.30 - Aircraft Trajectories - Case B

The system behaviour can be derived from the analysis of its logic evolution, with consideration similar to the ones expressed for the detailed analysis of the case A. In Figure 4.31 the mission automation logic signal is reported: the logic signal value 26 indicates that, already from the start of the simulation, the conflict detection system implemented on-board the ownship identifies a conflict condition, so leading to the activation of the conflict resolution manoeuver. Indeed, as evident from the analysis of Figure 4.32 and Table 4.4, the detected conflict condition involves two intruders (namely the intruder 1 and the intruder 2), so leading to the need of prioritizing the two conflicts according to the criterion described in the previous chapter.

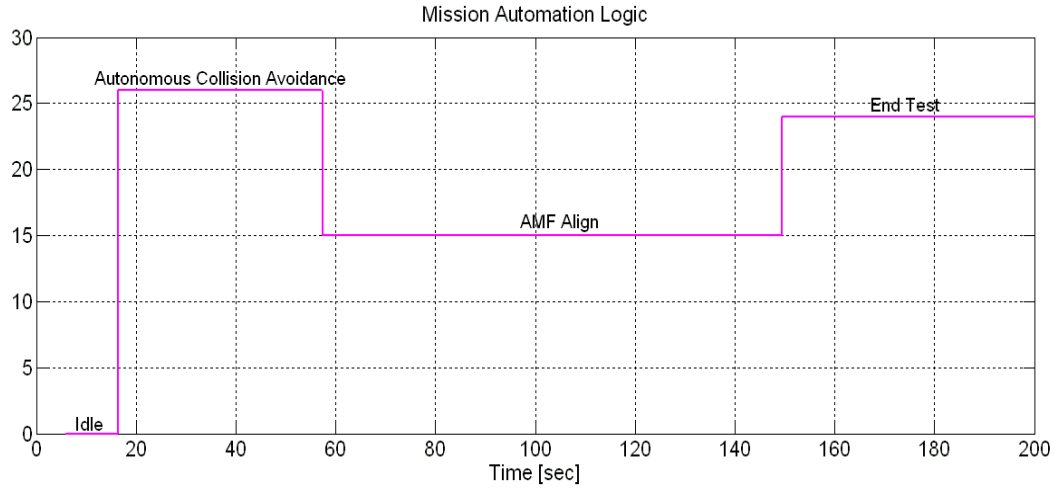

Figure 4.31 - Mission Automation Logic - Case B

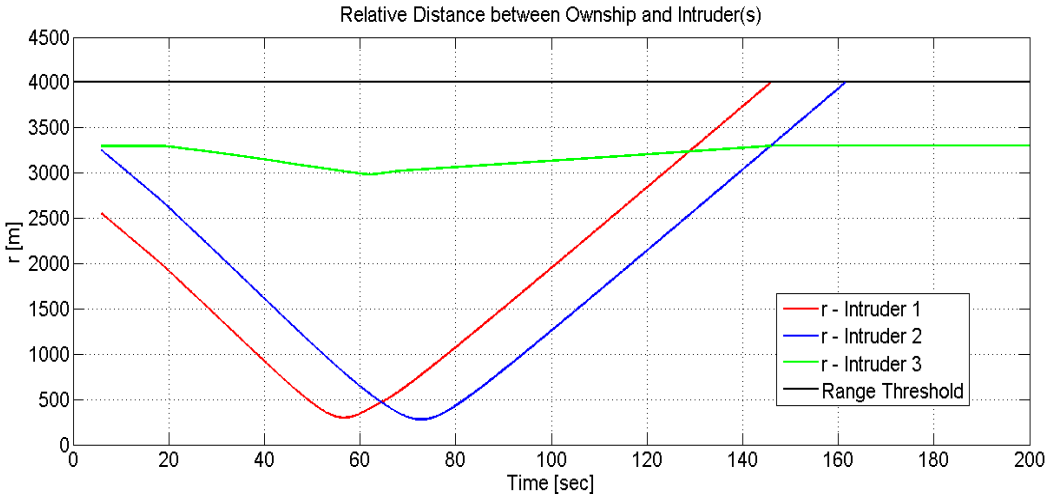

Figure 4.32 - Aircraft Relative Distance - Case B

	Intruder 1	**Intruder 2**
Relative Distance [m]	2552	3251
Closure Rate [m/sec]	45	45
TTG [sec]	57	72

Table 4.4 - Most significant values for conflict prioritization

Once the conflicts have been prioritized, the conflict resolution manoeuver is implemented with respect to the most relevant conflict according to the time-to-go prioritization criterion: in this scenario, the highest priority conflict is the one with the intruder 1. The collision avoidance manoeuver continues until the vehicles start diverging, i.e. up to *57.4 s* of the simulation time. After that, the mission automation logic value changes to 15, indicating the activation of the automatic navigation towards a destination waypoint different from the initial one due to the implementation of the collision avoidance manoeuver. The waypoint is captured at *149.5 s*, so that the mission automation logic changes to 24, indicating that the ownship continues in a straight levelled flight.

The collision avoidance maneuver consists in suitable modification of the ownship trajectory as well as velocity magnitude in order to assure that the ownship will pass behind intruder 1 (and in this case also behind the intruder 2, which represents lower priority conflict).

Based on these considerations, the overall flight evolution for the case B, can be summarized as:

- the conflict is detected only when the distance between intruders and ownship is lower than the coarse filtering threshold and the conflict detection condition is satisfied, i.e. in this case already from the simulation beginning;
- being detected two conflicts (with intruder 1 and with intruder 2), the two detected conflicts are prioritized according to the associated TTG;
- the resolution manoeuver is then calculated and implemented with respect to the most relevant conflict condition (the one with the intruder 1);
- the resolution manoeuver ends at *57.4 s*, when the ownship starts again its flight in order to capture the updated destination waypoint, after having deviated from its original route due to collision avoidance manoeuver implementation.

4.5 Real-Time Testing

4.5.1 Simulation Facility Description

Following the fast-time simulation campaign, dedicated real-time simulation campaign has been carried out in order to assess the behaviour of the proposed system in presence of the real-time implementation constraints. Suitable information about the real-time tests will be provided in the following section IV, whereas in this section the laboratory setup used for real-time simulation is described. Detailed description of this facility can be found in [103].

The laboratory setup comprises all the ground segment equipment and the Flight Control Computer that is designed to be installed on-board of the CIRA experimental platform FLARE. The flying platform is constituted by a VLA optionally piloted vehicle, i.e. a vehicle equipped for completely automatic flight that is managed by the Remote Pilot Station that can be, where needed, also piloted by the safety pilot on-board [104]. Furthermore, the laboratory facility is equipped with suitable flight simulator, reproducing the dynamical behaviour of the vehicle FLARE and the external environmental conditions where the vehicle is simulated to fly. In addition, the surrounding traffic is also simulated by means of dedicated traffic simulator.

The laboratory set-up functional architecture is shown in Figure 4.33, where it is emphasized that the main elements of the laboratory test rig are:

- Flight Control Computer;
- Ground Segment (Remote Pilot Station);
- Aircraft and Sensors simulator;
- Traffic simulator;
- Pilot Cockpit and Interceptor Commands Emulator.

It is worth noticing in Figure 4.33 that the aircraft and sensors simulator is interconnected not only with the Flight Control Computer but also with the Ground Control Computer. This connection is not present in the real experimental set-up, but it is necessary to simulate the direct connection between the pilot's

cockpit and the aircraft because in the laboratory set-up the Ground Control Computer manages also the communications with the pilot's cockpit simulation computer.

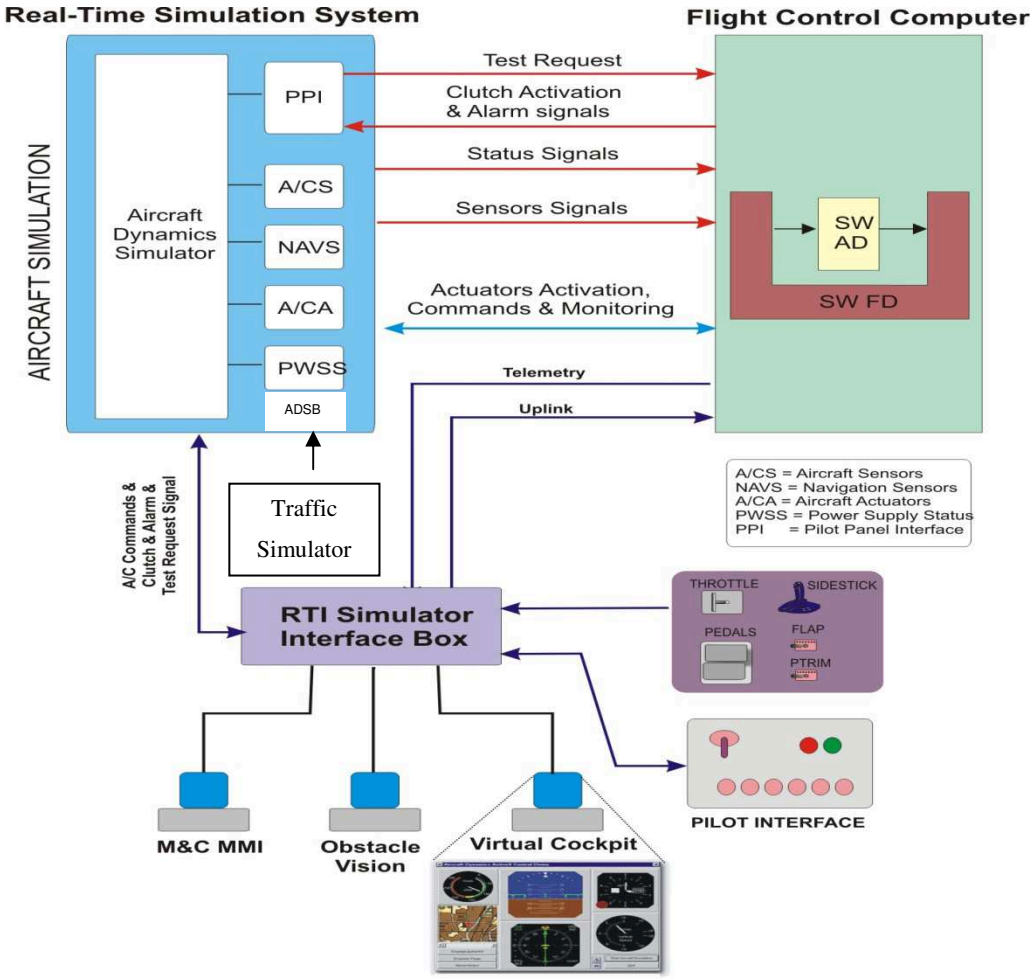

Figure 4.33 - Laboratory Setup Architecture

Furthermore, in the laboratory setup the same hardware platform is used for the acquisition of pilot direct link commands, for the management of the laboratory pilot real cockpit and for the data communications management between aircraft simulator and ground segment. This does not constitute a limitation of the proposed real-time validation test rig, because the software module devoted to the pilot commands acquisition and laboratory real cockpit management does not have any link with the software module devoted to the data

management between the ground segment and the on board segment, even if they are allocated on the same hardware.

The traffic simulator is connected only to aircraft and sensors simulator. It provides the simulation of the ADS-B OUT signals sent by the surrounding vehicles and received by the ADS-B IN device simulated on-board of the FLARE platform. The simulation of the ADS-B OUT signal transmission includes the possibility of reproducing also failures like link loss , delay and so on. Nevertheless, it is worth to emphasize here that simulation of failures and/or disturbances affecting the ADS-B signal broadcast has not been considered in the real-time simulation campaign addressed in this paper, where ideal behaviour of the ADS-B signal exchange has been reproduced. The external sensors interface of the ADSB module, similarly to the interfaces of the other sensors, reproduces the real protocol.

The aim of the laboratory set-up is to test the software implemented on the Flight Control Computer and the ground segment software needed for the mission management. Achieving this goal is done correctly simulating all sensors on board. The software architecture of the aircraft and sensors simulator is composed by the modules listed in the following:

- six degrees of freedom (6dof) aircraft model module;
- sensors simulation module;
- external interface sensors simulation module;
- actuators simulation module;
- external weather conditions simulation module;
- pilot's cockpit management module.

The 6dof aircraft model module is the core of the whole simulation software. The sensors and external interface sensors simulation modules are based on the COTS elements installed on the experimental set-up. The actuators simulation module implements the open loop model of each actuator. The external weather simulation is necessary to reproduce wind gust, shear and turbulence in all flight phases. Nevertheless, in the test cases presented in the next section, the wind disturbances have not been reproduced, because the provided description aims emphasizing the behaviour of the proposed conflict detection system and not

the guidance system robustness with respect to external disturbances. It is worth to emphasize here that for the description of the overall performances and functionalities of the Guidance, Navigation and Control system implemented on-board the FLARE vehicle the reader can be referred to literature papers in [105] - [108].

The Pilot's cockpit management, finally, is a software module which acquires the laboratory pilot commands trough an Ethernet link between the 6dof aircraft model of the vehicle and the pilot commands acquisition software implemented on a PC104.

4.5.2 Real-Time Testing Results

Up to date the proposed system has been validated by means of fast-time numerical simulations, including the analysis of relevant conflict scenarios. Those scenarios have been defined with the aim of assessing the applicability of ADS-B data for conflict detection purposes. The ownship dynamic has been simulated by means of a 6dof aircraft model with autopilot and auto-throttle system, whereas the intruders' motion model has been simulated by means of a kinematic 3dof motion model.

Based on the positive results obtained in the fast-time simulation campaign, the activities devoted to the development of the proposed system addressed the real-time simulation stage [109]. The real-time simulation campaign included several scenarios, involving different conflict geometries and one or more conflicting vehicles. Three significant real-time simulation trials are reported and discussed, which are considered suitable to describe the testing of the overall architecture paying particular attention to the conflict detection and the prioritization modules. In all the scenarios here reported nominal behavior of the ADS-B systems (both the OUT installed on-board the surrounding vehicles and the IN installed on-board the ownship) has been supposed and no external disturbances (such has wind) have been reproduced..

The considered scenarios are:

- CASE A – in this scenario the ownship and one intruder are flying, with constant velocity, at the same altitude in a typical head-on approach geometry;
- CASE B – the scenario presents two intruders and both represent a conflict condition with the ownship;
- CASE C – the scenario refers to the presence of two intruders which represent consecutive conflict conditions with the ownship.

For what concerns the CASE A, the flight evolution is reported in Figure 4.34. The ownship and the unique intruder are approaching according to an head-on geometry. Once the intruder vehicle approached at a distance equal or lower to *4000 m* the conflict condition is expected to be detected.

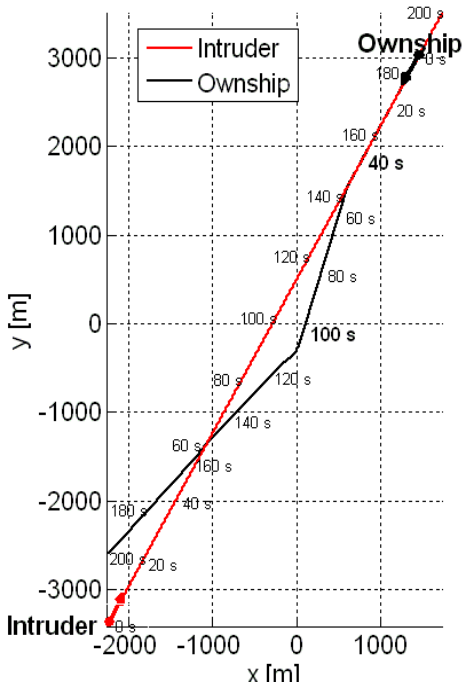

Figure 4.34 - Aircraft Trajectories - Case A (Real-Time Simulation)

Coherently with the system expected behavior, therefore, Figure 4.35 shows that at *46.1 s* the intruder enters the coarse filter radius and, therefore, the conflict resolution maneuver starts as reported in Figure 4.36, where the evolution of the system mission automation logic is reported. As mentioned before, the logic signal values 15 and 16 indicate flight modes related to the automatic waypoints

navigation. At *46.1 s* the signal changes from 16 to 26 indicating the activation of the collision avoidance maneuver and the satisfaction of the conflict detection. At *99.9 s* the logic signal returns to 16 indicating the end of the conflict condition. Finally, the mission automation logic changes to 24 indicating that the ownship continues in a straight leveled flight.

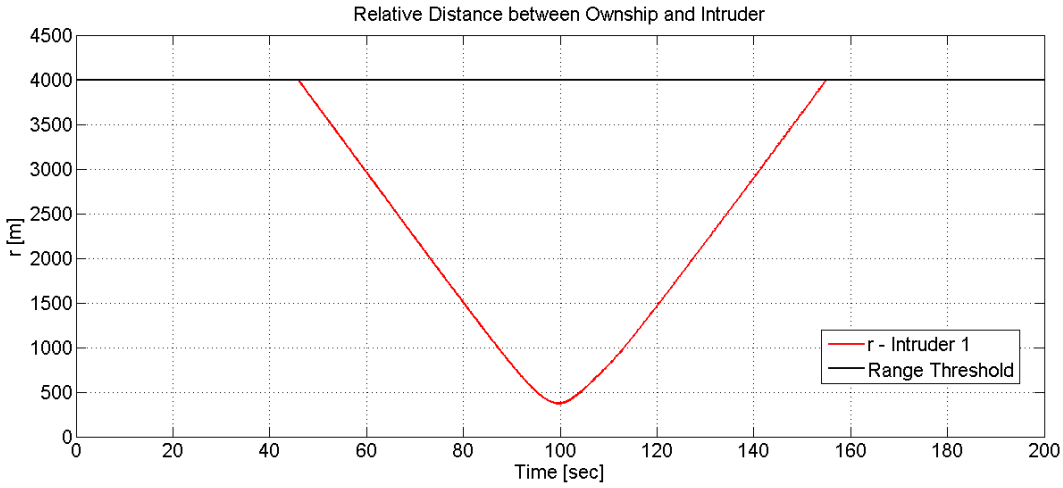

Figure 4.35 - Aircraft Relative Distance - Case A (Real-Time Simulation)

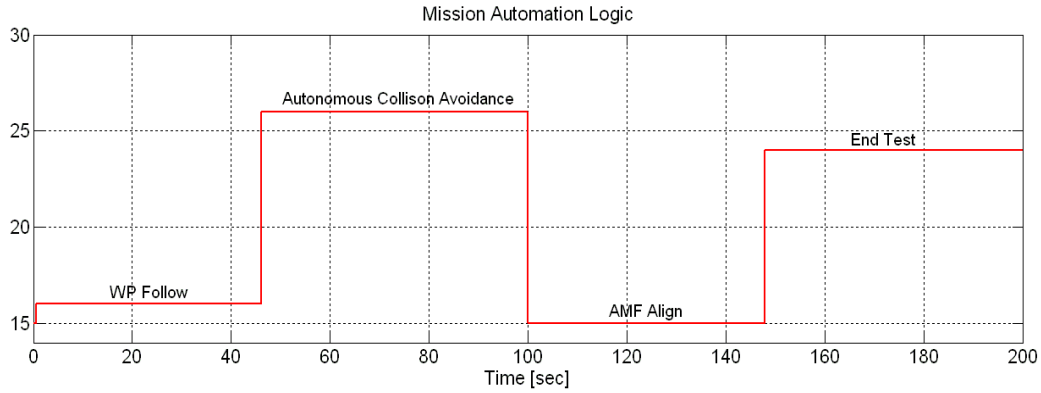

Figure 4.36 - Mission Automation Logic - Case A (Real-Time Simulation)

Hence, the collision avoidance maneuver continues until the aircraft start diverging.

The overall evolution for the Case A can be summarized as follows:

- the ownship and the single intruder are flying at same altitude in an head-on geometry;

- the conflict is detected when the intruder enters the coarse filter radius (i.e. *4000 m*) and the conflict detection condition is satisfied, i.e. at *46.1 s* of the simulation time;
- the conflict resolution maneuver is computed and executed;
- the conflict resolution maneuver ends when the aircraft start diverging, i.e. at *99.9 s*, so the ownship starts again the automatic waypoints navigation after a deviation from its original route.

For what concerns the CASE B, the evolution of the flights are reported in Figure 4.37. The two intruders start to send the ADS-B OUT data *36.1 s* after the simulation starts (corresponding to the achievement of the ownship assigned first waypoint, as set in the scenario simulation system). Both the intruders are flying at the ownship altitude with straight line trajectories.

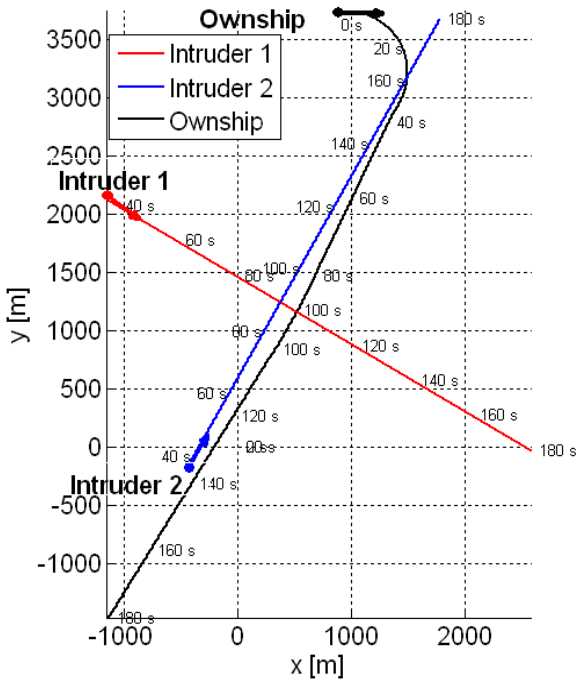

Figure 4.37 - Aircraft Trajectories - Case B (Real-Time Simulation)

As it can be seen in Figure 4.38, when the ownship start receiving ADS-B data, both intruders are inside the coarse filter threshold and it results that the detected conflict condition involves both the intruders and the prioritization of these conflicts by the system is needed.

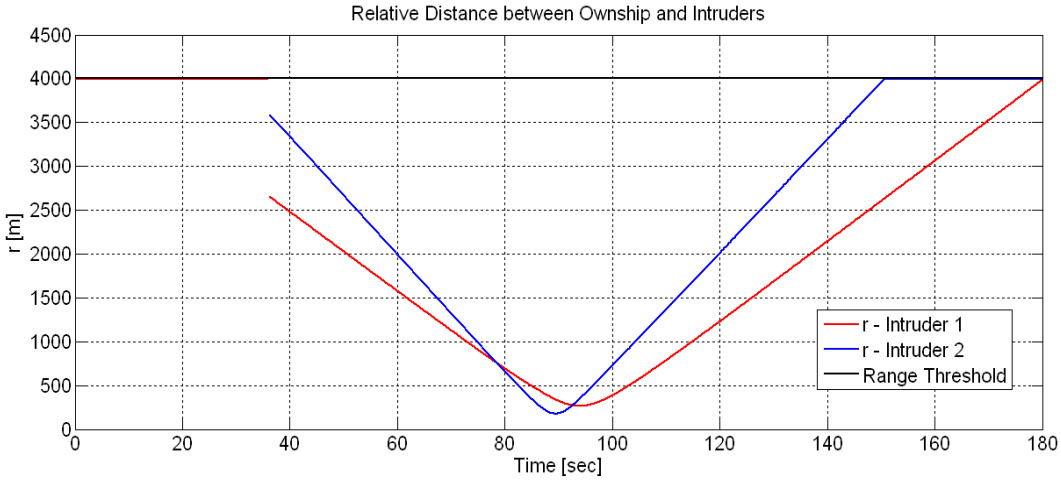

Figure 4.38 - Aircraft Relative Distance - Case B (Real-Time Simulation)

Once the conflicts have been prioritized, according to the criterion explained above, the collision avoidance maneuver is implemented with respect to the most relevant conflict, i.e. in this case Intruder 1. This intruder is the one with higher priority because, as it can be derived from the analysis of Table 4.5, it has a lower TTG with respect to the Intruder 2.

The logic evolution reported in Figure 4.39 shows, therefore, that the collision avoidance maneuver starts at *36.1 s* and lasts until *94.1 s* instant, when the Intruder 1 and the ownship start diverging. It is worth noticing here that, at the end of the conflict with Intruder 1, the Intruder 2 does not pose anymore a conflict with respect to the ownship, so the ownship continues its navigation towards the assigned waypoint.

	Intruder 1	**Intruder 2**
Relative Distance [m]	2660	3590
Closure Rate [m/sec]	59	55
TTG [sec]	45	64

Table 4.5 - Most significant values for conflict prioritization (Real-Time Simulation)

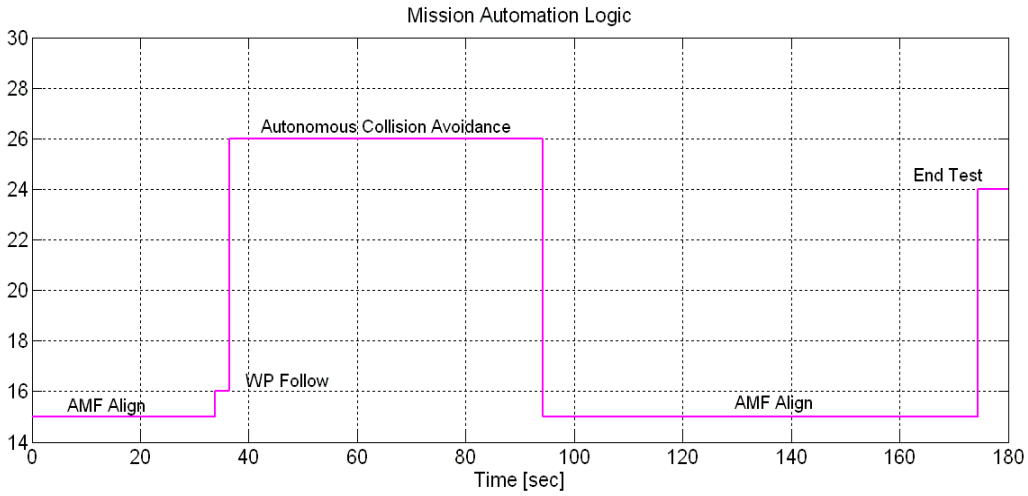

Figure 4.39 - Mission Automation Logic - Case B (Real-Time Simulation)

In this case, the collision avoidance maneuver consists in a suitable modification of the ownship trajectory as well as velocity magnitude in order to assure that the ownship will pass behind the Intruder 1.

The overall evolution for the Case B can be summarized as follows:

- the ownship starts receiving traffic ADS-B data at *36.1 s* and both intruders, which characterize the scenario, are inside the coarse filter radius and represent a conflict condition with respect to the ownship;
- the two conflicts are prioritized according to the TTG criterion explained earlier, i.e. the Intruder 1 represents the most relevant conflict;
- the conflict resolution maneuver is computed and executed with respect to the Intruder 1;
- the conflict resolution maneuver ends when the aircraft start diverging, i.e. at *99.1 s*;
- the ownship starts again the automatic waypoints navigation after a deviation from its original route, due to the circumstance that the resolution maneuver with respect to the intruder 1 is concluded and at this point intruder 2 does not represent anymore a conflict for the ownship.

It has to be noticed here that the conflict resolution manoeuver with respect to intruder 1 allowed also the simultaneous resolution of the conflict with respect to the intruder 2, in this particular case. Nevertheless, this is a result of this specific scenario and it is not a general feature of the system here proposed, which is aimed to solve only the primary conflict, without regard of the other conflicts that have been detected but have lower priority.

The last scenario (CASE C) considers the presence of two intruders which represent consecutive conflict conditions with the ownship. From the analysis of the flights evolution, reported in Figure 4.40 and Figure 4.41, it is clear that the two intruders enter the coarse filter radius in consecutive instants. Also in this case, the intruders send ADS-B data after they reached their first assigned waypoint (at *33.5 s*), according to the scenario simulation conditions that have been set.

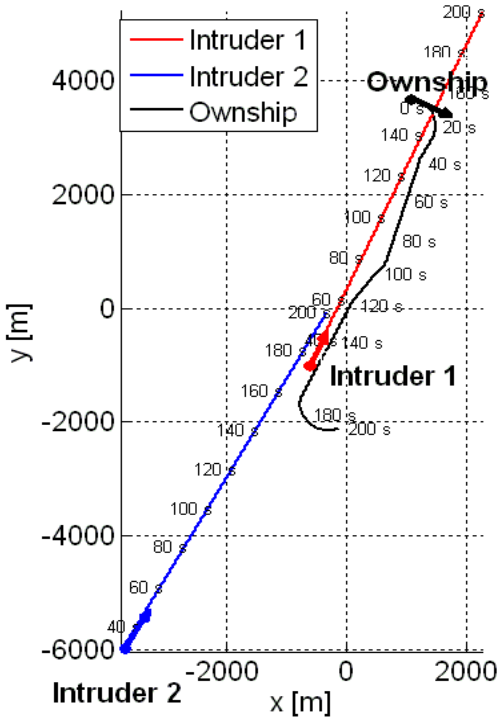

Figure 4.40 - Aircraft Trajectories - Case C (Real-Time Simulation)

The system behavior can be derived from the analysis of the logic evolution reported in Figure 4.42. At *33.5 s* the conflict resolution maneuver is activated since the Intruder 1 satisfies the conflict detection condition. The maneuver ends

at *86.5 s*, when the ownship and Intruder 1 start diverging. The ownship returns to its assigned waypoints navigation until *113.3 s*, when the conflict detection condition is satisfied once again but in this case with respect to Intruder 2. Therefore, the ownship deviates from its route and performs a collision avoidance maneuver with respect to the Intruder 2. At *165.8 s*, the ownship and the Intruder 2 exit from the conflict condition. It has to be noticed that in this case no conflict prioritization has been needed, because the two conflict are consecutives and do not apply at the same time as in the previous scenario (case B).

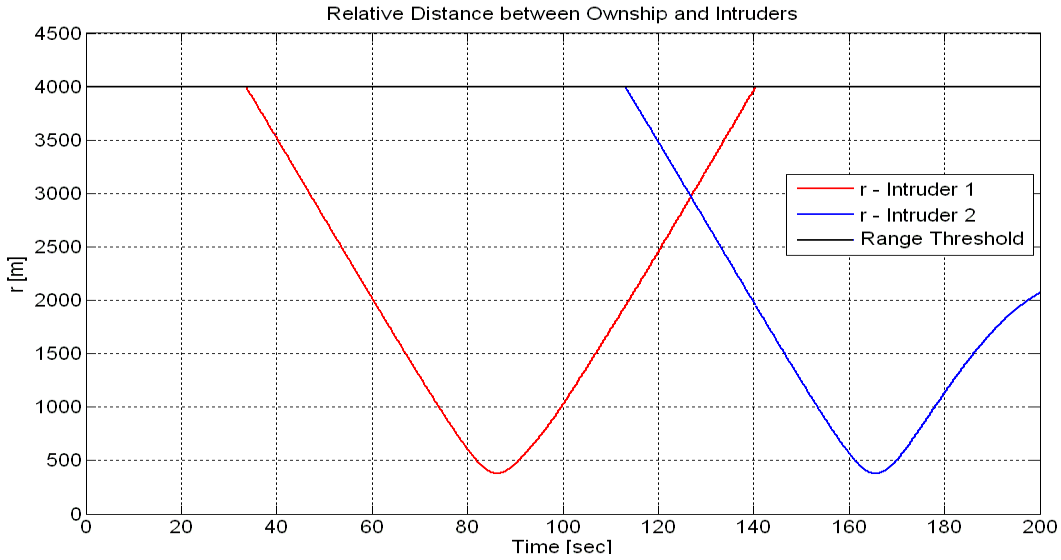

Figure 4.41 - Aircraft Relative Distance - Case C (Real-Time Simulation)

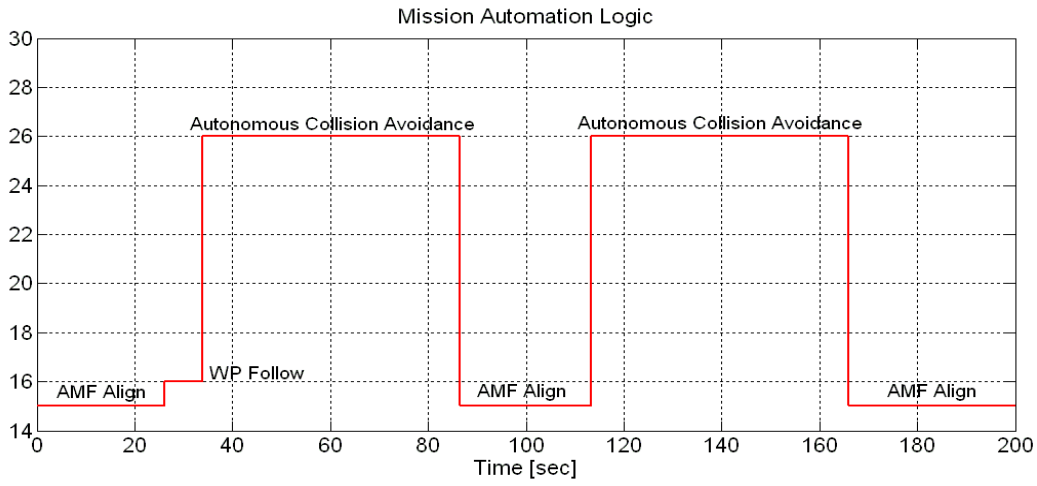

Figure 4.42 - Mission Automation Logic - Case C (Real-Time Simulation)

The overall evolution for the Case C can be summarized as follows:

- the ownship starts receiving traffic ADS-B data at *33.5 s* and one of the intruders, which characterize the scenario, is inside the coarse filter radius and represents a conflict condition with respect to the ownship;
- a conflict resolution maneuver is computed and executed with respect to the Intruder 1;
- the conflict resolution maneuver ends when the aircraft start diverging, i.e. at *86.5 s* and the ownship returns to its assigned waypoints navigation condition;
- at *113.4 s* a new conflict, with the Intruder 2, is detected;
- a conflict resolution maneuver is computed and executed with respect to the Intruder 2;
- the ownship starts again the automatic waypoints navigation after a deviation from its original route at *165.8 s*.

Conclusions

The aim of the work is to introduce an innovative ADS-B data based conflict detection system. The intended system applicability is for both manned commercial aircraft, as an aid to pilots system, and UAS, where high automation levels are required, as part of an autonomous sense and avoid system.

Based on the results of the simulations, the proposed approach shows to be able to implement the use of the surveillance data provided by the ADS-B IN for conflict detection purposes. This includes the possibility to support both advanced mission visualization displays for pilot situation awareness and automatic algorithms for conflict detection and resolution, for both tactical separation assurance and emergency collision avoidance.

Moreover, the real-time simulated scenarios above reported show that the proposed approach to conflict detection and prioritization based on the use of ADS-B surveillance data is suitable for efficient real-time implementation with no numerical and/or computational issues.

Test results demonstrated that the proposed system is suitable for integration as part of a complete airborne sense and avoid systems although a robust safety assessment would be needed through extensive simulation and flight test campaigns.

Currently the proposed algorithms are included in the on-going European project RAID (RPAS ATM Integration Demonstration) in the framework of SESAR JU program. The project aims to verify the possibility of the proposed system to support the airborne SAA system for either Self-Separation and Collision Avoidance functionalities in order to assist the integration of UAVs in the NAS.

References

[1] Han, J., Xu, Y., Di, L., Chen, Y.Q., Low-cost Multi-UAV Technologies for Contour Mapping of Nuclear Radiation Field, Journal of Intelligent & Robotic Systems, Volume 70, Issue 1-4, pp. 401-410, 2013.

[2] J. Zhang, W. Liu, Y. Wu, Novel Technique for Vision-Based UAV Navigation, IEEE Aerospace and Electronic System, Volume 47, Issue 4, pp. 2731 – 2741, 2011.

[3] Cook, S. P., Lacher, A. R., Maroney, D. R., Zeitlin, A. D., UAS Sense and Avoid Development – the Challenges of Technology, Standards, and Certification, 50th AIAA Aerospace Sciences Meeting, Nashville, Tennessee, 09 - 12 January, 2012.

[4] Marshall, D.M., Trapnell, B. M., Mendez, J. E., Berseth, B. L., Schultz, R. R., Semke, W. H., Regulatory and Technology Survey of Sense-and-Avoid for UAS, AIAA Infotech@Aerospace Conference and Exhibit, Rohnert Park, California, 7 – 10 May, 2007.

[5] Part 60-Scheduled Air Carrier Rules, 19 Fed. Reg. 6871, 1954.

[6] Code of Federal Regulations – Tiltle 14 Aeronautics and Space, Part 91 General operating and flight rules, Section 113, Right-of-way rules: Except water operations.

[7] Code of Federal Regulations – Tiltle 14 Aeronautics and Space, Part 91 General operating and flight rules, Section 111, Operating Near other Aircraft.

[8] 14 C.F.R. Section 1.1, 2005.

[9] 14 C.F.R. Part 101, 2005.

[10] Walker, J., 2010-2011 UAS Yearbook – UAS: The Global Perspective, 8th Edition, Copyright Blyenburgh & Co, Page 71, 2010.

[11] 72 FR 6689, 2007.

[12] Federal Aviation Administration, Sense And Avoid (SAA) for Unmanned Aircraft Systems (UAS), October 2009.

[13] http://www.rtca.org/content.asp?pl=108&sl=33&contentid=121

[14] http://www.rtca.org/content.asp?pl=108&sl=33&contentid=178

[15] Federal Aviation Administration, Order 7610.4K, Special Military Operation, 2004.

[16] Pellebergs, J., The MIDCAS Project, ICAS 2010, 27th International Congress of the Aeronautical Sciences, Nice, France, 19-24 September, 2010.

[17] Hottman, S. B., Hansen, K. R., Berry, M.,, Literature Review on Detect, Sense, and Avoid Technology for Unmanned Aircraft Systems, Federal Aviation Administration DOT/FAA/AR-08/41, September, 2009.

[18] Zeitlin, A., Progress on Requirements and Standards for Sense & Avoid, MITRE Corporation, 2010.

[19] RTCA, Inc., Minimum Operational Performance Standards for Traffic Alert and Collision Avoidance System II (TCAS II) Version 7.1, DO-185B, June, 2008.

[20] Sabatini, N., Statement of Nicholas A. Sabatini, Associate Administrator for Aviation Safety, Testimony – Statement of Nicholas A. Sabatini, 29 March, 2006.

[21] Insinna, V., Military, Industry Racing to Create Sense-and-Avoid Systems, National Defence Industrial Association, May, 2014.

[22] Muraru, A., A Critical Analysis of Sense and Avoid Technologies for Modern UAVs, Advances in Mechanical Engineering, Volume 2, Number 1 March, 2012.

[23] Billingsley, T.B., Kochenderfer, M.J., Collision Avoidance for General Aviation, IEEE Aerosp. Electron. Syst., 2012.

[24] Zeitlin, A. D., McLaughlin, M. P., Safety of cooperation collision avoidance for unmanned aircraft, IEEE Aerosp. Electron. Syst., 2007.

[25] International Civil Aviation Organization, ADS-B Implementation and Operations Guidance Document. Edition 3.0, 2007.

[26] Mozdzanowska, A., Weibel, R., Marais, K., Lester, E., Weigel, A., Hansman, R.J., Dynamics of Air Transportation System Transition and Implications for ADS-B Equipage in Proceedings of7th AIAA Aviation Technology, Integration and Operations Conference (ATIO), Belfast, Northern Ireland, 2007.

[27] SESAR Consortium, Work Programme for 2008-2013, Doc. SESAR Consortium No. DLM-0710-002-01-00, Bruxelles, Belgium, 2008.

[28] Joint Planning and Development Office, Concept of Operations for the Next Generation Air Transportation System, v.2.0, 2007.

[29] Skolnik, M.I., Radar Handbook, McGraw Hill Professional. New York, NY, USA, 1990.

[30] SELEX ES, LOAM – Laser Obstacle Avoidance System, from http://www.selexelsag.com/internet/?open0=5338&open1=5350&section=COMM&showentry=17089, 2015.

[31] Yu, X., Zhang, Y., Sense and avoid technologies with applications to unmanned aircraft systems: Review and prospects, Progress in Aerospace Sciences, Elsevier Ltd., 2015.

[32] Karhoff, B. C., Limb, J. I., Oravsky, S. W., Shephard, A. D., Eyes in the Domestic Sky: An Assessment of Sense and Avoid Technology for the Army's "Warrior" Unmanned Aerial Vehicle, in Proc. Of IEEE System and Information Engineering Design Symposium, Charlottesville, VA, USA, 2006.

[33] Lester, T., Cook, S., Noth, K., USAF Airborne Sense And Avoid (ABSAA) Airworthiness and Operational Approval Approach, Version 1.0, MITRE Corporation, 31 January, 2014.

[34] Lincoln Laboratory, Tech Notes on Airborne Sense and Avoid Radar Panel, Massachusetts Institute of Technology (MIT), October, 2014 from http://www.ll.mit.edu/publications/technotes/TechNote_ABSAAPanel.pdf

[35] Owen, M. P., Duffy, S. M., Edwards, M. W. M., Unmanned Aircraft Sense and Avoid Radar: Surrogate Flight Testing Performance Evaluation, in Proc. Of IEEE Radar Conference, Cincinnati, OH, USA, 2014.

[36] Itcia, E., Wasselin, J.P., Mazuel, S., Otten, M., Huizing, A., FMCW Radar for Sense Fucntion of Sense & Avoid Systems onboard UAVs, Proc. Of SPIE Vol 8899, Emerging Technologies in Security and Defence; and Quantum Security II; and Unmanned Sensor Systems X, 889914, 23 October, 2013.

[37] Moses, A., Rutherford, M. J., Valavanis, K. P., Radar-based detection and identification for miniature air vehicles, in Proc. Of the 2011 IEEE International Conference on Control Applications, Denver, CO, USA 2011.

[38] Lai, J., Mejias, L., Ford, J.J., Airborne vision-based collision-detection system, Journal of Field Robotics, Volume 28, Issue 2, pp. 137-157, 2011.

[39] Kopp, C., Active Electronically Steered Arrays, Air Power Australia website, 30 May, 2007. http://www.ausairpower.net/aesa-intro.html

[40] Zarandy, A., Zsedrovits, T., Nagy, Z., Kiss, A., Roska, T., Visual sense-and-avoid system for UAVs, Proc. Of 13th International Workshop on Cellular Nanoscale Networks and their Applications, pp. 1–5, 2012.

[41] Fasano, G., Accardo, D., Tirri, A. E., Moccia, A., De Lellis, E., Morphological filtering and target tracking for vision-based UAS sense and avoid, IEEE International Conference on Unmanned Aircraft Systems (ICUAS), Orlando, FL, 27-30 May, 2014.

[42] Kim, J.-H., Lee, D. W., Cho, K.-R., Jo, S.-Y., Kim, J.-H., Min, C.-O., Han, D.-I., Cho, S.-J., Development of an electro-optical system for small UAV, Aerospace Scince and Technology, Elsevier Masson SAS., 2010.

[43] Minwalla, C., Thomas, P., Ellis, K., Hornsey, R., Jenings, Flight Test Evaluation of a Prototype Optical Instrument for airborne Sense-and-Avoid Applications, Proc. Of SPIE Vol. 8387, 2012.

[44] Griffith, J. D., Kochenderfer M. J., Kuchar J. K., Electro-Optical System Analysis for Sense and Avoid, AIAA Guidance, Navigation and Control Conference and Exhibit, Honolulu, Hawaii, 18-21 August 2008.

[45] Finn, A., Franklin, S., Acoustic Sense and Avoid for UAV's, In Proc. Of 7th International conference on Intelligent Sensors, Sensor Networks and Information Processing, Adelaide, SA, Australia, 2011.

[46] Lo, K. W., Ferguson, B. G., Gai, Y. J., Maguer, A., Aircraft flight parameter estimation using acoustic multipath delays, IEEE Trans. Aerosp. Electron. Syst., 2003.

[47] Case, E. E., Zelnio, A. M., Rigling, B. D., Low-cost acoustic array for small UAV detection and tracking, in Proc. Of IEEE National Aerospace and Electronics Conference, Dayton, OH, USA, 2008.

[48] Milkie, T., Passive Acoustic Non-Cooperative Collision Alert System (PANCAS) for UAV Sense and Avoid. Unpublished white paper by SARA, Inc, 2007.

[49] Ramasamy, S., Sabatini, R., Gardi, A., Avionics Sensor Fusion for Small Size Unmanned Aircraft Sense-and-Avoid, IEEE Metrology for Aerospace (MetroAerospace) 2014, pp. 271-276, Benevento, Italy, 2014.

[50] Cornic, P., Garrec, P., KemKemian, S., Ratton, L., Sense and Avoid Radar using DataFusion with Other Sensors, IEEE Aerospace Conference, Big Sky, USA, March, 2010.

[51] Chen, R. H., Gevorkian, A., Fung, A., Chen, W.-Z., Multi-Sensor Data Integration for Autonomous Sense and Avoid, Infotech @ Aerospace 2011, St. Louis, Missouri, 29 -31 March, 2011.

[52] Graham, S., Chen, W.-Z., De Luca, J., Kay, J., Deschenes M., Weingarten, N., Raska, V., Lee, X., Multiple Intruder Autonomous Avoidance Flight Test, Infotech @ Aerospace 2011, St. Louis, Missouri, 29 -31 March, 2011.

[53] Sabatini, R., Gardi, A., Richardson, M. A., LIDAR Obstacle Warning and Avoidance System for Unmanned Aircraft, International Journal of Mechanical, Aerospace, Industrial and Mechatronics Engineering Vol8, No. 4, 2014.

[54] Fasano G., D. Accardo, A. Moccia, C. Carbone, U. Ciniglio, F. Corraro, S. Luongo, “Multi-Sensor-Based Fully Autonomous Non-Cooperative Collision Avoidance System for Unmanned Air Vehicles”, AIAA Journal of Aerospace Computing, Information, and Communication, vol. 5, pp. 338-360, DOI: 10.2514/1.35145, October 2008.

[55] Federal Aviation Administration, Aeronautical Information Manual – Official Guide to Basic Flight Information and ATC procedures, 3 August, 2006.

[56] Martel, F., Schultz, R. R., Semke, W. H., Wang, Z., Czarnomski, M., Unmanned Aircraft Systems Sense and Avoid Avionics Utilizing ADS-B Transceiver, AIAA Infotech@Aerospace Conference, Seattle, Washington, 6-9 April, 2009.

[57] Martel, F., Mullins, M., Kaabouch, N., Semke, W., Flight Testing of an ADS-B-based Miniature 4D Sense and Avoid System for Small UAS, AIAA Infotech@Aerospace Conference, St. Louis, Missouri, 29-31 March, 2011.

[58] Mullins, M., Holman, M., Foerster, K., Kaabouch, N., Semke, W., Dynamic Separation Thresholds for a Small Airborne Sense and Avoid System, AIAA Infotech@Aerospace Conference, Boston, MA, 19-22 August, 2013.

[59] Huiyao, W., Zhihao, C., Yingxun, W., UAVs Autonomous Collision Avoidance in Non-segregated Airspace using Dynamic Alerting Thresholds, AIAA Infotech@Aerospace Conference, Boston, MA, 19-22 August, 2013.

[60] Tadema, J., Theunissen, E., An Integrated Conflict Avoidance Concept for Aviation, IEEE/AIAA 28th Digital Avionics Systems Conference, Orlando, Florida, 23-29 October, 2009.

[61] Baek, K., Bang, H., ADS-B based Trajectory Prediction and Conflict Detection for Air Traffic Management, Int. J. of Aeronautical & Space Sci. 13(3), 2012.

[62] Sellem-Delmar, S., Farjon, J., D2.2.2-1 MID-air Collision Avoidance System (MIDCAS) Concept of Operations (CONOPS), EDA, 15 February, 2011.

[63] AA.VV., www.flarm.com/technology/.

[64] Automatic Dependent Surveillance – Broadcast (ADS-B) Out Performance Requirements to Support Air Traffic (ATC) Service; Final Rule, Federal Register, vol 75, May, 2010.

[65] http://www.duncanaviation.aero/straighttalk/adsb/how_it_works.php

[66] RTCA, DO-338 Minimum Aviation System Performance Standards (MASPS) for ADS-B Traffic Surveillance Systems and Applications (ATSSA), June, 2012.

[67] Federal Aviation Administration, TSO-C166b Extended Squitter Automatic Dependent Surveillance – Broadcast (ADS-B) and Traffic Information Service - Broadcast (TIS-B) Equipment Operating on the Radio Frequency of 1090 Megahertz (MHz), February, 2009.

[68] Kunzi, F., Hansman, J., ADS-B Benefits to General Aviation and Barriers to implementation, MIT International Center for Air Transportation (ICAT), May, 2011.

[69] http://www.ads-b.com/

[70] Federal Aviation Administration, 14 CFR Part 91 Automatic Dependent Surveillance – Broadcast (ADS-B) Out Performance Requirements To Support Air Traffic Control (ATC) Service; Final rule, Part II Department of Transportation, 28 May, 2010.

[71] ICAO, DOC 9871 Technical Provisions for Mode S Services and External Squitter, 2008.

[72] ICAO, DOC 9861 Manual on the Universal Access Transceiver (UAT), 2009.

[73] FAA, AC 20-165 Airworthiness Approval of Automatic Dependent Surveillance - Broadcast (ADS-B) Out Systems, 21 May, 2010.

[74] FAA, AC 90-114 Automatic Dependent Surveillance-Broadcast (ADS-B) Operations, 21 September, 2012.

[75] FAA, AC 150/5220-26 Airport Ground Vehicle Automatic Dependent Surveillance – Broadcast (ADS-B) Out Squitter Equipment, 1 September, 2012.

[76] FAA, AC 20-172A Airworthiness Approval for ADS-B In Systems and Applications, 23 March, 2012.

[77] FAA, TSO-C154c Universal Access Transceiver (UAT) Automatic Dependent Surveillance Broadcast (ADS-B) Equipment Operating on Frequency of 978 MHz, 2 December, 2009.

[78] FAA, TSO-C195a, Avionics Supporting Automatic Dependent Surveillance – Broadcast (ADS-B) Aircraft Surveillance Applications (ASA), 29 February, 2012.

[79] RTCA, DO-260B Minimum Operational Performance Standards for 1090 MHz Extended Squitter Automatic Dependent Surveillance - Broadcast (ADS-B) and Traffic Information Services - Broadcast (TIS-B), 2 December, 2009.

[80] RTCA, DO-282B Minimum Operational Performance Standards for Universal Access Transceiver (UAT) Automatic Dependent Surveillance - Broadcast (ADS-B), 2 December, 2009.

[81] RTCA, DO-317B Minimum Operational Performance Standards (MOPS) for Aircraft Surveillance Applications (ASA) System, 17 June, 2014.

[82] RTCA, DO-249 Development and Implementation Planning Guide for Automatic Dependent Surveillance Broadcast (ADS-B) Applications, 6 October, 1999.

[83] RTCA, DO-242A Minimum Aviation System Performance Standards for Automatic Dependent Surveillance Broadcast (ADS-B), 25 June, 2002.

[84] http://www.rtca.org/store_list.asp

[85] EUROCONTROL, UE 1207/2011 Requirements for the performance and the interoperability of surveillance for the SES, 22 November, 2011.

[86] Atienza, E., Falah, R., Garcia, S., Gutierrez, L., Martinez, M. A. L., Robles, O., ADS-B: An Air Navigation Revolution, Rey Juan Carlos University – Fuenlabrada Campus, 24 April, 2013

[87] Strohmeier, M., Schafer, M., Lenders, V., Martinovic, I., Realities and Challenges of NextGen Air Traffic Management, IEEE Communications Magazine, May, 2014.

[88] McCallie, D., Butts, J., Mills, R., Security Analysis of the ADS-B Implementation in the Next Generation Air Transportation System, Int'I. J. Critical Infrastructure Protection (IJCIP), vol. 4, August, 2011.

[89] Costin, A., Francillon, A., Ghost in the Air (Traffic): On Insecurity of ADS-B Protocol and Practical Attacks on ADS-B Devices, Black Hat, July, 2012.

[90] Schafer, M., Lenders, V., Martinovic, I., Experimental Analysis of Attacks on Next Generation Air Traffic Communication, Int'I. Conf. Applied Cryptografy and Network Security (ACNS), Springer, June, 2013.

[91] Samuelson, K., Valovage, E., Hall, D., Enhanced ADS-B Research, IEEE Aerospace Conference, Big Sky, MT, 2006.

[92] Stark, B., Stevenson, B., Chen, Y.Q., ADS-B for Small Unmanned Aerial Systems: Case Study and Regulatory Practices, 2013 International Conference

on Unmanned Aircraft Systems (ICUAS), Grand Hyatt Atlanta, Atlanta, GA, May 28-31, 2013.

[93] Unmanned Aircraft System Study Group (UASSG), The Use of Displayed ADS-B Data for a Collision Avoidance Capability in an Unmanned Aircraft System, Montreal, Canada, 23-27 April, 2012.

[94] RTCA, DO-317A Minimum Operational Performance Standards (MOPS) for Aircraft Surveillance Applications (ASA) System, December 2011.

[95] X. Rong Li, V. P. Jilkov, "A survey of Maneuvering Target Tracking: Dynamic Models" in Proceedings of SPIE Conference on Signal and Data Processing of Small Targets, Orlando, FL, USA (200).

[96] RTCA, DO-289 Minimum Aviation System Performance Standards for Aircraft Surveillance Applications (ASA), Volume1, December 9, 2003.

[97] RTCA, DO-317B Traffic Situation Awareness with Alerting (TSAA) Application Sample Algorithm, Appendix T, 2014.

[98] F. Kunzi, Development of a High-Precision ADS-B Based Conflict Alterting System for Operation in the Airport Enviroment, Massachusetts Institute of Technology, October 2013.

[99] ICAO, Airborne Collision Avoidance System (ACAS) Manual, Doc 9863 AN/461, 2006

[100] Munoz C., Narkawicz A., Chamberlain J., A TCAS-II Resolution Advisory Detection Algorithm, AIAA Guidance, Navigation and Control Conference, August 19-22, 2013, Boston, USA.

[101] Orefice, M., Luongo, S., Accardo, D., Fasano, G., Corraro, F., Tracking Architectures and Algorithms based on Cooperative and Non-Cooperative Sensors for Multiple UAV Applications, In Proceedings of the Italian Association of Aeronautics and Astronautics (AIDAA) XXII Conference, Naples, Italy, 9-12 September, 2013.

[102] Orefice, M., Di Vito, V., Corraro, F., Accardo, D., Fasano, G., Aircraft Conflict Detection Based on ADS-B Surveillance Data, In Proceedings of the IEEE International Workshop on Metrology for Aerospace 2014, Benevento, Italy, 29-30 May, 2014.

[103] Baraniello, V., “AsBuilt della facility FLARE HIL 0p0”, CIRA-CF-14-1512, 2014.

[104] De Lellis, E., Di Vito, V., Marrone, C., Ciniglio, U., Corraro, “Flight Testing of a Fully Adaptive Algorithm for Autonomous Fixed Wing Aircrafts Landing”, Infotech@Aerospace 2012 Conference, Garden Grove, California 19 - 21 June 2012.

[105] Genito, N. De Lellis, E., Di Vito, V., Garbarino, L., Marrone, C., “Autonomous Take Off System: Development and Experimental Validation”, 3rd CEAS Air&Space Conference, 21st AIDAA Congress, CEAS 2011 The International Conference of the European Aerospace Societies, Venice, Italy, 24-28 October 2011.

[106] De Lellis, E., Di Vito, V., Garbarino, L., Lai, C., Corraro, F., “Design Process and Real-Time Validation of an Innovative Autonomous Mid-Air Flight and Landing System”, World Academy of Science, Engineering and Technology (WASET), Issue 79-2011, Proceedings of the ICAAE 2011 - International Conference on Aeronautical and Astronautical Engineering, Paris, France, 27-29 July 2011.

[107] Di Vito, V., De Lellis, E., Marrone, C., Corraro, F., Ciniglio, U., “UAV Free Path Safe DGPS/AHRS Approach and Landing System with Dynamic and Performance Constraints”, UAV 2007 International Conference, Exhibition and Workshop, Paris, France, 12-14 June 2007.

[108] Di Vito, V., De Lellis, E., Genito, N., Marrone, C., Ciniglio, U., Corraro, F., “UAV Free Path Safe DGPS/AHRS Autolanding: algorithm and flight tests”, UAS 2008 International Technical Conference and Exhibition, Paris, France, 10-12 June 2008

[109] Orefice, M., Di Vito, V., Garbarino, L., Corraro, F., Accardo, D., Fasano, G., Real-Time Validation of an ADS-B Based Aircraft Conflict Detection System, in Proceedings of the American Institute of Aeronautics and Astronautics (AIAA) SciTech 2015 Conference, Kissimmee, Florida, 5-9 January, 2015.